UNIVERSITY OF AMSTERDAM

UvA-DARE (Digital Academic Repository)

Measurement of inclusive jet and dijet cross-sections in proton-proton collisions at $\sqrt{s}$=13 TeV with the ATLAS detector

The ATLAS Collaboration

DOI
10.1007/JHEP05(2018)195

Publication date
2018

Document Version
Final published version

Published in
The Journal of High Energy Physics

License
CC BY

Link to publication

Citation for published version (APA):
The ATLAS Collaboration (2018). Measurement of inclusive jet and dijet cross-sections in proton-proton collisions at $\sqrt{s}$=13 TeV with the ATLAS detector. *The Journal of High Energy Physics*, *2018*(5), Article 195. https://doi.org/10.1007/JHEP05(2018)195

General rights
It is not permitted to download or to forward/distribute the text or part of it without the consent of the author(s) and/or copyright holder(s), other than for strictly personal, individual use, unless the work is under an open content license (like Creative Commons).

Disclaimer/Complaints regulations
If you believe that digital publication of certain material infringes any of your rights or (privacy) interests, please let the Library know, stating your reasons. In case of a legitimate complaint, the Library will make the material inaccessible and/or remove it from the website. Please Ask the Library: https://uba.uva.nl/en/contact, or a letter to: Library of the University of Amsterdam, Secretariat, P.O. Box 19185, 1000 GD Amsterdam, The Netherlands. You will be contacted as soon as possible.

UvA-DARE is a service provided by the library of the University of Amsterdam (https://dare.uva.nl)

Download date:05 Sept 2026

Published for SISSA by Springer

Received: November 9, 2017
Revised: February 19, 2018
Accepted: March 13, 2018
Published: May 30, 2018

Measurement of inclusive jet and dijet cross-sections in proton-proton collisions at $\sqrt{s} = 13$ TeV with the ATLAS detector

The ATLAS collaboration

E-mail: atlas.publications@cern.ch

Abstract: Inclusive jet and dijet cross-sections are measured in proton-proton collisions at a centre-of-mass energy of 13 TeV. The measurement uses a dataset with an integrated luminosity of 3.2 fb^{-1} recorded in 2015 with the ATLAS detector at the Large Hadron Collider. Jets are identified using the anti-k_{t} algorithm with a radius parameter value of $R = 0.4$. The inclusive jet cross-sections are measured double-differentially as a function of the jet transverse momentum, covering the range from 100 GeV to 3.5 TeV, and the absolute jet rapidity up to $|y| = 3$. The double-differential dijet production cross-sections are presented as a function of the dijet mass, covering the range from 300 GeV to 9 TeV, and the half absolute rapidity separation between the two leading jets within $|y| < 3$, y^*, up to $y^* = 3$. Next-to-leading-order, and next-to-next-to-leading-order for the inclusive jet measurement, perturbative QCD calculations corrected for non-perturbative and electroweak effects are compared to the measured cross-sections.

Keywords: Hadron-Hadron scattering (experiments)

ArXiv ePrint: 1711.02692

Open Access, Copyright CERN,
for the benefit of the ATLAS Collaboration.
Article funded by SCOAP^3.

https://doi.org/10.1007/JHEP05(2018)195

Contents

1 Introduction **1**

2 ATLAS detector **2**

3 Cross-section definitions **3**

4 Dataset and Monte Carlo simulations **4**

5 Event and jet selection **5**

6 Jet energy calibration and resolution **5**
- 6.1 Jet reconstruction 5
- 6.2 Jet energy calibration 6
- 6.3 Jet energy scale uncertainties 7
- 6.4 Jet energy resolution and its uncertainties 8
- 6.5 Jet angular resolution and its uncertainties 8

7 Unfolding of detector effects **9**

8 Propagation of the uncertainties to the cross-sections **10**

9 Theoretical predictions **11**
- 9.1 Next-to-leading-order pQCD calculations 11
- 9.2 Non-perturbative corrections 13
- 9.3 Electroweak corrections 14
- 9.4 Next-to-next-to-leading-order pQCD calculations 14

10 Results **16**

11 Conclusion **22**

The ATLAS collaboration **30**

1 Introduction

Precise measurements of jet cross-sections are crucial in understanding physics at hadron colliders. In quantum chromodynamics (QCD), jets are interpreted as resulting from the fragmentation of quarks and gluons produced in a short-distance scattering process. Jet cross-sections provide valuable information about the strong coupling constant, α_s, and the structure of the proton. Also, inclusive jet and dijet events represent a background to many

JHEP05(2018)195

other processes at hadron colliders. The predictive power of fixed-order QCD calculations is therefore relevant in many searches for new physics.

Inclusive jet production cross-sections have been measured in collisions of hadrons at the Sp$\bar{\text{p}}$S and Tevatron colliders at various centre-of-mass energies. The latest and most precise results at $\sqrt{s} = 1.96\,\text{TeV}$ are detailed in refs. [1, 2]. At the Large Hadron Collider (LHC) [3] at CERN, the ALICE, ATLAS and CMS collaborations have measured inclusive jet cross-sections in proton-proton collisions at centre-of-mass energies of $\sqrt{s} = 2.76\,\text{TeV}$ [4–6] and $\sqrt{s} = 7\,\text{TeV}$ [7–10]. Recently, the ATLAS and CMS collaborations have measured the inclusive jet cross-sections at $\sqrt{s} = 8\,\text{TeV}$ [11, 12], and the CMS Collaboration also at $\sqrt{s} = 13\,\text{TeV}$ [13]. Dijet production at the LHC has been measured by the ATLAS and CMS collaborations at a centre-of-mass energy of $\sqrt{s} = 7\,\text{TeV}$ [7, 14], and also by the CMS Collaboration at $\sqrt{s} = 8\,\text{TeV}$ [15].

This paper presents measurements of the inclusive jet and dijet cross-sections in proton-proton collisions at $\sqrt{s} = 13\,\text{TeV}$ centre-of-mass energy by the ATLAS Collaboration at the LHC, using data collected in 2015 and corresponding to an integrated luminosity of $3.2\,\text{fb}^{-1}$. The inclusive jet cross-sections are measured double-differentially as a function of the jet transverse momentum, p_{T}, and absolute jet rapidity, $|y|$.[1] In addition, the double-differential dijet production cross-sections are presented as a function of the invariant mass of the dijet system, m_{jj}, and as a function of half the absolute rapidity separation between the two highest-p_{T} jets satisfying $|y| < 3$, denoted y^*.[2] Jets are reconstructed using the anti-k_t jet clustering algorithm [16] with a radius parameter value of $R = 0.4$. The measurements cover the kinematic region of $100\,\text{GeV} < p_{\text{T}} < 3.5\,\text{TeV}$ and $|y| < 3$ for the inclusive jet cross-section, and of $300\,\text{GeV} < m_{jj} < 9\,\text{TeV}$ and $y^* < 3$ for the dijet cross-section.

Next-to-leading-order (NLO) perturbative QCD (pQCD) predictions calculated using several parton distribution function (PDF) sets, corrected for electroweak and non-perturbative effects, are quantitatively compared to the measurement results. In addition, the inclusive jet cross-sections are compared to the recently published complete next-to-next-to-leading-order (NNLO) pQCD calculation [17, 18].

2 ATLAS detector

The ATLAS experiment [19, 20] at the LHC is a multi-purpose particle detector with a forward-backward symmetric cylindrical geometry and a near 4π coverage in solid angle.[3] It consists of an inner tracking detector, electromagnetic and hadron calorimeters, and a muon spectrometer. The inner tracking detector covers the pseudorapidity range $|\eta| < 2.5$

[1] The rapidity is defined as $y = 0.5 \times \ln[(E + p_z)/(E - p_z)]$, where E denotes the energy and p_z is the component of the momentum along the beam direction.

[2] The variable y^* is defined as $|y_1 - y_2|/2$, where the subscripts 1,2 label the highest and second highest-p_{T} jet in the event satisfying $|y| < 3.0$, respectively. This quantity is invariant under a Lorentz boost along the z-direction and is equal to the absolute rapidity of each jet in the dijet rest frame.

[3] ATLAS uses a right-handed coordinate system with its origin at the nominal interaction point (IP) in the centre of the detector and the z-axis along the beam pipe. The x-axis points from the IP to the centre of the LHC ring, and the y-axis points upward. Cylindrical coordinates (r, ϕ) are used in the transverse plane, ϕ being the azimuthal angle around the z-axis. The pseudorapidity is defined in terms of the polar angle θ as $\eta = -\ln\tan(\theta/2)$.

JHEP05(2018)195

and is used to reconstruct tracks and vertices. It consists of silicon pixel, silicon microstrip, and transition radiation tracking detectors, surrounded by a thin superconducting solenoid providing a 2 T axial magnetic field. Lead/liquid-argon (LAr) sampling calorimeters provide electromagnetic (EM) energy measurements with high granularity. They consist of a barrel ($|\eta| < 1.475$) and two endcap ($1.375 \leq |\eta| < 3.2$) regions. The hadron calorimeters are divided into five distinct regions: a barrel region ($|\eta| < 0.8$), two extended barrel regions ($0.8 \leq |\eta| < 1.7$) and two endcap regions ($1.5 \leq |\eta| < 3.2$). The barrel and extended barrel regions are instrumented with steel/scintillator tile calorimeters. The endcap regions are instrumented with LAr calorimeters for both the EM and hadronic energy measurements. The ATLAS calorimeters have very high lateral granularity and several samplings in depth over $|\eta| < 3.2$. The muon spectrometer surrounds the calorimeters and features three large air-core toroid superconducting magnets with eight coils each. The field integral of the toroids ranges between 2.0 and 6.0 Tm across most of the detector. It includes a system of precision tracking chambers for track measurement in the principal bending direction and fast detectors for triggering and measurement of the muon coordinate in the direction orthogonal to that determined by the precision-tracking chambers. A two-level trigger system is used to select events. The first-level trigger is implemented in hardware and uses a subset of the detector information. This is followed by the high-level trigger system [21], which is software-based and can run the offline reconstruction and calibration software, further reducing the event rate to an average of 1 kHz.

3 Cross-section definitions

The jet cross-sections are determined for so-called particle jets. These jets are built at the event generator level from stable particles, i.e. those fulfilling $c\tau > 10$ mm, where τ is the proper lifetime. This definition includes muons and neutrinos. Jets are identified using the anti-k_t jet algorithm [16] as implemented in the FastJet [22] package with radius parameter $R = 0.4$. The use of the anti-k_t algorithm is well motivated since it is infrared- and collinear-safe, and produces geometrically well-defined ("cone-like") jets.

Inclusive jet double-differential cross-sections are measured as a function of jet p_{T} in six equal-size bins of the absolute jet rapidity, $|y|$. Only jets in the kinematic range $p_{\mathrm{T}} > 100$ GeV and $|y| < 3.0$ are considered, to ensure that the jet energy scale is well understood, as described in section 6. The inclusive jet production cross-section can be expressed as a ratio of the number of jets in data after correcting for detector effects, N_{jets}, to the integrated luminosity of the data, $\mathcal{L}$, in a given interval of momentum and rapidity, Δp_{T} and Δy respectively:

$$\frac{\mathrm{d}^2\sigma}{\mathrm{d}p_{\mathrm{T}}\mathrm{d}y} = \frac{N_{\mathrm{jets}}}{\mathcal{L}\Delta p_{\mathrm{T}}\Delta y}.$$

The dijet double-differential cross-section is measured as a function of the invariant mass of the dijet system, m_{jj}, in six equal-size bins of y^*, for events with at least two jets with $p_{\mathrm{T}} > 75$ GeV and $|y| < 3.0$. In addition, the scalar sum of the p_{T} of the first and second leading jets, $H_{\mathrm{T},2} = p_{\mathrm{T}1} + p_{\mathrm{T}2}$, is required to be above 200 GeV. This requirement avoids instabilities in the NLO cross-section calculations due to the symmetric p_{T} requirement applied to the leading and sub-leading jets [23, 24].

JHEP05(2018)195

The dijet production cross-section is calculated as the ratio of the number of dijet events after correcting for detector effects, N_{dijet}, to the integrated luminosity of the data, in a given interval of the invariant mass and y^*, Δm_{jj} and Δy^* respectively:

$$\frac{\mathrm{d}^2\sigma}{\mathrm{d}m_{jj}\mathrm{d}y^*} = \frac{N_{\text{dijet}}}{\mathcal{L}\Delta m_{jj}\Delta y^*}.$$

The $H_{\mathrm{T},2}$ and p_{T} selections on the two leading jets determine the lower edge of the mass range in each y^* bin. The p_{T} (m_{jj}) binning is chosen according to the detector p_{T} (m_{jj}) resolution, such that the bin width is approximately twice the p_{T} (m_{jj}) resolution, with the exception of the highest p_{T} (m_{jj}) bins in each rapidity (y^*) range where the bin width is enlarged to avoid large statistical fluctuations and non-Gaussian statistical uncertainties due to a low number of entries per bin; as predicted by a MC simulation (see section 4).

4 Dataset and Monte Carlo simulations

The measurements use proton-proton collision data at a centre-of-mass energy of $\sqrt{s} = 13\,\text{TeV}$ collected by the ATLAS detector during the 2015 data-taking period of the LHC. The LHC beams were operated with proton bunches organised in "bunch trains", with a bunch spacing of 25 ns. The integrated collected luminosity is $3.2\,\text{fb}^{-1}$ with an uncertainty of 2.1%. The uncertainty in the luminosity is derived following a methodology similar to that detailed in ref. [25], from a calibration of the luminosity scale using x-y beam-separation scans performed in August 2015.

Simulated jet events were produced using three different Monte Carlo event generators for comparisons to data and to derive corrections. The Pythia 8 program (version 8.186 [26]) was used for the baseline comparisons, the deconvolution of detector effects and the propagation of systematic uncertainties. It uses LO pQCD matrix elements for $2 \to 2$ processes, along with a leading-logarithmic (LL) p_{T}-ordered parton shower [27] including photon radiation, underlying event[4] simulation with multiple parton interactions [28], and hadronisation with the Lund string model [29]. The samples were created using a set of tuned parameters called the A14 tune [30] and the NNPDF2.3LO [31] LO PDF set. The EvtGen 1.2.0 program [32] was used to model bottom and charm hadron decays. NLO samples of simulated events were produced using Powheg [24, 33] and showered with Pythia 8 for systematic studies as discussed in section 6.3, and for optimising bin widths. The A14 tune and the CT10 [34] PDF set were used. For the evaluation of non-perturbative effects, the Pythia 8 and Herwig++ [35] (v2.7.1 [36]) event generators were also employed as described in section 9.2.

In all the samples, the effects of multiple proton-proton interactions in the same and neighbouring bunch crossings (pile-up) were included by overlaying inelastic minimum-bias events generated with Pythia 8. The generated events were further weighted to reproduce the observed distribution of the average number of collisions per bunch crossing in data. The stable particles from the generated events were passed through the ATLAS detector

[4]The term underlying event is used to mean particles produced in the same proton-proton collision, but not originating from the primary hard partonic scatter or its products.

JHEP05(2018)195

simulation [37] based on Geant4 [38] and were reconstructed with the same version of the ATLAS software as was used to process the data.

5 Event and jet selection

A suite of single-jet triggers [21] with thresholds varying from 55 GeV to 360 GeV are used to record events with at least one jet with transverse energy, E_{T}, above the threshold in the region $|\eta| < 3.2$. To keep the trigger rate to an acceptable level, the triggers with lower E_{T} thresholds are prescaled by recording only a predefined fraction of events. The highest-threshold trigger accepts all events passing the threshold. The effective luminosities range from 81 nb^{-1} for $75 < p_{\mathrm{T}} < 100$ GeV, where the trigger prescaling is largest, to 3.2 fb^{-1} for $p_{\mathrm{T}} > 442$ GeV, where an unprescaled trigger is used.

A p_{T}-dependent trigger strategy is adopted in order to optimise the statistical power of the measurement. In the inclusive jet measurement, each p_{T} bin requires the trigger with the lowest prescale (i.e. with highest effective luminosity) that is fully efficient in that range. Due to the high prescale factors, trigger efficiencies are studied offline in data as a function of p_{T} and rapidity by emulating the online trigger decision. The efficiency for jets in a given p_{T} range is obtained as the fraction of those that pass the emulated trigger in an unbiased sample obtained by requiring at least one online jet passing the first-level trigger with $E_{\mathrm{T}} > 15$ GeV. The trigger efficiency is always larger than 99.9% in the p_{T} range where it is considered.

The trigger strategy for the dijet measurement is slightly different to account for different prescale combinations for dijet events in a given (m_{jj}, y^*) bin, which can be accepted by up to two jet triggers depending on the transverse momenta and pseudorapidities of the leading and sub-leading jets. Each pairing of triggers has a unique corresponding luminosity, which is used to calculate the differential cross section for that pairing. The separate cross sections from all pairings are then summed to obtain the final measurement. This strategy is described in detail in ref. [39]. It was carefully validated in the previous dijet analysis [7] using dedicated simulation samples containing a complete set of prescaled triggers, similar to those used in this measurement.

Events are required to have at least one reconstructed vertex with at least two associated well-reconstructed tracks. The vertex maximising $\sum p_{\mathrm{T}}^2$, where the sum is performed over the associated tracks, is chosen as the primary vertex. Quality criteria are applied to reject events with jets from beam-induced background due to proton losses upstream of the interaction point, cosmic-ray air showers overlapping with collision events and calorimeter noise from large-scale coherent noise or isolated pathological cells. These jet cleaning criteria are described in ref. [40].

6 Jet energy calibration and resolution

6.1 Jet reconstruction

The input objects to the jet algorithm are three-dimensional topological clusters (topoclusters) [41, 42] built from the energy deposits in calorimeter cells. A calibration is applied to the clusters to give the correct response for the energy deposited in electromagnetic showers,

JHEP05(2018)195

while it does not correct for the lower response to hadronic showers. The four-momentum of a jet is defined as the sum of the four-momenta of its clusters in the calorimeter, treating each cluster as a four-momentum with zero mass.

6.2 Jet energy calibration

Jets in data and simulation are calibrated following the procedure described in ref. [43]. The four-momenta of the jets are recalculated to originate from the hard-scatter vertex rather than from the centre of the detector. The jet energy is corrected for the effect of pile-up in both the collision data and simulated events using the methods described in ref. [44]. In addition, a jet energy- and η-dependent correction is applied to reconstructed jets in data and Monte Carlo (MC) simulation. It is derived from MC simulation and is designed to lead to agreement in energy and direction between reconstructed jets and particle jets on average. Further corrections are applied sequentially (Global Sequential Calibration [45]) using five jet substructure variables to reduce effects from fluctuations in the flavour composition of particles forming the jets and fluctuations in the hadronic shower caused by interactions of the hadrons with dead material in the calorimeter. Differences in energy response between data and simulation are evaluated using in situ techniques, where the p_{T} of the jet to be calibrated is balanced against well-measured objects. The full jet energy scale (JES) calibration procedure and its associated systematic uncertainties are described in more detail in the following.

Pile-up correction: jets are corrected for the contributions from additional proton-proton interactions within the same (in-time) or nearby (out-of-time) bunch crossings [44]. First, a correction based on the jet area and the average transverse energy density of the event is derived [46]. The jet area is a measure of the susceptibility of the jet to pile-up and is determined jet by jet, while the average energy density serves as a measure of the pile-up activity and is calculated event by event with k_t-jets with a radius parameter value of $R = 0.4$. After this correction, some dependence of the average jet p_{T} on pile-up activity remains. An additional correction is therefore derived by comparing reconstructed calorimeter jets to particle jets in simulated inclusive jet events. The correction is parameterised as a function of the mean number of interactions per bunch crossing, μ, and the number of reconstructed primary vertices in the event, N_{PV}, such that both the out-of-time and in-time effects are taken into account.

The correction for contributions from additional proton-proton interactions can also remove part of the soft-physics contributions to the jet energy, e.g. that from the underlying event. This contribution is restored on average by the MC-based jet energy scale correction discussed below.

Jet energy scale: this calibration is derived as a function of the energy and pseudorapidity of the jet using simulated samples of inclusive jet events. The jet energy and pseudorapidity are corrected for instrumental effects (non-compensating calorimeter response, energy losses in dead material and out-of-cone effects) so that they agree on average with the energy and direction of the matching particle jet.

JHEP05(2018)195

Global sequential calibration: the topology of the energy deposits in the calorimeter and of the tracks associated with the jets is exploited to correct for fluctuations in the jet's particle content [43, 45]. The calibration is based on the number of tracks, on the p_{T}-weighted average angular distance between the tracks and the calorimeter jet axis, on the longitudinal extent of the shower in the calorimeter and on the number of track segments in the muon spectrometer associated with the jet. This correction is performed such that the jet energy scale is unaltered on average, but the jet energy resolution is improved and the sensitivity to jet fragmentation effects such as differences between quark- or gluon-induced jets is reduced.

In situ techniques: an in situ calibration is derived to correct for remaining differences between the jet energy response in data and simulation. This correction is calculated using γ+jet, Z+jet, dijet and multijet p_{T}-balance techniques [43, 47, 48]. Up to a jet p_{T} of about 950 GeV, the p_{T} balance between a photon or a Z boson and a jet is exploited. The multijet p_{T}-balance technique calibrates high-p_{T} jets ($300 < p_{\mathrm{T}} < 2000$ GeV) recoiling against a collection of lower-p_{T} jets. Beyond 2000 GeV the response is considered constant. All these corrections are derived for the central jets, with $|\eta| < 1.2$. The relative response of all detector regions is equalised using a p_{T}-balance method exploiting dijet events (η-intercalibration) where the two leading jets are in different η-regions.

6.3 Jet energy scale uncertainties

The jet corrections are combined following the procedure described in refs. [43, 49]. The systematic and statistical uncertainties of each of the above-mentioned calibration steps contribute to the total JES uncertainty as independent systematic components.

Differences between the calorimeter responses to jets initiated by quarks or gluons and a lack of knowledge of the flavour composition of the analysed data lead to additional uncertainties. In order to reduce this contribution, Pythia 8 and Powheg+Pythia 8 Monte Carlo simulations are used to estimate the flavour composition of the sample as a function of p_{T} and rapidity. The result from Pythia 8 is taken as the nominal quark/gluon composition, and the difference between the two simulations as an estimate of the composition uncertainty.

A systematic uncertainty is also considered for the muon-segment-based correction, derived as the maximum difference in the jet response between data and MC dijet events as a function of the number of muon segments [45].

An uncertainty in the jet energy scale at high-p_{T}, for jets where in situ methods cannot be used, is derived from single-particle response measurements [50].

Four uncertainties are included to account for potential mismodelling of pile-up in the MC simulation: the number of reconstructed primary vertices, N_{PV}, the average number of interactions per bunch crossing, μ, the energy density in jets and the residual dependence of the jet p_{T} on pile-up. The description and evaluation of the pile-up uncertainties are described in detail in refs. [43, 44].

The measurements presented in this paper use the most detailed description of the systematic uncertainties considered in ATLAS. There are, in total, 76 independent sources

JHEP05(2018)195

of systematic uncertainty treated as being uncorrelated among each other [43]. All of these are treated as being fully correlated across p_{T} and η, with the exception of the statistical uncertainty of the η-intercalibration which is propagated as being uncorrelated between the 245 different η and p_{T} bins in which it was derived [43, 47]. The JES uncertainty is 1% in the $200 - 600\,\mathrm{GeV}$ range of jet p_{T}, 2% at 2 TeV, and reaches 3% above 3 TeV. The uncertainty is fairly constant as a function of η and reaches 2.5% at 80 GeV for the most forward jets [43].

6.4 Jet energy resolution and its uncertainties

The fractional uncertainty in the jet p_{T} resolution (JER) is derived using the data collected during 2012. It is obtained in situ from the standard deviation of the ratio of the p_{T} of a jet to the p_{T} of other well-measured objects (a photon or a Z boson [47, 48]) in an event, following techniques similar to those used to determine the JES uncertainty. The p_{T}-balance technique in dijet events (η-intercalibration) [47] allows a measurement of the JER at high jet rapidities and for a wide range of transverse momenta. Noise from the calorimeter electronics and pile-up forms a significant component of the JER at low p_{T}. A study in zero-bias data[5] allows this contribution to be constrained. In addition, a MC simulation is used in each in situ JER to correct for fluctuations present at particle level due to the underlying event and out-of-cone contributions from QCD radiation and hadronisation. The results from all these methods are combined in a way similar to that for the JES [49].

The JER uncertainty has in total 11 components. Eight of these components are obtained by combining the systematic uncertainties associated to the in situ methods. One component is the uncertainty due to the electronic and pile-up noise measurement. Another is the absolute JER difference between data and MC simulation as determined with the in situ methods. Finally, the JER uncertainties are completed with an extra component to account for the differences between the 2012 and 2015 data-taking conditions [51]. Each JER systematic component describes an uncertainty that is taken to be fully correlated in jet p_{T} and η. The 11 JER components are treated as fully uncorrelated with each other.

6.5 Jet angular resolution and its uncertainties

The jet angular resolution (JAR) is estimated in MC simulation from the differences in rapidity and azimuthal angle between reconstructed jets and matching particle jets. This estimate is validated by comparing the standard jets built from calorimeter energy deposits to those built from tracks in the inner detector [41, 52]. From these studies, the JAR is assigned an uncertainty of 10% to account for possible differences between data and MC simulation.

[5]The zero-bias sample contains data collected by recording events exactly one accelerator turn after a high p_{T} first-level calorimeter trigger. These events will thus be contained in a random filled bunch collision with a rate proportional to the instantaneous luminosity [49].

JHEP05(2018)195

7 Unfolding of detector effects

The reconstructed jet spectra in data are corrected for detector inefficiencies and resolution effects to obtain inclusive jet and dijet cross-sections that refer to the stable particles entering the detector. The unfolding of the detector resolution in jet p_{T} is based on a modified Bayesian technique, the iterative dynamically stabilised (IDS) method [53]. This unfolding method uses a transfer matrix constructed using samples of simulated events, which describes the migrations of jets (events) across p_{T} (m_{jj}) bins between particle level jets and reconstructed level jets. For the inclusive jet measurement, the transfer matrix is filled jet by jet by matching a particle jet with a reconstruction level jet, when both are closer to each other than to any other jet, lie within a radius of $R = 0.3$, have $p_{\mathrm{T}} > 75\,\mathrm{GeV}$ and belong to the same rapidity bin. For the dijet case, the transfer matrix is filled event by event with those events that lie in the same y^* bin and pass the selection requirements at both the reconstruction and the particle levels.

The unfolding technique is performed in three steps, correcting for the matching impurity at the reconstruction level, the smearing of matched jets (events) between p_{T} (m_{jj}) bins, and the matching inefficiency at the particle level,

$$N_i^{\mathrm{part}} = \sum_k N_k^{\mathrm{reco}} \cdot \mathcal{P}_k \cdot \mathcal{U}_{ik} \,/\, \mathcal{E}_i \,,$$

where i and k are the p_{T} (m_{jj}) bin indices of the jets (events) at the particle and reconstruction levels and N^{part} and N^{reco} are the numbers of particle level and reconstruction level jets (events) in a given bin. The symbols $\mathcal{P}$ and $\mathcal{E}$ denote respectively the matching purity and the matching efficiency. The symbol $\mathcal{U}$ denotes the unfolding matrix, where $\mathcal{U}_{ik}$ describes the probability for a jet (event) at reconstruction level in p_{T} (m_{jj}) bin k to originate from the particle level in p_{T} (m_{jj}) bin i.

For the inclusive jet cross-section measurements, the matching purity, $\mathcal{P}_k$, is defined as the fraction of reconstruction level jets that are matched to a particle level jet for a given p_{T} bin k. The matching efficiency, $\mathcal{E}_i$, is defined as the fraction of particle level jets that are matched to a reconstruction level jet for a given p_{T} bin i. If matched particle and reconstructed jets are in different rapidity bins then they are reassigned as being unmatched. For dijets, the efficiency (purity) is defined as the fraction of events passing the selection cuts at the particle (reconstruction) level for a given y^* bin that also pass the selection cuts and lie in the same y^* bin at the reconstruction (particle) level. In this way the migrations across jet $|y|$ and dijet y^* bins are effectively taken into account by bin-to-bin corrections. The jet matching efficiency is 98% (96%) at $p_{\mathrm{T}} = 100\,\mathrm{GeV}$ for low (high) jet rapidity, and reaches 99.7% at high p_{T}. The event dijet efficiency is 97% (85%) at $m_{jj} = 300\,\mathrm{GeV}$ ($m_{jj} = 1700\,\mathrm{GeV}$) for low (high) y^*, and reaches 99.7% at the highest dijet mass.

The unfolding matrix $\mathcal{U}$ depends on the details of the MC model, given that the transfer matrix is used to build it. This model improves when iterated, where the number of iterations is chosen such that the residual bias is within a tolerance of 1% in the bins with less than 10% statistical uncertainty. The residual bias is evaluated through a data-driven

JHEP05(2018)195

closure test [53, 54], in which the particle level spectrum in the MC simulation is reweighted to improve agreement between data and reweighted MC events in the reconstruction level spectra. The ratio of the spectra unfolded with reweighted and nominal MC simulation provides an estimate of the unfolding bias. In these measurements only one iteration is used, achieving an uncertainty bias of the order of a few per mille, except at high p_{T} ($\sim 1\,\mathrm{TeV}$) and high rapidity where it increases to 5%.

8 Propagation of the uncertainties to the cross-sections

The statistical uncertainties are propagated through the unfolding procedure using an ensemble of 1000 pseudo-experiments. Each pseudo-experiment is constructed by reweighting each event in data and simulation according to a Poisson distribution with expectation value equal to one. This procedure preserves the correlations between jets produced in the same event. The unfolding is performed for each pseudo-experiment and a covariance matrix is constructed for the cross-section in each $|y|$ or y^* bin. The total statistical uncertainty is obtained from the covariance matrix, where bin-to-bin correlations are also encoded. The separate contributions from the data and from the MC statistics are obtained from the same procedure by reweighting either the data or the simulated events.

All components of the JES uncertainty (see section 6) are propagated through the unfolding procedure using pseudo-data (MC simulations) to avoid the impact of the larger statistical fluctuations in data. The jet p_{T} in pseudo-data is scaled up and down by one standard deviation of each component. This procedure takes into account the correlations between various phase-space regions. The resulting pseudo-data spectra are unfolded for detector effects using the nominal unfolding matrix. The difference between the nominal unfolded cross-section and the systematically shifted unfolded cross-section is taken as a systematic uncertainty. The jet energy scale is the dominant uncertainty for $p_{\mathrm{T}} < 2500\,\mathrm{GeV}$ ($p_{\mathrm{T}} < 700\,\mathrm{GeV}$) in the first (last) rapidity bin for the inclusive jet measurement, and for $m_{jj} < 4000\,\mathrm{GeV}$ in the first y^* bin for the dijet mass measurement. In the complementary regions, including the whole m_{jj} range for the last y^* bin, the dominant source of uncertainty is the limited size of the sample.

The uncertainty in the JER is the second largest individual source of systematic uncertainty. There are 11 components, some of which can involve a JER degradation in part of $p_{\mathrm{T}} - \eta$ phase-space and a JER improvement in the complementary part, which allows (anti-)correlations to be accounted for. The effect of each of the components is evaluated by smearing the energy of the reconstructed jets. The degradation of the JER is achieved by smearing the reconstructed jets in the relevant phase space region in the MC simulation used as pseudo-data. On the other hand, an effective improvement of the JER is achieved by smearing the energy of the jets in the MC simulation used in constructing the transfer matrix. The difference between the modified spectrum unfolded with the systematically varied transfer matrix to the nominal spectrum unfolded with the nominal transfer matrix is taken as a systematic uncertainty.

An uncertainty for the jet cleaning procedure described in section 5 is estimated by measuring in situ the jet selection efficiency.

JHEP05(2018)195

The uncertainty in the luminosity measurement of 2.1% is propagated as being correlated across all measurement bins.

An uncertainty in the beam energy of 0.1% [55] is considered when comparing data with the theory prediction at a fixed beam energy. The induced uncertainty at the cross-section level is evaluated by comparing the theory predictions at the nominal and shifted beam energies. For the inclusive jet measurement, it amounts for 0.2% at low p_{T} and 0.9% at high p_{T} in the central region and rises to 2% at the highest p_{T} and high rapidity. In the dijet measurement, this uncertainty is 0.2% at low m_{jj} and 0.8% at high m_{jj} in the first y^* bin and reaches 1% at the highest m_{jj} and in the last y^* bin.

In order to assess the statistical precision of the systematic uncertainty estimates, each component is re-evaluated using a set of pseudo-experiments. The statistical fluctuations of the systematic uncertainty estimates are minimised using a smoothing procedure. To achieve this, for each component, the p_{T} (m_{jj}) bins are combined until the propagated uncertainty value in the bin has a Gaussian statistical significance larger than two standard deviations. A Gaussian kernel smoothing [52] is used to obtain the values in the original fine bins.

Figure 1 shows the individual components of the systematic uncertainties added in quadrature for the inclusive jet and dijet cross-section measurements in representative phase-space regions. In the central (forward) region the total uncertainty in the inclusive jet measurement is about 5% (8%) at medium p_{T} of 300–600 GeV. The uncertainty increases towards both lower and higher pT reaching 6% (10%) at low p_{T} and 30% ([-45%,+40%]) at high p_{T}.

The total uncertainty in the dijet measurement is about 5% (10%) at medium m_{jj} of 500–1000 GeV (2000–3000 GeV) in the first (last) y^* bin. The uncertainty increases towards both lower and higher m_{jj} reaching 6% at low m_{jj} and 30% at high m_{jj} in the first y^* bin. In the last y^* bin no significant dependence on m_{jj} is observed.

9 Theoretical predictions

Theoretical predictions of the cross-sections are obtained using NLO and NNLO pQCD calculations with corrections for non-perturbative and electroweak effects.

9.1 Next-to-leading-order pQCD calculations

The NLO pQCD predictions are calculated using NLOJET++ 4.1.3 [56] interfaced to APPLGRID [57] for fast and flexible calculations with various PDF sets and various values of the renormalisation and factorisation scales. The inclusive jet cross-section prediction is calculated using $p_{\mathrm{T}}^{\mathrm{max}}$, the transverse momentum of the leading jet in the event, as the renormalisation scale, μ_{R}, and the factorisation scale, μ_{F}. An alternative scale choice, $\mu_{\mathrm{R}} = \mu_{\mathrm{F}} = p_{\mathrm{T}}^{\mathrm{jet}}$, the p_{T} of each individual jet that enters the cross-section calculation, is also considered. This scale choice is proposed in ref. [58]. Both scale choices were used in the previous ATLAS analysis at $\sqrt{s} = 8$ TeV [11]. For the dijet cross-section calculation the scale choice is $\mu_{\mathrm{R}} = \mu_{\mathrm{F}} = p_{\mathrm{T}}^{\mathrm{max}} \exp(0.3y^*)$, as suggested in ref. [59] and previously used in the ATLAS dijet analysis at 7 TeV [7]. The predictions are calculated using several PDFs

JHEP05(2018)195

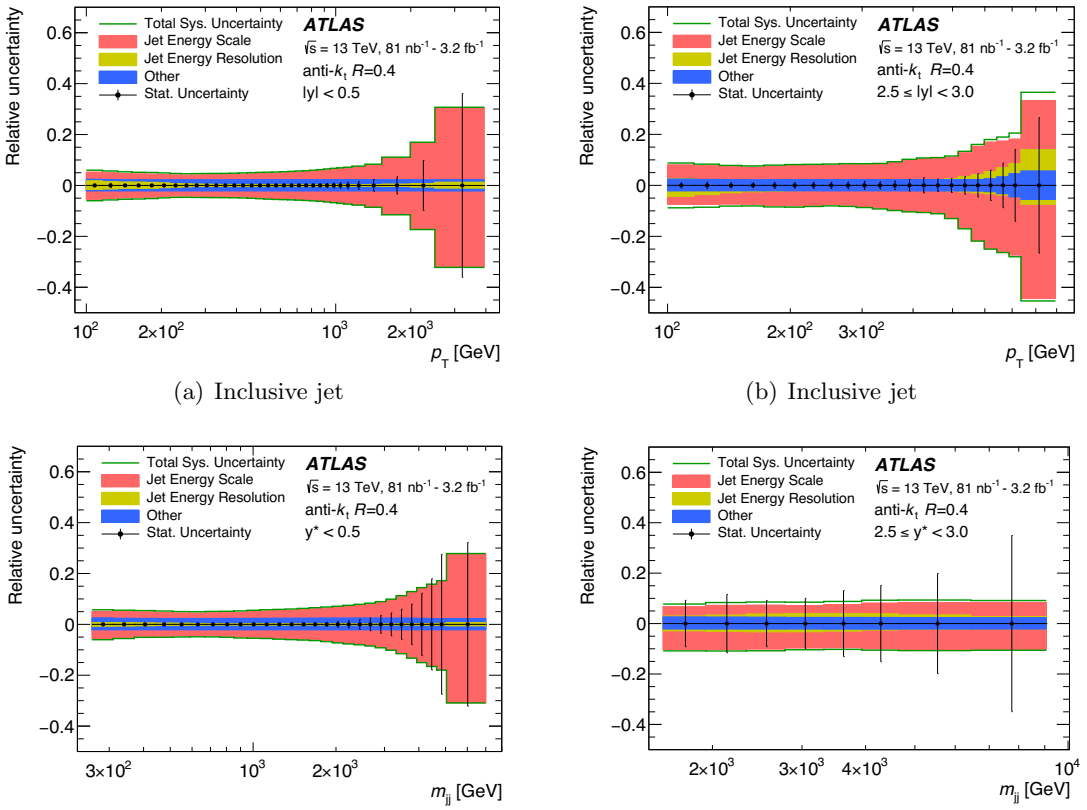

(a) Inclusive jet

(b) Inclusive jet

(c) Dijet

(d) Dijet

Figure 1. Relative systematic uncertainty for the inclusive jet cross-section as a function of the jet p_{T} for the first and last rapidity bins ((a) and (b) respectively) and for the dijet cross-section as a function of m_{jj} for the first and last y^* bins ((c) and (d) respectively). The individual uncertainties are shown in different colours: the jet energy scale, jet energy resolution and the other uncertainties (jet cleaning, luminosity and unfolding bias). The total systematic uncertainty, calculated by adding the individual uncertainties in quadrature, is shown as a green line. The statistical uncertainty is shown as vertical black lines.

provided by the LHAPDF6 [60] library: the NLO CT14 [61], MMHT 2014 [62], NNPDF 3.0 [63], and HERAPDF 2.0 [64] sets, and the NNLO ABMP16 [65] set. The value of the strong coupling constant, α_{s}, is taken from the corresponding PDF set.

The main uncertainties in the NLO predictions come from uncertainties associated with the PDFs, the choice of renormalisation and factorisation scales, and the uncertainty in the value of α_{s}. PDF uncertainties are defined at the 68% CL and propagated through the calculations following the prescription given for each PDF set, as recommended by the PDF4LHC group for PDF-sensitive analyses [66]. Calculations are redone with varied renormalisation and factorisation scales to estimate the uncertainty due to missing higher-order terms in the pQCD expansion. The nominal scales are independently varied up or down by a factor of two in both directions excluding opposite variations of μ_{R} and μ_{F}. The envelope of resulting variations of the prediction is taken as the scale uncertainty. The difference between the predictions obtained with the $p_{\mathrm{T}}^{\mathrm{max}}$ and the $p_{\mathrm{T}}^{\mathrm{jet}}$ scale choice is

JHEP05(2018)195

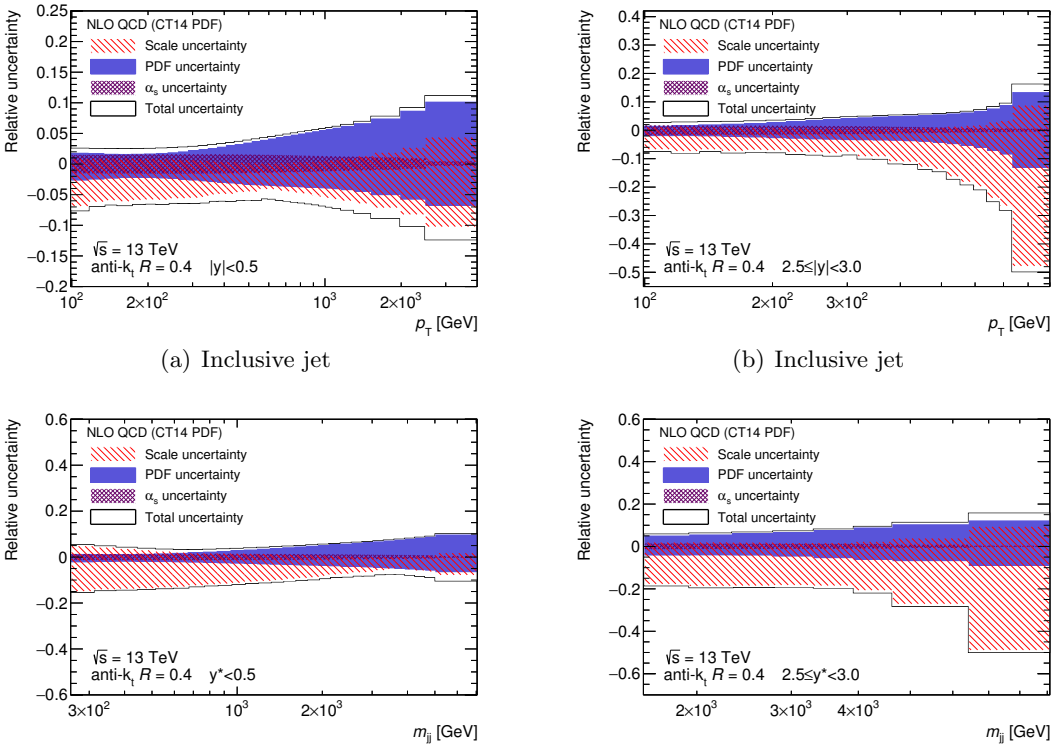

(a) Inclusive jet (b) Inclusive jet

(c) Dijet (d) Dijet

Figure 2. Relative NLO QCD uncertainties in the jet cross-sections calculated using the CT14 PDF set. Panels a,b (c,d) correspond respectively to the first and last $|y|$ (y^*) bins for the inclusive jet (dijet) measurement. The uncertainties due to the renormalisation and factorisation scale, the α_s, the PDF and the total uncertainty are shown. The total uncertainty, calculated by adding the individual uncertainties in quadrature, is shown as a black line.

treated as an additional uncertainty. The uncertainty from α_s is evaluated by calculating the cross-sections using two PDF sets that differ only in the value of α_s used and then scaling the cross-section difference corresponding to an α_s uncertainty $\Delta\alpha_s = 0.0015$ as recommended in ref. [66].

The uncertainties in the NLO QCD cross-section predictions obtained with the CT14 PDF set are shown in figure 2 for representative phase-space regions. The uncertainty due to the choice of renormalisation and factorisation scale is dominant in most phase-space regions, rising from 10% (20%) at about $p_T = 100$ GeV ($m_{jj} = 300$ GeV) in the central rapidity (y^*) bin to about 50% in the highest p_T (m_{jj}) bins in the most forward rapidity (large y^*) region. The PDF uncertainties vary from 2% to 12% depending on the jet p_T and rapidity (m_{jj} and y^*). The contribution from the α_s uncertainty is about 2% at low p_T (m_{jj}) and negligible for the highest p_T (m_{jj}) bin in each rapidity (y^*) range.

9.2 Non-perturbative corrections

Non-perturbative corrections are applied to the parton-level cross-sections from the NLO pQCD calculations. The correction factors are calculated using LO MC event generators, as

JHEP05(2018)195

	CTEQ6L1 [67]	CTEQ6L1 [67]	MSTW2008LO [68]	CT10	NNPDF2.3LO	NNPDF2.3LO	CTEQ6L1 [67]
Pythia 8	4C [69]	AU2 [70]	A14 [30]	AU2 [70]	MONASH [71]	A14 [30]	A14 [30]
Herwig++	UE-EE-5 [72, 73]	UE-EE-4 [72, 73]	UE-EE-5 [72, 73]				

Table 1. Summary of the soft-physics model tunes used for the evaluation of the non-perturbative corrections for each event generator and PDF set.

the bin-by-bin ratio of the nominal particle-level MC cross-sections to the MC cross-section derived from the partons remaining after showering, when the modelling of hadronisation and the underlying event are switched off. The correction factors are evaluated using several event generators and tunes, which are listed in table 1. The baseline correction is taken from Pythia 8 using the A14 tune with the NNPDF2.3 LO PDF set. The envelope of all corrections is considered as a systematic uncertainty.

The correction factors for a set of representative event generators and tunes for the inclusive jet (dijet) cross-section are shown in figure 3 in illustrative $|y|$ (y^*) bins as a function of p_{T} (m_{jj}). The values of the correction are in the range 0.92-1.03 at low p_{T} and 0.98-0.99 (0.97-1.01) at high p_{T} for the first (last) rapidity bin in the inclusive jet measurement, and 0.94-1.01 (0.98-0.99) at low (high) m_{jj} for the first y^* bin. For the last y^* bin in the dijet measurement, a fixed range 0.92-1.07 is conservatively taken for all m_{jj} bins due to lack of statistical precision at large m_{jj}.

9.3 Electroweak corrections

The NLO pQCD predictions are corrected for the effects of γ and $W^{\pm}/Z$ interactions at tree and one-loop level. They are derived using an NLO calculation of electroweak (EW) contributions to the LO pQCD process. The correction is defined as the ratio of a $2 \to 2$ calculation including tree-level effects of order α_{s}^2, α^2, and $\alpha_{\mathrm{s}}\alpha$ (from interference of QCD and EW diagrams), plus weak loop corrections of order $\alpha_{\mathrm{s}}^2\alpha$ to the LO QCD $2 \to 2$ calculation.

The correction factors are derived in the phase space considered for the measurements presented here and were provided by the authors of ref. [74]. No uncertainty associated with these corrections is presently estimated.

The electroweak correction factors for the inclusive jet (dijet) cross-section as a function of the jet p_{T} (event m_{jj}) in bins of $|y|$ (y^*) are shown in figure 4. The electroweak correction is small for low jet transverse momenta and for low m_{jj}. The correction reaches 8% at the highest p_{T} (3 TeV) for the central $|y|$ bin and is less than 4% for the rest of the $|y|$ bins. For dijets, the electroweak correction reaches 11% at $m_{jj} = 7$ TeV for the central y^* bin. For the rest of the y^* bins the correction is less than 3%.

9.4 Next-to-next-to-leading-order pQCD calculations

The NNLO pQCD predictions were provided by the authors of refs. [17, 18] using the NNLOJET program and the MMHT 2014 NNLO PDF set for two different choices of the μ_{R} and μ_{F} scales, respectively $p_{\mathrm{T}}^{\mathrm{jet}}$ and $p_{\mathrm{T}}^{\mathrm{max}}$. The non-perturbative and electroweak corrections described in sections 9.2 and 9.3, respectively, are applied to the predictions.

JHEP05(2018)195

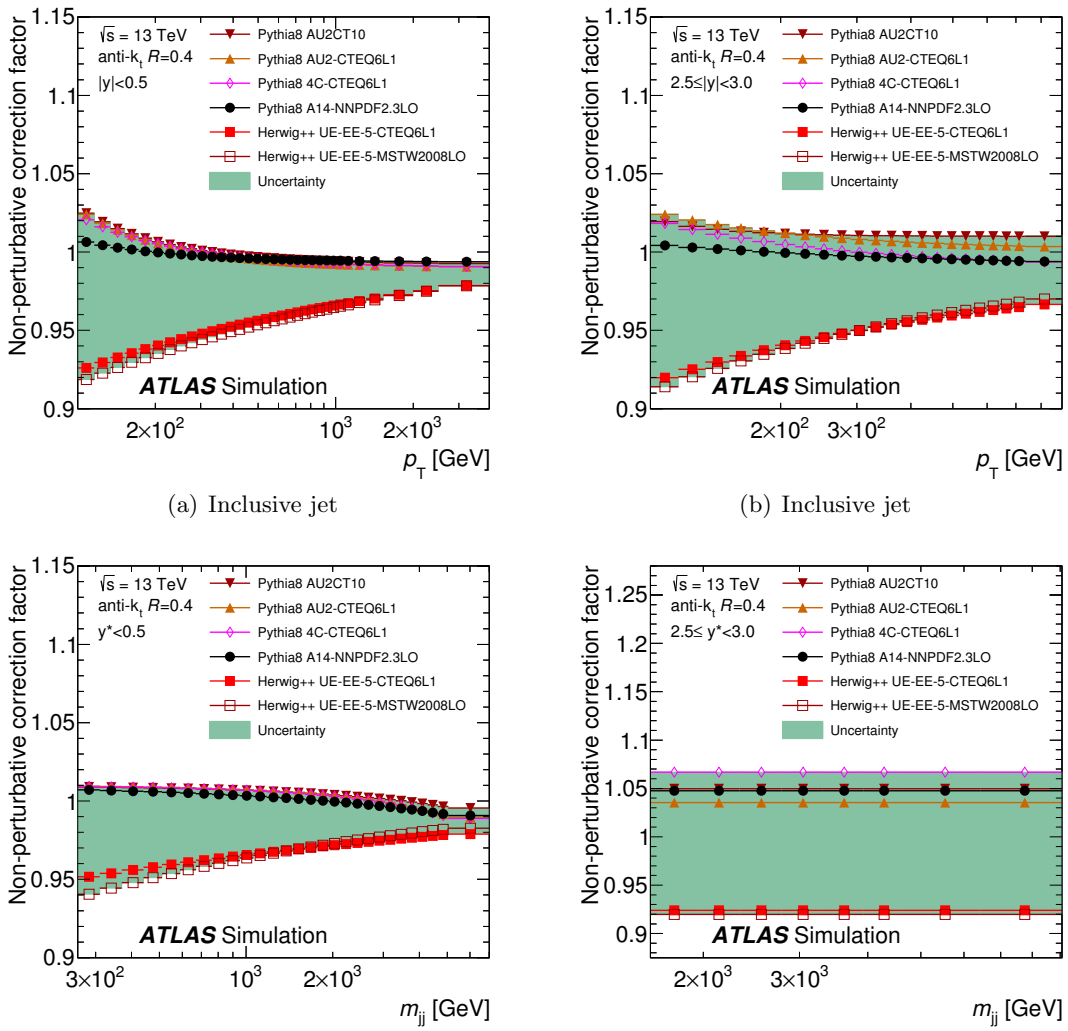

(a) Inclusive jet

(b) Inclusive jet

(c) Dijet

(d) Dijet

Figure 3. Non-perturbative correction factors for the (inclusive jet, dijet) NLO pQCD prediction as a function of (jet p_T, m_{jj}) for ((a), (c)) the first (rapidity, y^*) bin and for ((b), (d)) the last (rapidity, y^*) bin. The corrections are derived using Pythia 8 with the A14 tune with the NNPDF2.3 LO PDF set. The envelope of all MC configuration variations is shown as a band.

In addition to the statistical uncertainties on the calculations, which are larger for higher p_T and high rapidities, two sources of uncertainty are considered in this NNLO calculation: the scale uncertainty and the systematic uncertainty in the non-perturbative correction. To obtain the scale uncertainty, both scales (renormalisation and factorisation) are varied simultaneously by a factor of 0.5 or 2.[6] If both variations yield changes with the same sign, the scale uncertainty is obtained from the larger change.

[6] A different approach to estimate the scale uncertainty was used for NNLO due to computing time limitations. At NLO the simultaneous variations are not always the dominant ones, although they are at high p_T.

JHEP05(2018)195

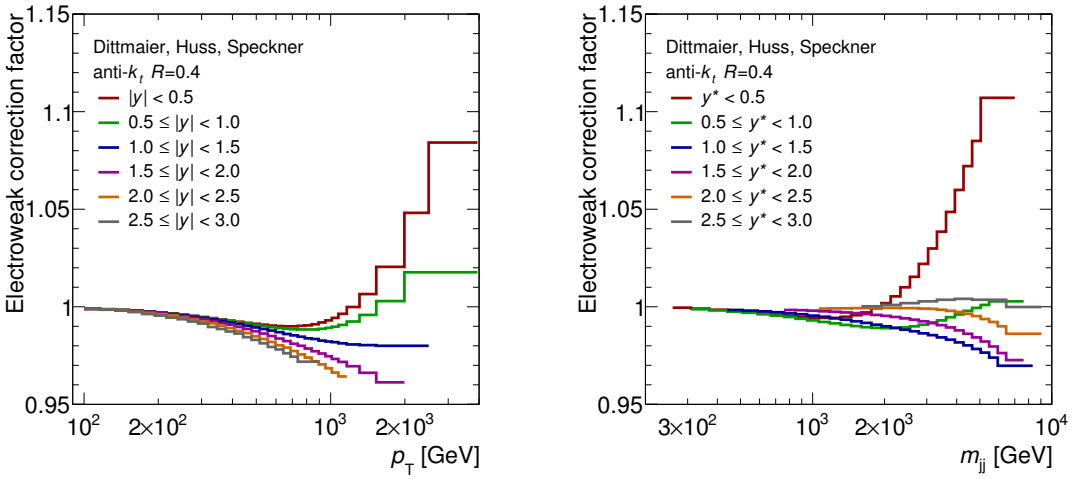

Figure 4. Electroweak correction factors for the inclusive jet (dijet) cross-section as a function of the jet p_T (m_{jj}) for all $|y|$ (y^*) bins.

10 Results

The measured double-differential inclusive jet cross-sections are shown in figure 5 as a function of p_T for the six jet rapidity bins, and the measured double-differential dijet cross-sections are shown in figure 6 as a function of m_{jj} for the six y^* bins. The measurements respectively cover the jet p_T range from 100 GeV to 3.5 TeV for $|y| < 3.0$, and the m_{jj} range from 300 GeV to 9 TeV for $y^* < 3.0$, thus attaining a significantly higher reach than the previous ATLAS measurements [11, 75, 76]. The NLO pQCD predictions using the CT14 PDF set corrected for non-perturbative and electroweak effects are also shown in both figures.

The ratios of the NLO pQCD predictions to the measured inclusive jet cross-sections as a function of p_T in the six jet rapidity bins are shown in figure 7 (figure 8) for the CT14, MMHT 2014 and NNPDF 3.0 (CT14, ABMP16 and HERAPDF 2.0) PDF sets. The CT14 case is repeated in both figures to serve as a reference for comparison. No significant deviation of the data points from the predictions is seen; the NLO pQCD predictions and data agree within uncertainties. This behaviour is compatible with the results of the comparison between data and the pQCD predictions in the previous ATLAS measurement at $\sqrt{s} = 8$ TeV [11]. In the forward region ($|y| > 2$) there is a tendency for the NLO pQCD prediction using the CT14, MMHT 2014 and NNPDF 3.0 PDF sets to overestimate the measured cross-section in the high p_T range, although the difference from data does not exceed the range covered by the experimental and theoretical uncertainties.

The ratios of the NLO pQCD predictions to the measured dijet cross-sections as a function of m_{jj} in the six y^* bins are shown in figures 9 and 10. No significant deviation of the data points from the predictions is seen, the NLO pQCD predictions and data agree within uncertainties.

The ratios of the NNLO pQCD predictions to the measured inclusive jet cross-sections as a function of p_T in the six jet rapidity bins are shown in figures 11 and 12 for the

JHEP05(2018)195

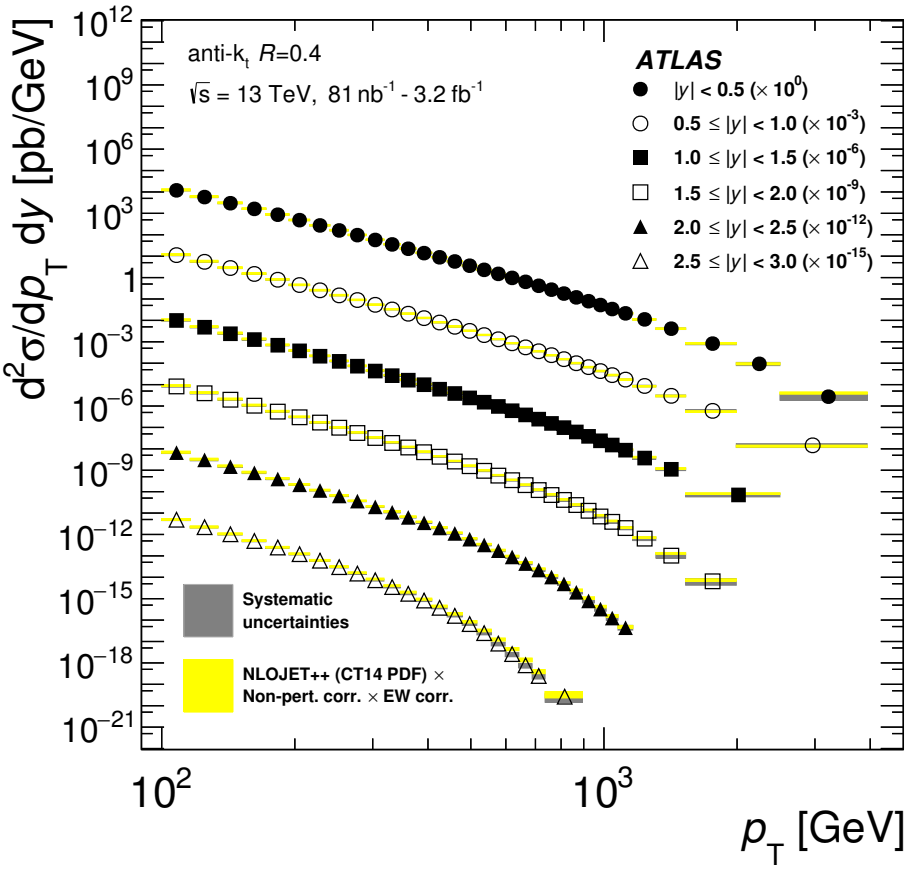

Figure 5. Inclusive jet cross-sections as a function of p_{T} and $|y|$, for anti-k_t jets with $R = 0.4$. The statistical uncertainties are smaller than the size of the symbols used to plot the cross-section values. The dark gray shaded areas indicate the experimental systematic uncertainties. The data are compared to NLO pQCD predictions calculated using NLOJET++ with $p_{\mathrm{T}}^{\mathrm{max}}$ as the QCD scale and the CT14 NLO PDF set, to which non-perturbative and electroweak corrections are applied. The light gray (yellow in the online version) shaded areas indicate the predictions with their uncertainties. At low and intermediate p_{T} bins the experimental systematic uncertainties are comparable to the theory uncertainties (drawn on top) and therefore are barely visible.

two different scale choices, respectively $p_{\mathrm{T}}^{\mathrm{jet}}$ and $p_{\mathrm{T}}^{\mathrm{max}}$, together with the NLO case for comparison. When using $p_{\mathrm{T}}^{\mathrm{jet}}$ as a scale, the NNLO pQCD predictions describe the data within uncertainties, with the exception of the forward ($|y| > 2$) high p_{T} range where it tends to overestimate the measured cross-section. The predictions using $p_{\mathrm{T}}^{\mathrm{max}}$ as the scale overestimate the measured cross-section.

The NLO pQCD predictions, corrected for non-perturbative and electroweak effects, are quantitatively compared to the measurement using the method described in ref. [76]. The χ^2 value and the corresponding observed p-value, P_{obs}, are computed taking into account the asymmetries and the (anti-)correlations of the experimental and theoretical uncertainties. The individual experimental and theoretical uncertainty components are assumed to be uncorrelated among each other and fully correlated across the p_{T} and $|y|$

JHEP05(2018)195

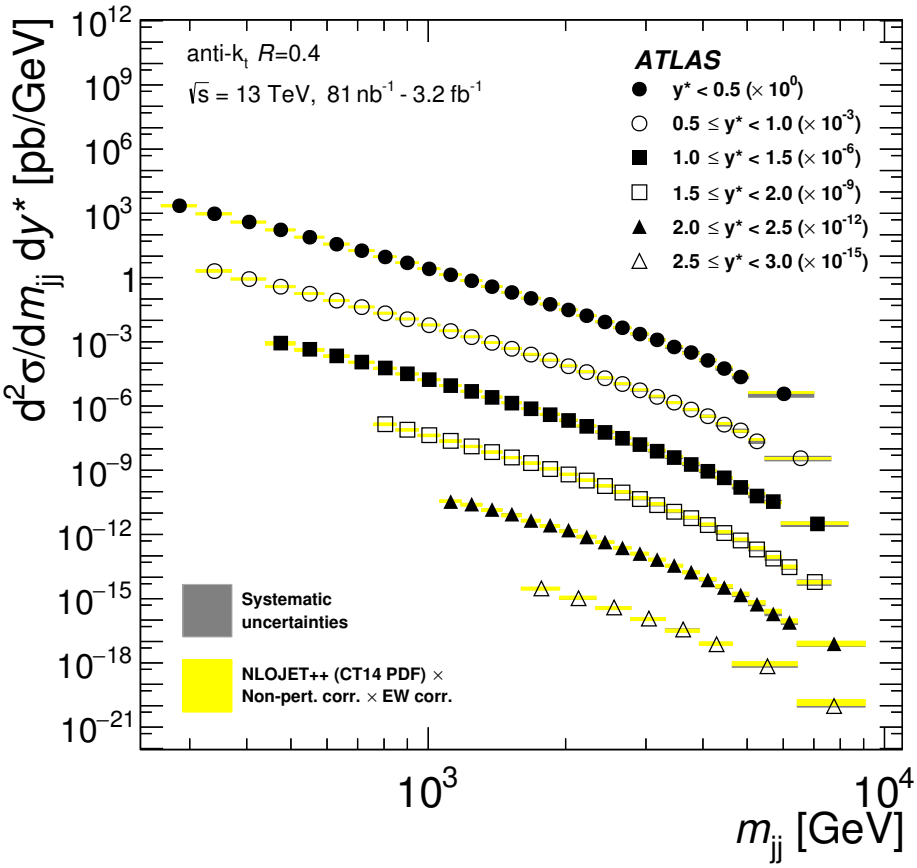

Figure 6. Dijet cross-sections as a function of m_{jj} and y^*, for anti-k_t jets with $R = 0.4$. The statistical uncertainties are smaller than the size of the symbols used to plot the cross-section values. The dark gray shaded areas indicate the experimental systematic uncertainties. The data are compared to NLO pQCD predictions calculated using NLOJET++ with $p_{\mathrm{T}}^{\mathrm{max}} \exp(0.3y^*)$ as the QCD scale and the CT14 NLO PDF set, to which non-perturbative and electroweak corrections are applied. The light gray (yellow in the online version) shaded areas indicate the predictions with their uncertainties. In most m_{jj} bins the experimental systematic uncertainty is smaller than the theory uncertainties and is therefore not visible.

(m_{jj} and y^* for dijets) bins. The correlations of the statistical uncertainties across different phase-space regions are taken into account using covariance matrices derived from 1000 pseudo-experiments obtained by fluctuating the data and the MC simulation (see section 8).

For the theoretical prediction and separately for each scale choice ($p_{\mathrm{T}}^{\mathrm{max}}$ and $p_{\mathrm{T}}^{\mathrm{jet}}$), the uncertainties related to the scale variations, the PDF eigenvectors, the non-perturbative corrections and the strong coupling constant are treated as additional uncertainty components. In the case of the NNPDF 3.0 PDF set, the replicas [63] are used to evaluate a covariance matrix, from which the eigenvectors are then determined.

Table 2 shows the summary of the observed P_{obs} values for each individual rapidity bin of the inclusive jet measurement. Table 3 reports the results obtained from a global fit to all the p_{T} and rapidity bins of the measurement. Given that in this case the observed P_{obs}

JHEP05(2018)195

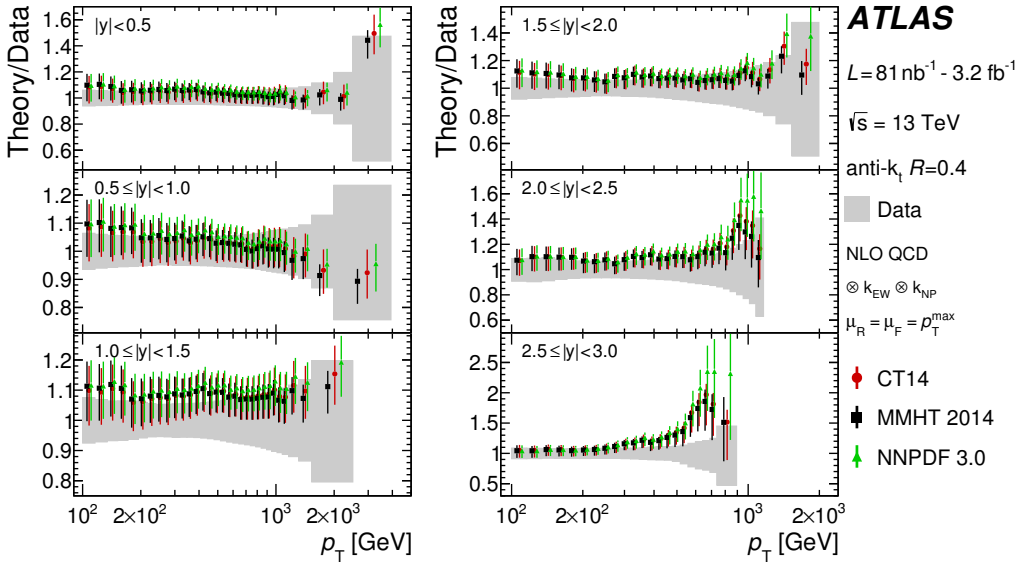

Figure 7. Comparison of the measured inclusive jet cross-sections and the NLO pQCD predictions shown as the ratios of predictions to the measured cross-sections. The ratios are shown as a function of the jet p_{T} in six $|y|$ bins for anti-k_t jets with $R = 0.4$. The predictions are calculated using NLOJET++ with three different PDF sets (CT14, MMHT 2014, NNPDF 3.0) and non-perturbative and electroweak corrections are applied. The uncertainties of the predictions, shown by the coloured lines, include all the uncertainties discussed in section 9. The grey bands show the total data uncertainty including both the systematic (JES, JER, unfolding, jet cleaning, luminosity) and statistical uncertainties.

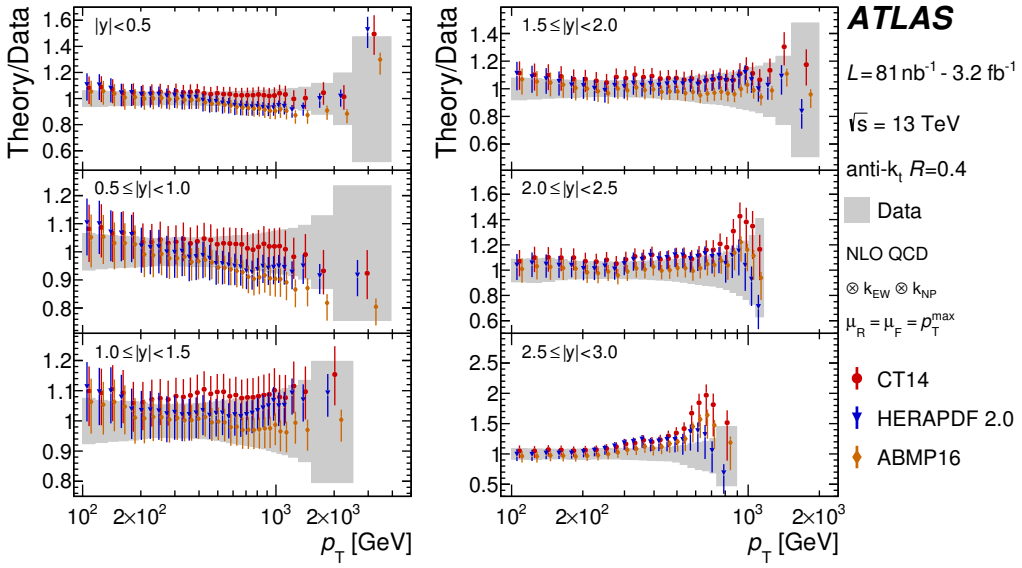

Figure 8. Comparison of the measured inclusive jet cross-sections and the NLO pQCD predictions shown as the ratios of predictions to the measured cross-sections. The ratios are shown as a function of the jet p_{T} in six $|y|$ bins for anti-k_t jets with $R = 0.4$. The predictions are calculated using NLOJET++ with three different PDF sets (CT14, HERAPDF 2.0, ABMP16) and non-perturbative and electroweak corrections are applied. The uncertainties of the predictions, shown by the coloured lines, include all the uncertainties discussed in section 9. The grey bands show the total data uncertainty including both the systematic (JES, JER, unfolding, jet cleaning, luminosity) and statistical uncertainties.

JHEP05(2018)195

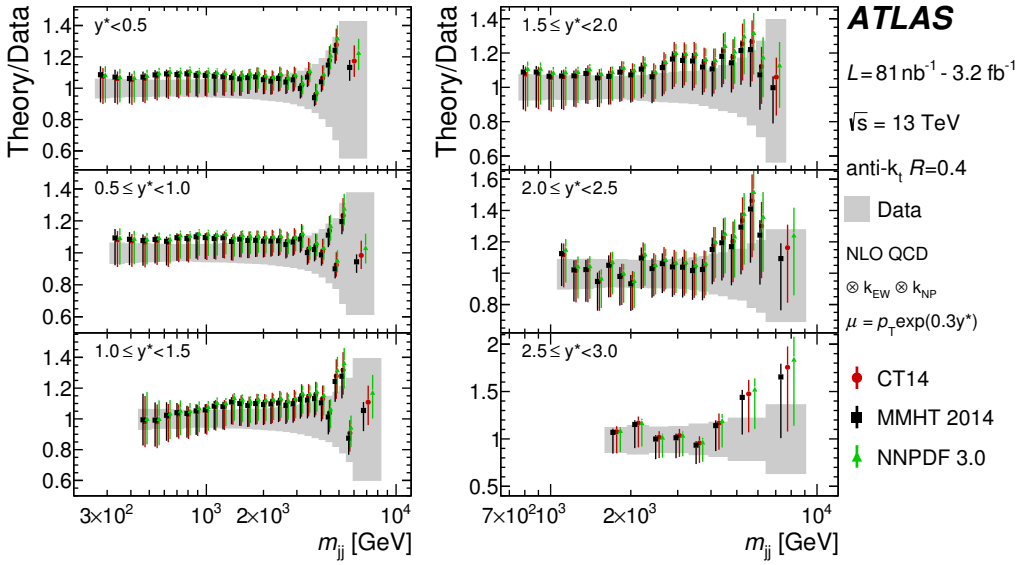

Figure 9. Comparison of the measured dijet cross-sections and the NLO pQCD predictions shown as the ratios of predictions to the measured cross-sections. The ratios are shown as a function of the jet m_{jj} in six y^* bins for anti-k_t jets with $R = 0.4$. The predictions are calculated using NLOJET++ with three different PDF sets (CT14, MMHT 2014, NNPDF 3.0) and non-perturbative and electroweak corrections are applied. The uncertainties of the predictions, shown by the coloured lines, include all the uncertainties discussed in section 9. The grey bands show the total data uncertainty including both the systematic (JES, JER, unfolding, jet cleaning, luminosity) and statistical uncertainties.

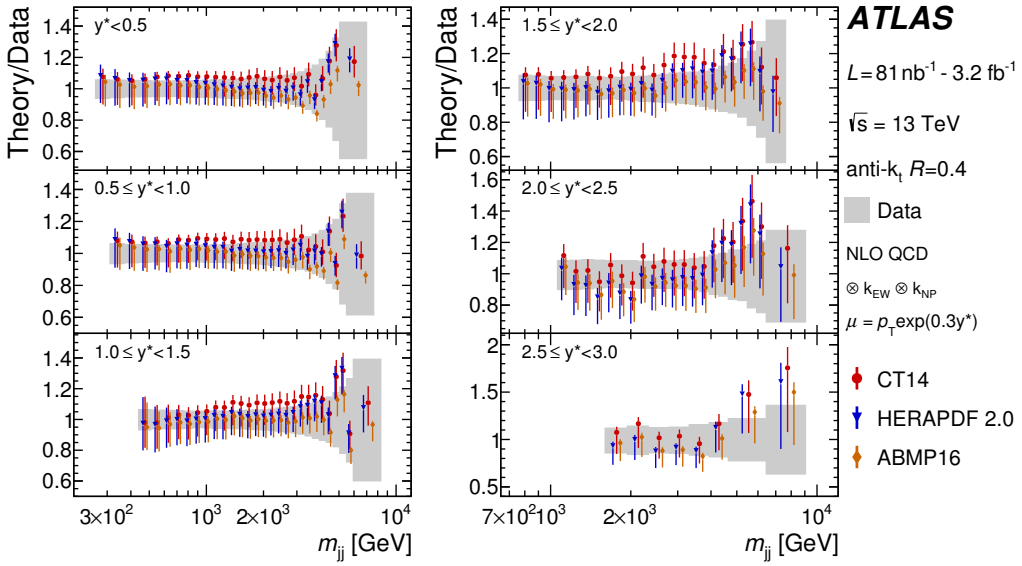

Figure 10. Comparison of the measured dijet cross-sections and the NLO pQCD predictions shown as the ratios of predictions to the measured cross-sections. The ratios are shown as a function of the jet m_{jj} in six y^* bins for anti-k_t jets with $R = 0.4$. The predictions are calculated using NLOJET++ with three different PDF sets (CT14, HERAPDF 2.0, ABMP16) and non-perturbative and electroweak corrections are applied. The uncertainties of the predictions, shown by the coloured lines, include all the uncertainties discussed in section 9. The grey bands show the total data uncertainty including both the systematic (JES, JER, unfolding, jet cleaning, luminosity) and statistical uncertainties.

JHEP05(2018)195

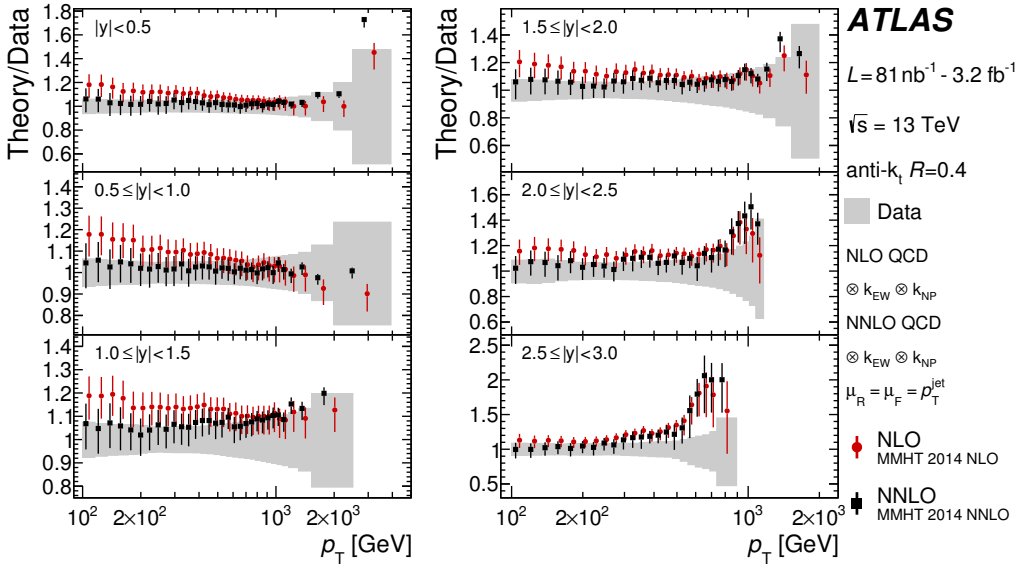

Figure 11. Ratios of the NLO and NNLO pQCD predictions to the measured inclusive jet cross-sections, shown as a function of the jet p_{T} in six $|y|$ bins for anti-k_t jets with $R = 0.4$. The NLO predictions are calculated using NLOJET++ with the MMHT 2014 NLO PDF set. The NNLO predictions are provided by the authors of refs. [17, 18] using NNLOJET with $p_{\mathrm{T}}^{\mathrm{jet}}$ as the QCD scale and the MMHT 2014 NNLO PDF set. Non-perturbative and electroweak corrections are applied to the predictions. The NLO and NNLO uncertainties are shown by the coloured lines, including all the uncertainties discussed in section 9. The grey bands show the total data uncertainty including both the systematic (JES, JER, unfolding, jet cleaning, luminosity) and statistical uncertainties.

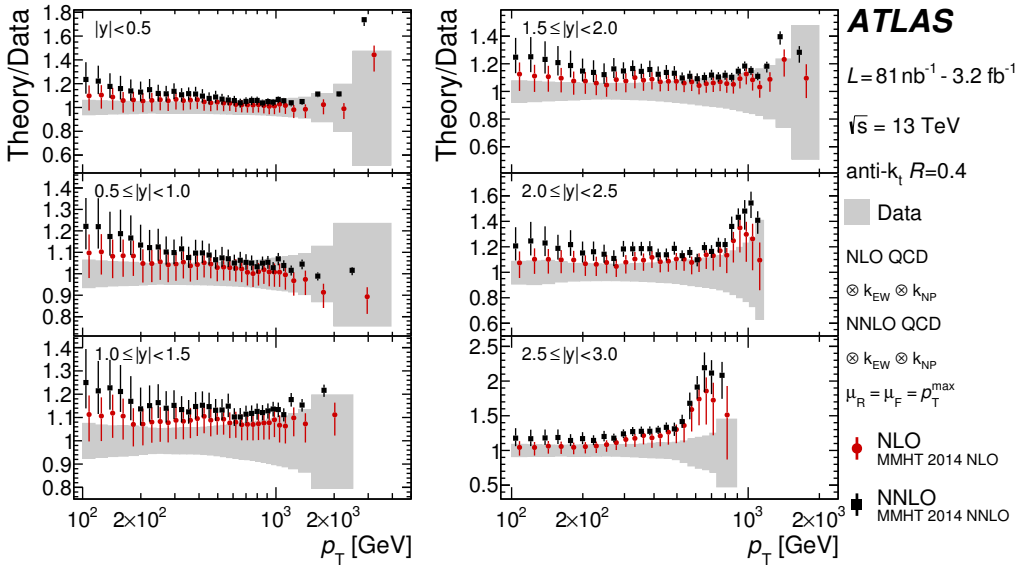

Figure 12. Ratios of the NLO and NNLO pQCD predictions to the measured inclusive jet cross-sections, shown as a function of the jet p_{T} in six $|y|$ bins for anti-k_t jets with $R = 0.4$. The NLO predictions are calculated using NLOJET++ with the MMHT 2014 NLO PDF set. The NNLO predictions are provided by the authors of refs. [17, 18] using NNLOJET with $p_{\mathrm{T}}^{\mathrm{max}}$ as the QCD scale and the MMHT 2014 NNLO PDF set. Non-perturbative and electroweak corrections are applied to the predictions. The NLO and NNLO uncertainties are shown by the coloured lines, including all the uncertainties discussed in section 9. The grey bands show the total data uncertainty including both the systematic (JES, JER, unfolding, jet cleaning, luminosity) and statistical uncertainties.

JHEP05(2018)195

values are very small, the results are presented in terms of the χ^2 per degree of freedom (dof). Table 4 shows the summary of observed P_{obs} values for each y^* bin of the dijet measurement, as well as those from a global fit using all the m_{jj} and y^* bins.

Fair agreement is seen (with p-values in the percent range) when considering jet cross-sections in individual jet rapidity or y^* bins treated independently, with some tension present in the 1.5–2.5 rapidity region. Comparable results are obtained for PDF sets determined with similar data. Strong tension between data and theory is observed when considering data points from all jet transverse momentum and rapidity regions in the inclusive jet measurement (table 3), a behaviour already observed in the previous ATLAS measurement at $\sqrt{s} = 8\,\text{TeV}$ [11]. For the dijet measurement, the agreement is fair when considering events from all y^* regions, as observed in the previous ATLAS measurement at $\sqrt{s} = 7\,\text{TeV}$ [76].

Consideration of all data points together requires a good understanding of the correlations of the experimental and theoretical systematic uncertainties in jet p_{T} and rapidity. Although the correlations of most uncertainties are generally well known, the systematic uncertainties that are based on simple comparisons between two options (two-point uncertainties) are not well defined. This is the case for instance for the in situ multijet balance uncertainties due to different fragmentation models and the theoretical uncertainty related to the alternative scale choice. In these cases, alternative decorrelation scenarios can in principle be used instead of the default full correlation model. In these, systematic uncertainties are split into sub-components whose size varies with jet rapidity and p_{T}, keeping their sum in quadrature equal to the original uncertainty.

Reference [11] presents a detailed discussion about the alternative correlation options that can be considered acceptable. The same conclusions are applicable here. Decorrelation scenarios were applied simultaneously to the largest sources of two-point experimental uncertainties (the JES flavour response, the JES multijet p_{T}-balance fragmentation, and the pile-up energy density in jets) as well as the theoretical uncertainties (the scale variations, the alternative scale choice and the non-perturbative corrections) using the splitting options that yielded the largest χ^2 reduction for each single component in ref. [11]. The χ^2 using the CT14 PDF set and the $p_{\text{T}}^{\text{max}}$ scale choice is found to be reduced by 58 units ($\chi^2/\text{dof} = 361/177$) compared to the nominal configuration, but the corresponding p-value is still $\ll 10^{-3}$, in agreement with the conclusions of the previous ATLAS measurement at $\sqrt{s} = 8\,\text{TeV}$ [11].

Since the uncertainties in the NNLO pQCD predictions do not yet include the contributions from the PDF and α_{s} uncertainties, it is not possible to perform a quantitative comparison to the measurements. However, one can conclude from figure 11 (figure 12) that the differences between data and the theoretical predictions at NNLO are smaller (larger) than at NLO for the $p_{\text{T}}^{\text{jet}}$ ($p_{\text{T}}^{\text{max}}$) scale choice.

11 Conclusion

The inclusive jet and dijet cross-sections in proton-proton collisions at $\sqrt{s} = 13$ TeV are measured for jets reconstructed with the anti-k_t algorithm with a jet radius parameter

JHEP05(2018)195

Rapidity ranges	P_{obs} CT14	MMHT 2014	NNPDF 3.0	HERAPDF 2.0	ABMP16
$p_{\text{T}}^{\text{max}}$					
$\|y\| < 0.5$	67%	65%	62%	31%	50%
$0.5 \le \|y\| < 1.0$	5.8%	6.3%	6.0%	3.0%	2.0%
$1.0 \le \|y\| < 1.5$	65%	61%	67%	50%	55%
$1.5 \le \|y\| < 2.0$	0.7%	0.8%	0.8%	0.1%	0.4%
$2.0 \le \|y\| < 2.5$	2.3%	2.3%	2.8%	0.7%	1.5%
$2.5 \le \|y\| < 3.0$	62%	71%	69%	25%	55%
$p_{\text{T}}^{\text{jet}}$					
$\|y\| < 0.5$	69%	67%	66%	30%	46%
$0.5 \le \|y\| < 1.0$	7.4%	8.9%	8.6%	3.4%	2.0%
$1.0 \le \|y\| < 1.5$	69%	62%	68%	45%	54%
$1.5 \le \|y\| < 2.0$	1.3%	1.6%	1.4%	0.1%	0.5%
$2.0 \le \|y\| < 2.5$	8.7%	6.6%	7.4%	1.0%	3.6%
$2.5 \le \|y\| < 3.0$	65%	72%	72%	28%	59%

Table 2. Summary of observed P_{obs} values from the comparison of the inclusive jet cross-section and the NLO pQCD prediction corrected for non-perturbative and electroweak effects for various PDF sets, for the two scale choices and for each rapidity bin of the measurement.

χ^2/dof all $\|y\|$ bins	CT14	MMHT 2014	NNPDF 3.0	HERAPDF 2.0	ABMP16
$p_{\text{T}}^{\text{max}}$	419/177	431/177	404/177	432/177	475/177
$p_{\text{T}}^{\text{jet}}$	399/177	405/177	384/177	428/177	455/177

Table 3. Summary of χ^2/dof values obtained from a global fit using all p_{T} and rapidity bins, comparing the inclusive jet cross-section and the NLO pQCD prediction corrected for non-perturbative and electroweak effects for several PDF sets and for the two scale choices. All the corresponding p-values are $\ll 10^{-3}$.

y^* ranges	P_{obs} CT14	MMHT 2014	NNPDF 3.0	HERAPDF 2.0	ABMP16
$y^* < 0.5$	79%	59%	50%	71%	71%
$0.5 \le y^* < 1.0$	27%	23%	19%	32%	31%
$1.0 \le y^* < 1.5$	66%	55%	48%	66%	69%
$1.5 \le y^* < 2.0$	26%	26%	28%	9.9%	25%
$2.0 \le y^* < 2.5$	41%	34%	29%	3.6%	20%
$2.5 \le y^* < 3.0$	45%	46%	40%	25%	38%
all y^* bins	9.4%	6.5%	11%	0.1%	5.1%

Table 4. Summary of observed P_{obs} values obtained from the comparison of the dijet cross-section and the NLO pQCD prediction corrected for non-perturbative and electroweak effects for various PDF sets and for each individual y^* range. The last row of the table corresponds to a global fit using all m_{jj} and y^* bins of the dijet measurement.

JHEP05(2018)195

value of $R = 0.4$. The measurements use data collected at the LHC with the ATLAS detector during 2015 corresponding to an integrated luminosity of 3.2 fb^{-1}. The inclusive jet cross-sections are measured double-differentially in the jet transverse momentum and jet rapidity in a kinematic region between 100 GeV and 3.5 TeV with $|y| < 3$. The dijet cross-sections are measured double-differentially in the invariant mass of the dijet system and half the absolute rapidity separation between the two leading jets with $|y| < 3$, covering 300 GeV $< m_{jj} <$ 9 TeV and $y^* < 3$. The dominant systematic uncertainty arises from the jet energy calibration.

A quantitative comparison of the measurements to fixed-order NLO QCD calculations, corrected for non-perturbative and electroweak effects, shows overall fair agreement (with p-values in the percent range) when considering jet cross-sections in individual jet rapidity bins independently. In the inclusive jet measurement, a significant tension (with p-values $\ll 10^{-3}$) between data and theory is observed when considering data points from all jet transverse momentum and rapidity regions. No significant differences between the inclusive jet cross-sections and the fixed-order NNLO QCD calculations corrected for non-perturbative and electroweak effects are observed when using $p_{\mathrm{T}}^{\mathrm{jet}}$ as the QCD scale. The NNLO pQCD predictions using $p_{\mathrm{T}}^{\mathrm{max}}$ as the scale overestimate the measured inclusive jet cross-sections.

Acknowledgments

We thank CERN for the very successful operation of the LHC, as well as the support staff from our institutions without whom ATLAS could not be operated efficiently.

We acknowledge the support of ANPCyT, Argentina; YerPhI, Armenia; ARC, Australia; BMWFW and FWF, Austria; ANAS, Azerbaijan; SSTC, Belarus; CNPq and FAPESP, Brazil; NSERC, NRC and CFI, Canada; CERN; CONICYT, Chile; CAS, MOST and NSFC, China; COLCIENCIAS, Colombia; MSMT CR, MPO CR and VSC CR, Czech Republic; DNRF and DNSRC, Denmark; IN2P3-CNRS, CEA-DRF/IRFU, France; SRNSFG, Georgia; BMBF, HGF, and MPG, Germany; GSRT, Greece; RGC, Hong Kong SAR, China; ISF, I-CORE and Benoziyo Center, Israel; INFN, Italy; MEXT and JSPS, Japan; CNRST, Morocco; NWO, Netherlands; RCN, Norway; MNiSW and NCN, Poland; FCT, Portugal; MNE/IFA, Romania; MES of Russia and NRC KI, Russian Federation; JINR; MESTD, Serbia; MSSR, Slovakia; ARRS and MIZŠ, Slovenia; DST/NRF, South Africa; MINECO, Spain; SRC and Wallenberg Foundation, Sweden; SERI, SNSF and Cantons of Bern and Geneva, Switzerland; MOST, Taiwan; TAEK, Turkey; STFC, United Kingdom; DOE and NSF, United States of America. In addition, individual groups and members have received support from BCKDF, the Canada Council, CANARIE, CRC, Compute Canada, FQRNT, and the Ontario Innovation Trust, Canada; EPLANET, ERC, ERDF, FP7, Horizon 2020 and Marie Skłodowska-Curie Actions, European Union; Investissements d'Avenir Labex and Idex, ANR, Région Auvergne and Fondation Partager le Savoir, France; DFG and AvH Foundation, Germany; Herakleitos, Thales and Aristeia programmes co-financed by EU-ESF and the Greek NSRF; BSF, GIF and Minerva, Israel; BRF, Norway; CERCA Programme Generalitat de Catalunya, Generalitat Valenciana, Spain; the Royal Society and Leverhulme Trust, United Kingdom.

JHEP05(2018)195

The crucial computing support from all WLCG partners is acknowledged gratefully, in particular from CERN, the ATLAS Tier-1 facilities at TRIUMF (Canada), NDGF (Denmark, Norway, Sweden), CC-IN2P3 (France), KIT/GridKA (Germany), INFN-CNAF (Italy), NL-T1 (Netherlands), PIC (Spain), ASGC (Taiwan), RAL (U.K.) and BNL (U.S.A.), the Tier-2 facilities worldwide and large non-WLCG resource providers. Major contributors of computing resources are listed in ref. [77].

Open Access. This article is distributed under the terms of the Creative Commons Attribution License (CC-BY 4.0), which permits any use, distribution and reproduction in any medium, provided the original author(s) and source are credited.

JHEP05(2018)195

References

[1] CDF collaboration, T. Aaltonen et al., *Measurement of the inclusive jet cross section at the Fermilab Tevatron $p\bar{p}$ collider using a cone-based jet algorithm*, *Phys. Rev.* **D 78** (2008) 052006 [*Erratum ibid.* **D 79** (2009) 119902] [arXiv:0807.2204] [INSPIRE].

[2] D0 collaboration, V.M. Abazov et al., *Measurement of the inclusive jet cross section in $p\bar{p}$ collisions at $\sqrt{s} = 1.96$ TeV*, *Phys. Rev.* **D 85** (2012) 052006 [arXiv:1110.3771] [INSPIRE].

[3] L. Evans and P. Bryant, *LHC machine*, 2008 *JINST* **3** S08001 [INSPIRE].

[4] ALICE collaboration, *Measurement of the inclusive differential jet cross section in pp collisions at $\sqrt{s} = 2.76$ TeV*, *Phys. Lett.* **B 722** (2013) 262 [arXiv:1301.3475] [INSPIRE].

[5] ATLAS collaboration, *Measurement of the inclusive jet cross section in pp collisions at $\sqrt{s} = 2.76$ TeV and comparison to the inclusive jet cross section at $\sqrt{s} = 7$ TeV using the ATLAS detector*, *Eur. Phys. J.* **C 73** (2013) 2509 [arXiv:1304.4739] [INSPIRE].

[6] CMS collaboration, *Measurement of the inclusive jet cross section in pp collisions at $\sqrt{s} = 2.76$ TeV*, *Eur. Phys. J.* **C 76** (2016) 265 [arXiv:1512.06212] [INSPIRE].

[7] ATLAS collaboration, *Measurement of inclusive jet and dijet cross sections in proton-proton collisions at 7 TeV centre-of-mass energy with the ATLAS detector*, *Eur. Phys. J.* **C 71** (2011) 1512 [arXiv:1009.5908] [INSPIRE].

[8] CMS collaboration, *Measurements of differential jet cross sections in proton-proton collisions at $\sqrt{s} = 7$ TeV with the CMS detector*, *Phys. Rev.* **D 87** (2013) 112002 [arXiv:1212.6660] [INSPIRE].

[9] CMS collaboration, *Measurement of the ratio of inclusive jet cross sections using the anti-k_T algorithm with radius parameters $R = 0.5$ and 0.7 in pp collisions at $\sqrt{s} = 7$ TeV*, *Phys. Rev.* **D 90** (2014) 072006 [arXiv:1406.0324] [INSPIRE].

[10] CMS collaboration, *Measurement of the inclusive jet cross section in pp collisions at $\sqrt{s} = 7$ TeV*, *Phys. Rev. Lett.* **107** (2011) 132001 [arXiv:1106.0208] [INSPIRE].

[11] ATLAS collaboration, *Measurement of the inclusive jet cross-sections in proton-proton collisions at $\sqrt{s} = 8$ TeV with the ATLAS detector*, *JHEP* **09** (2017) 020 [arXiv:1706.03192] [INSPIRE].

[12] CMS collaboration, *Measurement and QCD analysis of double-differential inclusive jet cross sections in pp collisions at $\sqrt{s} = 8$ TeV and cross section ratios to 2.76 and 7 TeV*, *JHEP* **03** (2017) 156 [arXiv:1609.05331] [INSPIRE].

[13] CMS collaboration, *Measurement of the double-differential inclusive jet cross section in proton–proton collisions at* $\sqrt{s} = 13$ *TeV*, *Eur. Phys. J.* **C 76** (2016) 451 [arXiv:1605.04436] [INSPIRE].

[14] CMS collaboration, *Measurement of the differential dijet production cross section in proton-proton collisions at* $\sqrt{s} = 7$ *TeV*, *Phys. Lett.* **B 700** (2011) 187 [arXiv:1104.1693] [INSPIRE].

[15] CMS collaboration, *Measurement of the triple-differential dijet cross section in proton-proton collisions at* $\sqrt{s} = 8$ *TeV and constraints on parton distribution functions*, *Eur. Phys. J.* **C 77** (2017) 746 [arXiv:1705.02628] [INSPIRE].

[16] M. Cacciari, G.P. Salam and G. Soyez, *The anti-*k_t *jet clustering algorithm*, *JHEP* **04** (2008) 063 [arXiv:0802.1189] [INSPIRE].

[17] J. Currie, E.W.N. Glover and J. Pires, *Next-to-next-to leading order QCD predictions for single jet inclusive production at the LHC*, *Phys. Rev. Lett.* **118** (2017) 072002 [arXiv:1611.01460] [INSPIRE].

[18] J. Currie et al., *Single jet inclusive production for the individual jet* p_{T} *scale choice at the LHC*, *Acta Phys. Polon.* **B 48** (2017) 955 [arXiv:1704.00923] [INSPIRE].

[19] ATLAS collaboration, *The ATLAS experiment at the CERN Large Hadron Collider*, 2008 *JINST* **3** S08003 [INSPIRE].

[20] ATLAS collaboration, *ATLAS insertable B-layer technical design report*, ATLAS-TDR-19 (2010) [ATLAS-TDR-19-ADD-1].

[21] ATLAS collaboration, *Performance of the ATLAS Trigger System in 2015*, *Eur. Phys. J.* **C 77** (2017) 317 [arXiv:1611.09661] [INSPIRE].

[22] M. Cacciari, G.P. Salam and G. Soyez, *FastJet user manual*, *Eur. Phys. J.* **C 72** (2012) 1896 [arXiv:1111.6097] [INSPIRE].

[23] S. Frixione and G. Ridolfi, *Jet photoproduction at HERA*, *Nucl. Phys.* **B 507** (1997) 315 [hep-ph/9707345] [INSPIRE].

[24] S. Alioli, K. Hamilton, P. Nason, C. Oleari and E. Re, *Jet pair production in POWHEG*, *JHEP* **04** (2011) 081 [arXiv:1012.3380] [INSPIRE].

[25] ATLAS collaboration, *Luminosity determination in pp collisions at* $\sqrt{s} = 8$ *TeV using the ATLAS detector at the LHC*, *Eur. Phys. J.* **C 76** (2016) 653 [arXiv:1608.03953] [INSPIRE].

[26] T. Sjöstrand, S. Mrenna and P.Z. Skands, *A brief introduction to PYTHIA 8.1*, *Comput. Phys. Commun.* **178** (2008) 852 [arXiv:0710.3820] [INSPIRE].

[27] T. Sjöstrand and P.Z. Skands, *Transverse-momentum-ordered showers and interleaved multiple interactions*, *Eur. Phys.* **C 39** (2005) 129.

[28] T. Sjöstrand and P.Z. Skands, *Multiple interactions and the structure of beam remnants*, *JHEP* **03** (2004) 053 [hep-ph/0402078] [INSPIRE].

[29] B. Andersson, G. Gustafson, G. Ingelman and T. Sjöstrand, *Parton fragmentation and string dynamics*, *Phys. Rept.* **97** (1983) 31.

[30] ATLAS collaboration, *ATLAS Run 1 PYTHIA8 tunes*, ATL-PHYS-PUB-2014-021 (2014).

[31] R.D. Ball et al., *Parton distributions with LHC data*, *Nucl. Phys.* **B 867** (2013) 244 [arXiv:1207.1303] [INSPIRE].

JHEP05(2018)195

[32] D.J. Lange, *The EvtGen particle decay simulation package*, *Nucl. Instrum. Meth.* **A 462** (2001) 152 [INSPIRE].

[33] P. Nason, *A new method for combining NLO QCD with shower Monte Carlo algorithms*, *JHEP* **11** (2004) 040 [hep-ph/0409146] [INSPIRE].

[34] H.-L. Lai et al., *New parton distributions for collider physics*, *Phys. Rev.* **D 82** (2010) 074024 [arXiv:1007.2241] [INSPIRE].

[35] M. Bahr et al., *HERWIG++ physics and manual*, *Eur. Phys. J.* **C 58** (2008) 639 [arXiv:0803.0883] [INSPIRE].

[36] J. Bellm et al., *HERWIG++ 2.7 release note*, arXiv:1310.6877 [INSPIRE].

[37] ATLAS collaboration, *The ATLAS simulation infrastructure*, *Eur. Phys. J.* **C 70** (2010) 823 [arXiv:1005.4568] [INSPIRE].

[38] GEANT4 collaboration, S. Agostinelli et al., *GEANT4: a simulation toolkit*, *Nucl. Instrum. Meth.* **A 506** (2003) 250 [INSPIRE].

[39] V. Lendermann et al., *Combining triggers in HEP data analysis*, *Nucl. Instrum. Meth.* **A 604** (2009) 707 [arXiv:0901.4118] [INSPIRE].

[40] ATLAS collaboration, *Selection of jets produced in 13TeV proton-proton collisions with the ATLAS detector*, ATLAS-CONF-2015-029 (2015).

[41] ATLAS collaboration, *Jet energy measurement with the ATLAS detector in proton-proton collisions at* $\sqrt{s} = 7$ *TeV*, *Eur. Phys. J.* **C 73** (2013) 2304 [arXiv:1112.6426] [INSPIRE].

[42] W. Lampl et al., *Calorimeter clustering algorithms: description and performance*, ATL-LARG-PUB-2008-002 (2008).

[43] ATLAS collaboration, *Jet energy scale measurements and their systematic uncertainties in proton-proton collisions at* $\sqrt{s} = 13$ *TeV with the ATLAS detector*, *Phys. Rev.* **D 96** (2017) 072002 [arXiv:1703.09665] [INSPIRE].

[44] ATLAS collaboration, *Performance of pile-up mitigation techniques for jets in pp collisions at* $\sqrt{s} = 8$ *TeV using the ATLAS detector*, *Eur. Phys. J.* **C 76** (2016) 581 [arXiv:1510.03823] [INSPIRE].

[45] ATLAS collaboration, *Jet global sequential corrections with the ATLAS detector in proton-proton collisions at* $\sqrt{s} = 8$ *TeV*, ATLAS-CONF-2015-002 (2015).

[46] M. Cacciari and G.P. Salam, *Pileup subtraction using jet areas*, *Phys. Lett.* **B 659** (2008) 119 [arXiv:0707.1378] [INSPIRE].

[47] ATLAS collaboration, *Data-driven determination of the energy scale and resolution of jets reconstructed in the ATLAS calorimeters using dijet and multijet events at* $\sqrt{s} = 8$ *TeV*, ATLAS-CONF-2015-017 (2015).

[48] ATLAS collaboration, *Determination of the jet energy scale and resolution at ATLAS using* Z/γ*-jet events in data at* $\sqrt{s} = 8$ *TeV*, ATLAS-CONF-2015-057 (2015).

[49] ATLAS collaboration, *Monte Carlo calibration and combination of in-situ measurements of jet energy scale, jet energy resolution and jet mass in ATLAS*, ATLAS-CONF-2015-037 (2015).

[50] ATLAS collaboration, *A measurement of the calorimeter response to single hadrons and determination of the jet energy scale uncertainty using LHC Run-1 pp-collision data with the ATLAS detector*, *Eur. Phys. J.* **C 77** (2017) 26 [arXiv:1607.08842] [INSPIRE].

JHEP05(2018)195

[51] ATLAS collaboration, *Jet calibration and systematic uncertainties for jets reconstructed in the ATLAS detector at* $\sqrt{s} = 13$ *TeV*, ATL-PHYS-PUB-2015-015 (2015).

[52] ATLAS collaboration, *Jet energy measurement and its systematic uncertainty in proton-proton collisions at* $\sqrt{s} = 7$ *TeV with the ATLAS detector*, *Eur. Phys. J.* **C 75** (2015) 17 [arXiv:1406.0076] [INSPIRE].

[53] B. Malaescu, *An Iterative, Dynamically Stabilized (IDS) method of data unfolding*, in the proceedongs of the *PHYSTAT 2011 Workshop on Statistical Issues Related to Discovery Claims in Search Experiments and Unfolding*, January 17–20, CERN, Geneva, Switzerland (2011), arXiv:1106.3107 [INSPIRE].

[54] ATLAS collaboration, *Measurement of inclusive jet and dijet production in pp collisions at* $\sqrt{s} = 7$ *TeV using the ATLAS detector*, *Phys. Rev.* **D 86** (2012) 014022 [arXiv:1112.6297] [INSPIRE].

[55] J. Wenninger and E. Todesco, *Large Hadron Collider momentum calibration and accuracy*, *Phys. Rev. Accel. Beams* **20** (2017) 081003.

[56] Z. Nagy, *Next-to-leading order calculation of three jet observables in hadron hadron collision*, *Phys. Rev.* **D 68** (2003) 094002 [hep-ph/0307268] [INSPIRE].

[57] T. Carli et al., *A posteriori inclusion of parton density functions in NLO QCD final-state calculations at hadron colliders: The APPLGRID Project*, *Eur. Phys. J.* **C 66** (2010) 503 [arXiv:0911.2985] [INSPIRE].

[58] S. Carrazza and J. Pires, *Perturbative QCD description of jet data from LHC Run-I and Tevatron Run-II*, *JHEP* **10** (2014) 145 [arXiv:1407.7031] [INSPIRE].

[59] S.D. Ellis, Z. Kunszt and D.E. Soper, *Two jet production in hadron collisions at order* α_S^3 *in QCD*, *Phys. Rev. Lett.* **69** (1992) 1496 [INSPIRE].

[60] A. Buckley et al., *LHAPDF6: parton density access in the LHC precision era*, *Eur. Phys. J.* **C 75** (2015) 132 [arXiv:1412.7420] [INSPIRE].

[61] S. Dulat et al., *New parton distribution functions from a global analysis of quantum chromodynamics*, *Phys. Rev.* **D 93** (2016) 033006 [arXiv:1506.07443] [INSPIRE].

[62] L.A. Harland-Lang, A.D. Martin, P. Motylinski and R.S. Thorne, *Parton distributions in the LHC era: MMHT 2014 PDFs*, *Eur. Phys. J.* **C 75** (2015) 204 [arXiv:1412.3989] [INSPIRE].

[63] NNPDF collaboration, R.D. Ball et al., *Parton distributions for the LHC Run II*, *JHEP* **04** (2015) 040 [arXiv:1410.8849] [INSPIRE].

[64] ZEUS, H1 collaboration, H. Abramowicz et al., *Combination of measurements of inclusive deep inelastic* $e^{\pm}p$ *scattering cross sections and QCD analysis of HERA data*, *Eur. Phys. J.* **C 75** (2015) 580 [arXiv:1506.06042] [INSPIRE].

[65] S. Alekhin, J. Blümlein, S. Moch and R. Placakyte, *Parton distribution functions,* α_s *and heavy-quark masses for LHC Run II*, *Phys. Rev.* **D 96** (2017) 014011 [arXiv:1701.05838] [INSPIRE].

[66] J. Butterworth et al., *PDF4LHC recommendations for LHC Run II*, *J. Phys.* **G 43** (2016) 023001 [arXiv:1510.03865] [INSPIRE].

[67] J. Pumplin et al., *New generation of parton distributions with uncertainties from global QCD analysis*, *JHEP* **07** (2002) 012 [hep-ph/0201195] [INSPIRE].

JHEP05(2018)195

[68] A.D. Martin, W.J. Stirling, R.S. Thorne and G. Watt, *Parton distributions for the LHC*, *Eur. Phys. J.* **C 63** (2009) 189 [arXiv:0901.0002] [INSPIRE].

[69] R. Corke and T. Sjöstrand, *Interleaved parton showers and tuning prospects*, *JHEP* **03** (2011) 032 [arXiv:1011.1759] [INSPIRE].

[70] ATLAS collaboration, *Summary of ATLAS Pythia8 tunes*, ATLAS-PHYS-PUB-2012-003 (2012).

[71] P. Skands, S. Carrazza and J. Rojo, *Tuning PYTHIA 8.1: the Monash 2013 Tune*, *Eur. Phys. J.* **C 74** (2014) 3024 [arXiv:1404.5630] [INSPIRE].

[72] S. Gieseke, C. Rohr and A. Siodmok, *Colour reconnections in HERWIG++*, *Eur. Phys. J.* **C 72** (2012) 2225 [arXiv:1206.0041] [INSPIRE].

[73] M.H. Seymour and A. Siodmok, *Constraining MPI models using σ_{eff} and recent Tevatron and LHC Underlying Event data*, *JHEP* **10** (2013) 113 [arXiv:1307.5015] [INSPIRE].

[74] S. Dittmaier, A. Huss and C. Speckner, *Weak radiative corrections to dijet production at hadron colliders*, *JHEP* **11** (2012) 095 [arXiv:1210.0438] [INSPIRE].

[75] ATLAS collaboration, *Measurement of the inclusive jet cross-section in proton-proton collisions at $\sqrt{s} = 7$ TeV using 4.5 fb^{-1} of data with the ATLAS detector*, *JHEP* **02** (2015) 153 [*Erratum ibid.* **09** (2015) 141] [arXiv:1410.8857] [INSPIRE].

[76] ATLAS collaboration, *Measurement of dijet cross sections in pp collisions at 7 TeV centre-of-mass energy using the ATLAS detector*, *JHEP* **05** (2014) 059 [arXiv:1312.3524] [INSPIRE].

[77] ATLAS collaboration, *ATLAS computing acknowledgements*, ATL-GEN-PUB-2016-002 (2016).

JHEP05(2018)195

The ATLAS collaboration

M. Aaboud[137d], G. Aad[88], B. Abbott[115], O. Abdinov[12,*], B. Abeloos[119], S.H. Abidi[161], O.S. AbouZeid[139], N.L. Abraham[151], H. Abramowicz[155], H. Abreu[154], R. Abreu[118], Y. Abulaiti[148a,148b], B.S. Acharya[167a,167b,a], S. Adachi[157], L. Adamczyk[41a], J. Adelman[110], M. Adersberger[102], T. Adye[133], A.A. Affolder[139], Y. Afik[154], T. Agatonovic-Jovin[14], C. Agheorghiesei[28c], J.A. Aguilar-Saavedra[128a,128f], S.P. Ahlen[24], F. Ahmadov[68,b], G. Aielli[135a,135b], S. Akatsuka[71], H. Akerstedt[148a,148b], T.P.A. Åkesson[84], E. Akilli[52], A.V. Akimov[98], G.L. Alberghi[22a,22b], J. Albert[172], P. Albicocco[50], M.J. Alconada Verzini[74], S.C. Alderweireldt[108], M. Aleksa[32], I.N. Aleksandrov[68], C. Alexa[28b], G. Alexander[155], T. Alexopoulos[10], M. Alhroob[115], B. Ali[130], M. Aliev[76a,76b], G. Alimonti[94a], J. Alison[33], S.P. Alkire[38], B.M.M. Allbrooke[151], B.W. Allen[118], P.P. Allport[19], A. Aloisio[106a,106b], A. Alonso[39], F. Alonso[74], C. Alpigiani[140], A.A. Alshehri[56], M.I. Alstaty[88], B. Alvarez Gonzalez[32], D. Álvarez Piqueras[170], M.G. Alviggi[106a,106b], B.T. Amadio[16], Y. Amaral Coutinho[26a], C. Amelung[25], D. Amidei[92], S.P. Amor Dos Santos[128a,128c], S. Amoroso[32], G. Amundsen[25], C. Anastopoulos[141], L.S. Ancu[52], N. Andari[19], T. Andeen[11], C.F. Anders[60b], J.K. Anders[77], K.J. Anderson[33], A. Andreazza[94a,94b], V. Andrei[60a], S. Angelidakis[37], I. Angelozzi[109], A. Angerami[38], A.V. Anisenkov[111,c], N. Anjos[13], A. Annovi[126a], C. Antel[60a], M. Antonelli[50], A. Antonov[100,*], D.J. Antrim[166], F. Anulli[134a], M. Aoki[69], L. Aperio Bella[32], G. Arabidze[93], Y. Arai[69], J.P. Araque[128a], V. Araujo Ferraz[26a], A.T.H. Arce[48], R.E. Ardell[80], F.A. Arduh[74], J-F. Arguin[97], S. Argyropoulos[66], M. Arik[20a], A.J. Armbruster[32], L.J. Armitage[79], O. Arnaez[161], H. Arnold[51], M. Arratia[30], O. Arslan[23], A. Artamonov[99,*], G. Artoni[122], S. Artz[86], S. Asai[157], N. Asbah[45], A. Ashkenazi[155], L. Asquith[151], K. Assamagan[27], R. Astalos[146a], M. Atkinson[169], N.B. Atlay[143], K. Augsten[130], G. Avolio[32], B. Axen[16], M.K. Ayoub[35a], G. Azuelos[97,d], A.E. Baas[60a], M.J. Baca[19], H. Bachacou[138], K. Bachas[76a,76b], M. Backes[122], P. Bagnaia[134a,134b], M. Bahmani[42], H. Bahrasemani[144], J.T. Baines[133], M. Bajic[39], O.K. Baker[179], P.J. Bakker[109], E.M. Baldin[111,c], P. Balek[175], F. Balli[138], W.K. Balunas[124], E. Banas[42], A. Bandyopadhyay[23], Sw. Banerjee[176,e], A.A.E. Bannoura[178], L. Barak[155], E.L. Barberio[91], D. Barberis[53a,53b], M. Barbero[88], T. Barillari[103], M-S Barisits[32], J.T. Barkeloo[118], T. Barklow[145], N. Barlow[30], S.L. Barnes[36c], B.M. Barnett[133], R.M. Barnett[16], Z. Barnovska-Blenessy[36a], A. Baroncelli[136a], G. Barone[25], A.J. Barr[122], L. Barranco Navarro[170], F. Barreiro[85], J. Barreiro Guimarães da Costa[35a], R. Bartoldus[145], A.E. Barton[75], P. Bartos[146a], A. Basalaev[125], A. Bassalat[119,f], R.L. Bates[56], S.J. Batista[161], J.R. Batley[30], M. Battaglia[139], M. Bauce[134a,134b], F. Bauer[138], H.S. Bawa[145,g], J.B. Beacham[113], M.D. Beattie[75], T. Beau[83], P.H. Beauchemin[165], P. Bechtle[23], H.P. Beck[18,h], H.C. Beck[57], K. Becker[122], M. Becker[86], C. Becot[112], A.J. Beddall[20e], A. Beddall[20b], V.A. Bednyakov[68], M. Bedognetti[109], C.P. Bee[150], T.A. Beermann[32], M. Begalli[26a], M. Begel[27], J.K. Behr[45], A.S. Bell[81], G. Bella[155], L. Bellagamba[22a], A. Bellerive[31], M. Bellomo[154], K. Belotskiy[100], O. Beltramello[32], N.L. Belyaev[100], O. Benary[155,*], D. Benchekroun[137a], M. Bender[102], N. Benekos[10], Y. Benhammou[155], E. Benhar Noccioli[179], J. Benitez[66], D.P. Benjamin[48], M. Benoit[52], J.R. Bensinger[25], S. Bentvelsen[109], L. Beresford[122], M. Beretta[50], D. Berge[109], E. Bergeaas Kuutmann[168], N. Berger[5], J. Beringer[16], S. Berlendis[58], N.R. Bernard[89], G. Bernardi[83], C. Bernius[145], F.U. Bernlochner[23], T. Berry[80], P. Berta[86], C. Bertella[35a], G. Bertoli[148a,148b], I.A. Bertram[75], C. Bertsche[45], D. Bertsche[115], G.J. Besjes[39], O. Bessidskaia Bylund[148a,148b], M. Bessner[45], N. Besson[138], A. Bethani[87], S. Bethke[103], A. Betti[23], A.J. Bevan[79], J. Beyer[103], R.M. Bianchi[127], O. Biebel[102], D. Biedermann[17], R. Bielski[87], K. Bierwagen[86], N.V. Biesuz[126a,126b], M. Biglietti[136a], T.R.V. Billoud[97], H. Bilokon[50], M. Bindi[57], A. Bingul[20b], C. Bini[134a,134b], S. Biondi[22a,22b], T. Bisanz[57], C. Bittrich[47], D.M. Bjergaard[48], J.E. Black[145], K.M. Black[24], R.E. Blair[6], T. Blazek[146a],

JHEP05(2018)195

I. Bloch[45], C. Blocker[25], A. Blue[56], U. Blumenschein[79], Dr. Blunier[34a], G.J. Bobbink[109], V.S. Bobrovnikov[111,c], S.S. Bocchetta[84], A. Bocci[48], C. Bock[102], M. Boehler[51], D. Boerner[178], D. Bogavac[102], A.G. Bogdanchikov[111], C. Bohm[148a], V. Boisvert[80], P. Bokan[168,i], T. Bold[41a], A.S. Boldyrev[101], A.E. Bolz[60b], M. Bomben[83], M. Bona[79], M. Boonekamp[138], A. Borisov[132], G. Borissov[75], J. Bortfeldt[32], D. Bortoletto[122], V. Bortolotto[62a], D. Boscherini[22a], M. Bosman[13], J.D. Bossio Sola[29], J. Boudreau[127], E.V. Bouhova-Thacker[75], D. Boumediene[37], C. Bourdarios[119], S.K. Boutle[56], A. Boveia[113], J. Boyd[32], I.R. Boyko[68], A.J. Bozson[80], J. Bracinik[19], A. Brandt[8], G. Brandt[57], O. Brandt[60a], F. Braren[45], U. Bratzler[158], B. Brau[89], J.E. Brau[118], W.D. Breaden Madden[56], K. Brendlinger[45], A.J. Brennan[91], L. Brenner[109], R. Brenner[168], S. Bressler[175], D.L. Briglin[19], T.M. Bristow[49], D. Britton[56], D. Britzger[45], F.M. Brochu[30], I. Brock[23], R. Brock[93], G. Brooijmans[38], T. Brooks[80], W.K. Brooks[34b], J. Brosamer[16], E. Brost[110], J.H Broughton[19], P.A. Bruckman de Renstrom[42], D. Bruncko[146b], A. Bruni[22a], G. Bruni[22a], L.S. Bruni[109], S. Bruno[135a,135b], BH Brunt[30], M. Bruschi[22a], N. Bruscino[127], P. Bryant[33], L. Bryngemark[45], T. Buanes[15], Q. Buat[144], P. Buchholz[143], A.G. Buckley[56], I.A. Budagov[68], F. Buehrer[51], M.K. Bugge[121], O. Bulekov[100], D. Bullock[8], T.J. Burch[110], S. Burdin[77], C.D. Burgard[109], A.M. Burger[5], B. Burghgrave[110], K. Burka[42], S. Burke[133], I. Burmeister[46], J.T.P. Burr[122], D. Büscher[51], V. Büscher[86], P. Bussey[56], J.M. Butler[24], C.M. Buttar[56], J.M. Butterworth[81], P. Butti[32], W. Buttinger[27], A. Buzatu[153], A.R. Buzykaev[111,c], S. Cabrera Urbán[170], D. Caforio[130], H. Cai[169], V.M. Cairo[40a,40b], O. Cakir[4a], N. Calace[52], P. Calafiura[16], A. Calandri[88], G. Calderini[83], P. Calfayan[64], G. Callea[40a,40b], L.P. Caloba[26a], S. Calvente Lopez[85], D. Calvet[37], S. Calvet[37], T.P. Calvet[88], R. Camacho Toro[33], S. Camarda[32], P. Camarri[135a,135b], D. Cameron[121], R. Caminal Armadans[169], C. Camincher[58], S. Campana[32], M. Campanelli[81], A. Camplani[94a,94b], A. Campoverde[143], V. Canale[106a,106b], M. Cano Bret[36c], J. Cantero[116], T. Cao[155], M.D.M. Capeans Garrido[32], I. Caprini[28b], M. Caprini[28b], M. Capua[40a,40b], R.M. Carbone[38], R. Cardarelli[135a], F. Cardillo[51], I. Carli[131], T. Carli[32], G. Carlino[106a], B.T. Carlson[127], L. Carminati[94a,94b], R.M.D. Carney[148a,148b], S. Caron[108], E. Carquin[34b], S. Carrá[94a,94b], G.D. Carrillo-Montoya[32], D. Casadei[19], M.P. Casado[13,j], A.F. Casha[161], M. Casolino[13], D.W. Casper[166], R. Castelijn[109], V. Castillo Gimenez[170], N.F. Castro[128a,k], A. Catinaccio[32], J.R. Catmore[121], A. Cattai[32], J. Caudron[23], V. Cavaliere[169], E. Cavallaro[13], D. Cavalli[94a], M. Cavalli-Sforza[13], V. Cavasinni[126a,126b], E. Celebi[20d], F. Ceradini[136a,136b], L. Cerda Alberich[170], A.S. Cerqueira[26b], A. Cerri[151], L. Cerrito[135a,135b], F. Cerutti[16], A. Cervelli[22a,22b], S.A. Cetin[20d], A. Chafaq[137a], D. Chakraborty[110], S.K. Chan[59], W.S. Chan[109], Y.L. Chan[62a], P. Chang[169], J.D. Chapman[30], D.G. Charlton[19], C.C. Chau[31], C.A. Chavez Barajas[151], S. Che[113], S. Cheatham[167a,167c], A. Chegwidden[93], S. Chekanov[6], S.V. Chekulaev[163a], G.A. Chelkov[68,l], M.A. Chelstowska[32], C. Chen[36a], C. Chen[67], H. Chen[27], J. Chen[36a], S. Chen[35b], S. Chen[157], X. Chen[35c,m], Y. Chen[70], H.C. Cheng[92], H.J. Cheng[35a,35d], A. Cheplakov[68], E. Cheremushkina[132], R. Cherkaoui El Moursli[137e], E. Cheu[7], K. Cheung[63], L. Chevalier[138], V. Chiarella[50], G. Chiarelli[126a], G. Chiodini[76a], A.S. Chisholm[32], A. Chitan[28b], Y.H. Chiu[172], M.V. Chizhov[68], K. Choi[64], A.R. Chomont[37], S. Chouridou[156], Y.S. Chow[62a], V. Christodoulou[81], M.C. Chu[62a], J. Chudoba[129], A.J. Chuinard[90], J.J. Chwastowski[42], L. Chytka[117], A.K. Ciftci[4a], D. Cinca[46], V. Cindro[78], I.A. Cioara[23], A. Ciocio[16], F. Cirotto[106a,106b], Z.H. Citron[175], M. Citterio[94a], M. Ciubancan[28b], A. Clark[52], B.L. Clark[59], M.R. Clark[38], P.J. Clark[49], R.N. Clarke[16], C. Clement[148a,148b], Y. Coadou[88], M. Cobal[167a,167c], A. Coccaro[52], J. Cochran[67], L. Colasurdo[108], B. Cole[38], A.P. Colijn[109], J. Collot[58], T. Colombo[166], P. Conde Muiño[128a,128b], E. Coniavitis[51], S.H. Connell[147b], I.A. Connelly[87], S. Constantinescu[28b], G. Conti[32], F. Conventi[106a,n], M. Cooke[16], A.M. Cooper-Sarkar[122], F. Cormier[171], K.J.R. Cormier[161], M. Corradi[134a,134b], F. Corriveau[90,o], A. Cortes-Gonzalez[32], G. Costa[94a], M.J. Costa[170], D. Costanzo[141], G. Cottin[30],

JHEP05(2018)195

G. Cowan[80], B.E. Cox[87], K. Cranmer[112], S.J. Crawley[56], R.A. Creager[124], G. Cree[31], S. Crépé-Renaudin[58], F. Crescioli[83], W.A. Cribbs[148a,148b], M. Cristinziani[23], V. Croft[112], G. Crosetti[40a,40b], A. Cueto[85], T. Cuhadar Donszelmann[141], A.R. Cukierman[145], J. Cummings[179], M. Curatolo[50], J. Cúth[86], S. Czekierda[42], P. Czodrowski[32], G. D'amen[22a,22b], S. D'Auria[56], L. D'eramo[83], M. D'Onofrio[77], M.J. Da Cunha Sargedas De Sousa[128a,128b], C. Da Via[87], W. Dabrowski[41a], T. Dado[146a], T. Dai[92], O. Dale[15], F. Dallaire[97], C. Dallapiccola[89], M. Dam[39], J.R. Dandoy[124], M.F. Daneri[29], N.P. Dang[176], A.C. Daniells[19], N.S. Dann[87], M. Danninger[171], M. Dano Hoffmann[138], V. Dao[150], G. Darbo[53a], S. Darmora[8], J. Dassoulas[3], A. Dattagupta[118], T. Daubney[45], W. Davey[23], C. David[45], T. Davidek[131], D.R. Davis[48], P. Davison[81], E. Dawe[91], I. Dawson[141], K. De[8], R. de Asmundis[106a], A. De Benedetti[115], S. De Castro[22a,22b], S. De Cecco[83], N. De Groot[108], P. de Jong[109], H. De la Torre[93], F. De Lorenzi[67], A. De Maria[57], D. De Pedis[134a], A. De Salvo[134a], U. De Sanctis[135a,135b], A. De Santo[151], K. De Vasconcelos Corga[88], J.B. De Vivie De Regie[119], R. Debbe[27], C. Debenedetti[139], D.V. Dedovich[68], N. Dehghanian[3], I. Deigaard[109], M. Del Gaudio[40a,40b], J. Del Peso[85], D. Delgove[119], F. Deliot[138], C.M. Delitzsch[7], A. Dell'Acqua[32], L. Dell'Asta[24], M. Dell'Orso[126a,126b], M. Della Pietra[106a,106b], D. della Volpe[52], M. Delmastro[5], C. Delporte[119], P.A. Delsart[58], D.A. DeMarco[161], S. Demers[179], M. Demichev[68], A. Demilly[83], S.P. Denisov[132], D. Denysiuk[138], D. Derendarz[42], J.E. Derkaoui[137d], F. Derue[83], P. Dervan[77], K. Desch[23], C. Deterre[45], K. Dette[161], M.R. Devesa[29], P.O. Deviveiros[32], A. Dewhurst[133], S. Dhaliwal[25], F.A. Di Bello[52], A. Di Ciaccio[135a,135b], L. Di Ciaccio[5], W.K. Di Clemente[124], C. Di Donato[106a,106b], A. Di Girolamo[32], B. Di Girolamo[32], B. Di Micco[136a,136b], R. Di Nardo[32], K.F. Di Petrillo[59], A. Di Simone[51], R. Di Sipio[161], D. Di Valentino[31], C. Diaconu[88], M. Diamond[161], F.A. Dias[39], M.A. Diaz[34a], J. Dickinson[16], E.B. Diehl[92], J. Dietrich[17], S. Díez Cornell[45], A. Dimitrievska[14], J. Dingfelder[23], P. Dita[28b], S. Dita[28b], F. Dittus[32], F. Djama[88], T. Djobava[54b], J.I. Djuvsland[60a], M.A.B. do Vale[26c], D. Dobos[32], M. Dobre[28b], D. Dodsworth[25], C. Doglioni[84], J. Dolejsi[131], Z. Dolezal[131], M. Donadelli[26d], S. Donati[126a,126b], P. Dondero[123a,123b], J. Donini[37], J. Dopke[133], A. Doria[106a], M.T. Dova[74], A.T. Doyle[56], E. Drechsler[57], M. Dris[10], Y. Du[36b], J. Duarte-Campderros[155], F. Dubinin[98], A. Dubreuil[52], E. Duchovni[175], G. Duckeck[102], A. Ducourthial[83], O.A. Ducu[97,p], D. Duda[109], A. Dudarev[32], A.Chr. Dudder[86], E.M. Duffield[16], L. Duflot[119], M. Dührssen[32], C. Dulsen[178], M. Dumancic[175], A.E. Dumitriu[28b], A.K. Duncan[56], M. Dunford[60a], A. Duperrin[88], H. Duran Yildiz[4a], M. Düren[55], A. Durglishvili[54b], D. Duschinger[47], B. Dutta[45], D. Duvnjak[1], M. Dyndal[45], B.S. Dziedzic[42], C. Eckardt[45], K.M. Ecker[103], R.C. Edgar[92], T. Eifert[32], G. Eigen[15], K. Einsweiler[16], T. Ekelof[168], M. El Kacimi[137c], R. El Kosseifi[88], V. Ellajosyula[88], M. Ellert[168], S. Elles[5], F. Ellinghaus[178], A.A. Elliot[172], N. Ellis[32], J. Elmsheuser[27], M. Elsing[32], D. Emeliyanov[133], Y. Enari[157], J.S. Ennis[173], M.B. Epland[48], J. Erdmann[46], A. Ereditato[18], M. Ernst[27], S. Errede[169], M. Escalier[119], C. Escobar[170], B. Esposito[50], O. Estrada Pastor[170], A.I. Etienvre[138], E. Etzion[155], H. Evans[64], A. Ezhilov[125], M. Ezzi[137e], F. Fabbri[22a,22b], L. Fabbri[22a,22b], V. Fabiani[108], G. Facini[81], R.M. Fakhrutdinov[132], S. Falciano[134a], R.J. Falla[81], J. Faltova[32], Y. Fang[35a], M. Fanti[94a,94b], A. Farbin[8], A. Farilla[136a], C. Farina[127], E.M. Farina[123a,123b], T. Farooque[93], S. Farrell[16], S.M. Farrington[173], P. Farthouat[32], F. Fassi[137e], P. Fassnacht[32], D. Fassouliotis[9], M. Faucci Giannelli[49], A. Favareto[53a,53b], W.J. Fawcett[122], L. Fayard[119], O.L. Fedin[125,q], W. Fedorko[171], S. Feigl[121], L. Feligioni[88], C. Feng[36b], E.J. Feng[32], M.J. Fenton[56], A.B. Fenyuk[132], L. Feremenga[8], P. Fernandez Martinez[170], J. Ferrando[45], A. Ferrari[168], P. Ferrari[109], R. Ferrari[123a], D.E. Ferreira de Lima[60b], A. Ferrer[170], D. Ferrere[52], C. Ferretti[92], F. Fiedler[86], A. Filipčič[78], M. Filipuzzi[45], F. Filthaut[108], M. Fincke-Keeler[172], K.D. Finelli[24], M.C.N. Fiolhais[128a,128c,r], L. Fiorini[170], A. Fischer[2], C. Fischer[13], J. Fischer[178], W.C. Fisher[93], N. Flaschel[45], I. Fleck[143], P. Fleischmann[92], R.R.M. Fletcher[124], T. Flick[178], B.M. Flierl[102], L.R. Flores Castillo[62a], M.J. Flowerdew[103], G.T. Forcolin[87], A. Formica[138],

JHEP05(2018)195

F.A. Förster[13], A. Forti[87], A.G. Foster[19], D. Fournier[119], H. Fox[75], S. Fracchia[141], P. Francavilla[126a,126b], M. Franchini[22a,22b], S. Franchino[60a], D. Francis[32], L. Franconi[121], M. Franklin[59], M. Frate[166], M. Fraternali[123a,123b], D. Freeborn[81], S.M. Fressard-Batraneanu[32], B. Freund[97], D. Froidevaux[32], J.A. Frost[122], C. Fukunaga[158], E. Fullana Torregrosa[170], T. Fusayasu[104], J. Fuster[170], O. Gabizon[154], A. Gabrielli[22a,22b], A. Gabrielli[16], G.P. Gach[41a], S. Gadatsch[32], S. Gadomski[80], G. Gagliardi[53a,53b], L.G. Gagnon[97], C. Galea[108], B. Galhardo[128a,128c], E.J. Gallas[122], B.J. Gallop[133], P. Gallus[130], G. Galster[39], K.K. Gan[113], S. Ganguly[37], Y. Gao[77], Y.S. Gao[145,g], F.M. Garay Walls[34a], C. García[170], J.E. García Navarro[170], J.A. García Pascual[35a], M. Garcia-Sciveres[16], R.W. Gardner[33], N. Garelli[145], V. Garonne[121], A. Gascon Bravo[45], K. Gasnikova[45], C. Gatti[50], A. Gaudiello[53a,53b], G. Gaudio[123a], I.L. Gavrilenko[98], C. Gay[171], G. Gaycken[23], E.N. Gazis[10], C.N.P. Gee[133], J. Geisen[57], M. Geisen[86], M.P. Geisler[60a], K. Gellerstedt[148a,148b], C. Gemme[53a], M.H. Genest[58], C. Geng[92], S. Gentile[134a,134b], C. Gentsos[156], S. George[80], D. Gerbaudo[13], G. Geßner[46], S. Ghasemi[143], M. Ghneimat[23], B. Giacobbe[22a], S. Giagu[134a,134b], N. Giangiacomi[22a,22b], P. Giannetti[126a], S.M. Gibson[80], M. Gignac[171], M. Gilchriese[16], D. Gillberg[31], G. Gilles[178], D.M. Gingrich[3,d], M.P. Giordani[167a,167c], F.M. Giorgi[22a], P.F. Giraud[138], P. Giromini[59], G. Giugliarelli[167a,167c], D. Giugni[94a], F. Giuli[122], C. Giuliani[103], M. Giulini[60b], B.K. Gjelsten[121], S. Gkaitatzis[156], I. Gkialas[9,s], E.L. Gkougkousis[13], P. Gkountoumis[10], L.K. Gladilin[101], C. Glasman[85], J. Glatzer[13], P.C.F. Glaysher[45], A. Glazov[45], M. Goblirsch-Kolb[25], J. Godlewski[42], S. Goldfarb[91], T. Golling[52], D. Golubkov[132], A. Gomes[128a,128b,128d], R. Gonçalo[128a], R. Goncalves Gama[26a], J. Goncalves Pinto Firmino Da Costa[138], G. Gonella[51], L. Gonella[19], A. Gongadze[68], J.L. Gonski[59], S. González de la Hoz[170], S. Gonzalez-Sevilla[52], L. Goossens[32], P.A. Gorbounov[99], H.A. Gordon[27], I. Gorelov[107], B. Gorini[32], E. Gorini[76a,76b], A. Gorišek[78], A.T. Goshaw[48], C. Gössling[46], M.I. Gostkin[68], C.A. Gottardo[23], C.R. Goudet[119], D. Goujdami[137c], A.G. Goussiou[140], N. Govender[147b,t], E. Gozani[154], I. Grabowska-Bold[41a], P.O.J. Gradin[168], J. Gramling[166], E. Gramstad[121], S. Grancagnolo[17], V. Gratchev[125], P.M. Gravila[28f], C. Gray[56], H.M. Gray[16], Z.D. Greenwood[82,u], C. Grefe[23], K. Gregersen[81], I.M. Gregor[45], P. Grenier[145], K. Grevtsov[5], J. Griffiths[8], A.A. Grillo[139], K. Grimm[75], S. Grinstein[13,v], Ph. Gris[37], J.-F. Grivaz[119], S. Groh[86], E. Gross[175], J. Grosse-Knetter[57], G.C. Grossi[82], Z.J. Grout[81], A. Grummer[107], L. Guan[92], W. Guan[176], J. Guenther[32], F. Guescini[163a], D. Guest[166], O. Gueta[155], B. Gui[113], E. Guido[53a,53b], T. Guillemin[5], S. Guindon[32], U. Gul[56], C. Gumpert[32], J. Guo[36c], W. Guo[92], Y. Guo[36a,w], R. Gupta[43], S. Gurbuz[20a], G. Gustavino[115], B.J. Gutelman[154], P. Gutierrez[115], N.G. Gutierrez Ortiz[81], C. Gutschow[81], C. Guyot[138], M.P. Guzik[41a], C. Gwenlan[122], C.B. Gwilliam[77], A. Haas[112], C. Haber[16], H.K. Hadavand[8], N. Haddad[137e], A. Hadef[88], S. Hageböck[23], M. Hagihara[164], H. Hakobyan[180,*], M. Haleem[45], J. Haley[116], G. Halladjian[93], G.D. Hallewell[88], K. Hamacher[178], P. Hamal[117], K. Hamano[172], A. Hamilton[147a], G.N. Hamity[141], P.G. Hamnett[45], L. Han[36a], S. Han[35a,35d], K. Hanagaki[69,x], K. Hanawa[157], M. Hance[139], D.M. Handl[102], B. Haney[124], P. Hanke[60a], J.B. Hansen[39], J.D. Hansen[39], M.C. Hansen[23], P.H. Hansen[39], K. Hara[164], A.S. Hard[176], T. Harenberg[178], F. Hariri[119], S. Harkusha[95], P.F. Harrison[173], N.M. Hartmann[102], Y. Hasegawa[142], A. Hasib[49], S. Hassani[138], S. Haug[18], R. Hauser[93], L. Hauswald[47], L.B. Havener[38], M. Havranek[130], C.M. Hawkes[19], R.J. Hawkings[32], D. Hayakawa[159], D. Hayden[93], C.P. Hays[122], J.M. Hays[79], H.S. Hayward[77], S.J. Haywood[133], S.J. Head[19], T. Heck[86], V. Hedberg[84], L. Heelan[8], S. Heer[23], K.K. Heidegger[51], S. Heim[45], T. Heim[16], B. Heinemann[45,y], J.J. Heinrich[102], L. Heinrich[112], C. Heinz[55], J. Hejbal[129], L. Helary[32], A. Held[171], S. Hellman[148a,148b], C. Helsens[32], R.C.W. Henderson[75], Y. Heng[176], S. Henkelmann[171], A.M. Henriques Correia[32], S. Henrot-Versille[119], G.H. Herbert[17], H. Herde[25], V. Herget[177], Y. Hernández Jiménez[147c], H. Herr[86], G. Herten[51], R. Hertenberger[102], L. Hervas[32],

JHEP05(2018)195

T.C. Herwig[124], G.G. Hesketh[81], N.P. Hessey[163a], J.W. Hetherly[43], S. Higashino[69], E. Higón-Rodriguez[170], K. Hildebrand[33], E. Hill[172], J.C. Hill[30], K.H. Hiller[45], S.J. Hillier[19], M. Hils[47], I. Hinchliffe[16], M. Hirose[51], D. Hirschbuehl[178], B. Hiti[78], O. Hladik[129], D.R. Hlaluku[147c], X. Hoad[49], J. Hobbs[150], N. Hod[163a], M.C. Hodgkinson[141], P. Hodgson[141], A. Hoecker[32], M.R. Hoeferkamp[107], F. Hoenig[102], D. Hohn[23], T.R. Holmes[33], M. Holzbock[102], M. Homann[46], S. Honda[164], T. Honda[69], T.M. Hong[127], B.H. Hooberman[169], W.H. Hopkins[118], Y. Horii[105], A.J. Horton[144], J-Y. Hostachy[58], A. Hostiuc[140], S. Hou[153], A. Hoummada[137a], J. Howarth[87], J. Hoya[74], M. Hrabovsky[117], J. Hrdinka[32], I. Hristova[17], J. Hrivnac[119], T. Hryn'ova[5], A. Hrynevich[96], P.J. Hsu[63], S.-C. Hsu[140], Q. Hu[27], S. Hu[36c], Y. Huang[35a], Z. Hubacek[130], F. Hubaut[88], F. Huegging[23], T.B. Huffman[122], E.W. Hughes[38], M. Huhtinen[32], R.F.H. Hunter[31], P. Huo[150], N. Huseynov[68,b], J. Huston[93], J. Huth[59], R. Hyneman[92], G. Iacobucci[52], G. Iakovidis[27], I. Ibragimov[143], L. Iconomidou-Fayard[119], Z. Idrissi[137e], P. Iengo[32], O. Igonkina[109,z], T. Iizawa[174], Y. Ikegami[69], M. Ikeno[69], Y. Ilchenko[11,aa], D. Iliadis[156], N. Ilic[145], F. Iltzsche[47], G. Introzzi[123a,123b], P. Ioannou[9,*], M. Iodice[136a], K. Iordanidou[38], V. Ippolito[59], M.F. Isacson[168], N. Ishijima[120], M. Ishino[157], M. Ishitsuka[159], C. Issever[122], S. Istin[20a], F. Ito[164], J.M. Iturbe Ponce[62a], R. Iuppa[162a,162b], H. Iwasaki[69], J.M. Izen[44], V. Izzo[106a], S. Jabbar[3], P. Jackson[1], R.M. Jacobs[23], V. Jain[2], K.B. Jakobi[86], K. Jakobs[51], S. Jakobsen[65], T. Jakoubek[129], D.O. Jamin[116], D.K. Jana[82], R. Jansky[52], J. Janssen[23], M. Janus[57], P.A. Janus[41a], G. Jarlskog[84], N. Javadov[68,b], T. Javůrek[51], M. Javurkova[51], F. Jeanneau[138], L. Jeanty[16], J. Jejelava[54a,ab], A. Jelinskas[173], P. Jenni[51,ac], C. Jeske[173], S. Jézéquel[5], H. Ji[176], J. Jia[150], H. Jiang[67], Y. Jiang[36a], Z. Jiang[145], S. Jiggins[81], J. Jimenez Pena[170], S. Jin[35b], A. Jinaru[28b], O. Jinnouchi[159], H. Jivan[147c], P. Johansson[141], K.A. Johns[7], C.A. Johnson[64], W.J. Johnson[140], K. Jon-And[148a,148b], R.W.L. Jones[75], S.D. Jones[151], S. Jones[7], T.J. Jones[77], J. Jongmanns[60a], P.M. Jorge[128a,128b], J. Jovicevic[163a], X. Ju[176], A. Juste Rozas[13,v], M.K. Köhler[175], A. Kaczmarska[42], M. Kado[119], H. Kagan[113], M. Kagan[145], S.J. Kahn[88], T. Kaji[174], E. Kajomovitz[154], C.W. Kalderon[84], A. Kaluza[86], S. Kama[43], A. Kamenshchikov[132], N. Kanaya[157], L. Kanjir[78], V.A. Kantserov[100], J. Kanzaki[69], B. Kaplan[112], L.S. Kaplan[176], D. Kar[147c], K. Karakostas[10], N. Karastathis[10], M.J. Kareem[163b], E. Karentzos[10], S.N. Karpov[68], Z.M. Karpova[68], K. Karthik[112], V. Kartvelishvili[75], A.N. Karyukhin[132], K. Kasahara[164], L. Kashif[176], R.D. Kass[113], A. Kastanas[149], Y. Kataoka[157], C. Kato[157], A. Katre[52], J. Katzy[45], K. Kawade[70], K. Kawagoe[73], T. Kawamoto[157], G. Kawamura[57], E.F. Kay[77], V.F. Kazanin[111,c], R. Keeler[172], R. Kehoe[43], J.S. Keller[31], E. Kellermann[84], J.J. Kempster[80], J Kendrick[19], H. Keoshkerian[161], O. Kepka[129], B.P. Kerševan[78], S. Kersten[178], R.A. Keyes[90], M. Khader[169], F. Khalil-zada[12], A. Khanov[116], A.G. Kharlamov[111,c], T. Kharlamova[111,c], A. Khodinov[160], T.J. Khoo[52], V. Khovanskiy[99,*], E. Khramov[68], J. Khubua[54b,ad], S. Kido[70], C.R. Kilby[80], H.Y. Kim[8], S.H. Kim[164], Y.K. Kim[33], N. Kimura[156], O.M. Kind[17], B.T. King[77], D. Kirchmeier[47], J. Kirk[133], A.E. Kiryunin[103], T. Kishimoto[157], D. Kisielewska[41a], V. Kitali[45], O. Kivernyk[5], E. Kladiva[146b], T. Klapdor-Kleingrothaus[51], M.H. Klein[92], M. Klein[77], U. Klein[77], K. Kleinknecht[86], P. Klimek[110], A. Klimentov[27], R. Klingenberg[46,*], T. Klingl[23], T. Klioutchnikova[32], F.F. Klitzner[102], E.-E. Kluge[60a], P. Kluit[109], S. Kluth[103], E. Kneringer[65], E.B.F.G. Knoops[88], A. Knue[103], A. Kobayashi[157], D. Kobayashi[73], T. Kobayashi[157], M. Kobel[47], M. Kocian[145], P. Kodys[131], T. Koffas[31], E. Koffeman[109], N.M. Köhler[103], T. Koi[145], M. Kolb[60b], I. Koletsou[5], A.A. Komar[98,*], T. Kondo[69], N. Kondrashova[36c], K. Köneke[51], A.C. König[108], T. Kono[69,ae], R. Konoplich[112,af], N. Konstantinidis[81], B. Konya[84], R. Kopeliansky[64], S. Koperny[41a], A.K. Kopp[51], K. Korcyl[42], K. Kordas[156], A. Korn[81], A.A. Korol[111,c], I. Korolkov[13], E.V. Korolkova[141], O. Kortner[103], S. Kortner[103], T. Kosek[131], V.V. Kostyukhin[23], A. Kotwal[48], A. Koulouris[10], A. Kourkoumeli-Charalampidi[123a,123b], C. Kourkoumelis[9], E. Kourlitis[141], V. Kouskoura[27], A.B. Kowalewska[42], R. Kowalewski[172], T.Z. Kowalski[41a],

JHEP05(2018)195

C. Kozakai[157], W. Kozanecki[138], A.S. Kozhin[132], V.A. Kramarenko[101], G. Kramberger[78], D. Krasnopevtsev[100], M.W. Krasny[83], A. Krasznahorkay[32], D. Krauss[103], J.A. Kremer[41a], J. Kretzschmar[77], K. Kreutzfeldt[55], P. Krieger[161], K. Krizka[16], K. Kroeninger[46], H. Kroha[103], J. Kroll[129], J. Kroll[124], J. Kroseberg[23], J. Krstic[14], U. Kruchonak[68], H. Krüger[23], N. Krumnack[67], M.C. Kruse[48], T. Kubota[91], H. Kucuk[81], S. Kuday[4b], J.T. Kuechler[178], S. Kuehn[32], A. Kugel[60a], F. Kuger[177], T. Kuhl[45], V. Kukhtin[68], R. Kukla[88], Y. Kulchitsky[95], S. Kuleshov[34b], Y.P. Kulinich[169], M. Kuna[134a,134b], T. Kunigo[71], A. Kupco[129], T. Kupfer[46], O. Kuprash[155], H. Kurashige[70], L.L. Kurchaninov[163a], Y.A. Kurochkin[95], M.G. Kurth[35a,35d], E.S. Kuwertz[172], M. Kuze[159], J. Kvita[117], T. Kwan[172], D. Kyriazopoulos[141], A. La Rosa[103], J.L. La Rosa Navarro[26d], L. La Rotonda[40a,40b], F. La Ruffa[40a,40b], C. Lacasta[170], F. Lacava[134a,134b], J. Lacey[45], D.P.J. Lack[87], H. Lacker[17], D. Lacour[83], E. Ladygin[68], R. Lafaye[5], B. Laforge[83], T. Lagouri[179], S. Lai[57], S. Lammers[64], W. Lampl[7], E. Lançon[27], U. Landgraf[51], M.P.J. Landon[79], M.C. Lanfermann[52], V.S. Lang[45], J.C. Lange[13], R.J. Langenberg[32], A.J. Lankford[166], F. Lanni[27], K. Lantzsch[23], A. Lanza[123a], A. Lapertosa[53a,53b], S. Laplace[83], J.F. Laporte[138], T. Lari[94a], F. Lasagni Manghi[22a,22b], M. Lassnig[32], T.S. Lau[62a], P. Laurelli[50], W. Lavrijsen[16], A.T. Law[139], P. Laycock[77], T. Lazovich[59], M. Lazzaroni[94a,94b], B. Le[91], O. Le Dortz[83], E. Le Guirriec[88], E.P. Le Quilleuc[138], M. LeBlanc[172], T. LeCompte[6], F. Ledroit-Guillon[58], C.A. Lee[27], G.R. Lee[34a], S.C. Lee[153], L. Lee[59], B. Lefebvre[90], G. Lefebvre[83], M. Lefebvre[172], F. Legger[102], C. Leggett[16], G. Lehmann Miotto[32], X. Lei[7], W.A. Leight[45], M.A.L. Leite[26d], R. Leitner[131], D. Lellouch[175], B. Lemmer[57], K.J.C. Leney[81], T. Lenz[23], B. Lenzi[32], R. Leone[7], S. Leone[126a], C. Leonidopoulos[49], G. Lerner[151], C. Leroy[97], R. Les[161], A.A.J. Lesage[138], C.G. Lester[30], M. Levchenko[125], J. Levêque[5], D. Levin[92], L.J. Levinson[175], M. Levy[19], D. Lewis[79], B. Li[36a,w], C.-Q. Li[36a], H. Li[150], L. Li[36c], Q. Li[35a,35d], Q. Li[36a], S. Li[48], X. Li[36c], Y. Li[143], Z. Liang[35a], B. Liberti[135a], A. Liblong[161], K. Lie[62c], J. Liebal[23], W. Liebig[15], A. Limosani[152], C.Y. Lin[30], K. Lin[93], S.C. Lin[182], T.H. Lin[86], R.A. Linck[64], B.E. Lindquist[150], A.E. Lionti[52], E. Lipeles[124], A. Lipniacka[15], M. Lisovyi[60b], T.M. Liss[169,ag], A. Lister[171], A.M. Litke[139], B. Liu[67], H. Liu[92], H. Liu[27], J.K.K. Liu[122], J. Liu[36b], J.B. Liu[36a], K. Liu[88], L. Liu[169], M. Liu[36a], Y.L. Liu[36a], Y. Liu[36a], M. Livan[123a,123b], A. Lleres[58], J. Llorente Merino[35a], S.L. Lloyd[79], C.Y. Lo[62b], F. Lo Sterzo[43], E.M. Lobodzinska[45], P. Loch[7], F.K. Loebinger[87], A. Loesle[51], K.M. Loew[25], T. Lohse[17], K. Lohwasser[141], M. Lokajicek[129], B.A. Long[24], J.D. Long[169], R.E. Long[75], L. Longo[76a,76b], K.A. Looper[113], J.A. Lopez[34b], I. Lopez Paz[13], A. Lopez Solis[83], J. Lorenz[102], N. Lorenzo Martinez[5], M. Losada[21], P.J. Lösel[102], X. Lou[35a], A. Lounis[119], J. Love[6], P.A. Love[75], H. Lu[62a], N. Lu[92], Y.J. Lu[63], H.J. Lubatti[140], C. Luci[134a,134b], A. Lucotte[58], C. Luedtke[51], F. Luehring[64], W. Lukas[65], L. Luminari[134a], O. Lundberg[148a,148b], B. Lund-Jensen[149], M.S. Lutz[89], P.M. Luzi[83], D. Lynn[27], R. Lysak[129], E. Lytken[84], F. Lyu[35a], V. Lyubushkin[68], H. Ma[27], L.L. Ma[36b], Y. Ma[36b], G. Maccarrone[50], A. Macchiolo[103], C.M. Macdonald[141], B. Maček[78], J. Machado Miguens[124,128b], D. Madaffari[170], R. Madar[37], W.F. Mader[47], A. Madsen[45], N. Madysa[47], J. Maeda[70], S. Maeland[15], T. Maeno[27], A.S. Maevskiy[101], V. Magerl[51], C. Maiani[119], C. Maidantchik[26a], T. Maier[102], A. Maio[128a,128b,128d], O. Majersky[146a], S. Majewski[118], Y. Makida[69], N. Makovec[119], B. Malaescu[83], Pa. Malecki[42], V.P. Maleev[125], F. Malek[58], U. Mallik[66], D. Malon[6], C. Malone[30], S. Maltezos[10], S. Malyukov[32], J. Mamuzic[170], G. Mancini[50], I. Mandić[78], J. Maneira[128a,128b], L. Manhaes de Andrade Filho[26b], J. Manjarres Ramos[47], K.H. Mankinen[84], A. Mann[102], A. Manousos[32], B. Mansoulie[138], J.D. Mansour[35a], R. Mantifel[90], M. Mantoani[57], S. Manzoni[94a,94b], L. Mapelli[32], G. Marceca[29], L. March[52], L. Marchese[122], G. Marchiori[83], M. Marcisovsky[129], C.A. Marin Tobon[32], M. Marjanovic[37], D.E. Marley[92], F. Marroquim[26a], S.P. Marsden[87], Z. Marshall[16], M.U.F Martensson[168], S. Marti-Garcia[170], C.B. Martin[113], T.A. Martin[173], V.J. Martin[49], B. Martin dit Latour[15], M. Martinez[13,v],

JHEP05(2018)195

V.I. Martinez Outschoorn[169], S. Martin-Haugh[133], V.S. Martoiu[28b], A.C. Martyniuk[81], A. Marzin[32], L. Masetti[86], T. Mashimo[157], R. Mashinistov[98], J. Masik[87], A.L. Maslennikov[111,c], L.H. Mason[91], L. Massa[135a,135b], P. Mastrandrea[5], A. Mastroberardino[40a,40b], T. Masubuchi[157], P. Mättig[178], J. Maurer[28b], S.J. Maxfield[77], D.A. Maximov[111,c], R. Mazini[153], I. Maznas[156], S.M. Mazza[94a,94b], N.C. Mc Fadden[107], G. Mc Goldrick[161], S.P. Mc Kee[92], A. McCarn[92], R.L. McCarthy[150], T.G. McCarthy[103], L.I. McClymont[81], E.F. McDonald[91], J.A. Mcfayden[32], G. Mchedlidze[57], S.J. McMahon[133], P.C. McNamara[91], C.J. McNicol[173], R.A. McPherson[172,o], S. Meehan[140], T.J. Megy[51], S. Mehlhase[102], A. Mehta[77], T. Meideck[58], K. Meier[60a], B. Meirose[44], D. Melini[170,ah], B.R. Mellado Garcia[147c], J.D. Mellenthin[57], M. Melo[146a], F. Meloni[18], A. Melzer[23], S.B. Menary[87], L. Meng[77], X.T. Meng[92], A. Mengarelli[22a,22b], S. Menke[103], E. Meoni[40a,40b], S. Mergelmeyer[17], C. Merlassino[18], P. Mermod[52], L. Merola[106a,106b], C. Meroni[94a], F.S. Merritt[33], A. Messina[134a,134b], J. Metcalfe[6], A.S. Mete[166], C. Meyer[124], J-P. Meyer[138], J. Meyer[109], H. Meyer Zu Theenhausen[60a], F. Miano[151], R.P. Middleton[133], S. Miglioranzi[53a,53b], L. Mijović[49], G. Mikenberg[175], M. Mikestikova[129], M. Mikuž[78], M. Milesi[91], A. Milic[161], D.A. Millar[79], D.W. Miller[33], C. Mills[49], A. Milov[175], D.A. Milstead[148a,148b], A.A. Minaenko[132], Y. Minami[157], I.A. Minashvili[54b], A.I. Mincer[112], B. Mindur[41a], M. Mineev[68], Y. Minegishi[157], Y. Ming[176], L.M. Mir[13], A. Mirto[76a,76b], K.P. Mistry[124], T. Mitani[174], J. Mitrevski[102], V.A. Mitsou[170], A. Miucci[18], P.S. Miyagawa[141], A. Mizukami[69], J.U. Mjörnmark[84], T. Mkrtchyan[180], M. Mlynarikova[131], T. Moa[148a,148b], K. Mochizuki[97], P. Mogg[51], S. Mohapatra[38], S. Molander[148a,148b], R. Moles-Valls[23], M.C. Mondragon[93], K. Mönig[45], J. Monk[39], E. Monnier[88], A. Montalbano[150], J. Montejo Berlingen[32], F. Monticelli[74], S. Monzani[94a], R.W. Moore[3], N. Morange[119], D. Moreno[21], M. Moreno Llácer[32], P. Morettini[53a], S. Morgenstern[32], D. Mori[144], T. Mori[157], M. Morii[59], M. Morinaga[174], V. Morisbak[121], A.K. Morley[32], G. Mornacchi[32], J.D. Morris[79], L. Morvaj[150], P. Moschovakos[10], M. Mosidze[54b], H.J. Moss[141], J. Moss[145,ai], K. Motohashi[159], R. Mount[145], E. Mountricha[27], E.J.W. Moyse[89], S. Muanza[88], F. Mueller[103], J. Mueller[127], R.S.P. Mueller[102], D. Muenstermann[75], P. Mullen[56], G.A. Mullier[18], F.J. Munoz Sanchez[87], W.J. Murray[173,133], H. Musheghyan[32], M. Muškinja[78], A.G. Myagkov[132,aj], M. Myska[130], B.P. Nachman[16], O. Nackenhorst[52], K. Nagai[122], R. Nagai[69,ae], K. Nagano[69], Y. Nagasaka[61], K. Nagata[164], M. Nagel[51], E. Nagy[88], A.M. Nairz[32], Y. Nakahama[105], K. Nakamura[69], T. Nakamura[157], I. Nakano[114], R.F. Naranjo Garcia[45], R. Narayan[11], D.I. Narrias Villar[60a], I. Naryshkin[125], T. Naumann[45], G. Navarro[21], R. Nayyar[7], H.A. Neal[92], P.Yu. Nechaeva[98], T.J. Neep[138], A. Negri[123a,123b], M. Negrini[22a], S. Nektarijevic[108], C. Nellist[57], A. Nelson[166], M.E. Nelson[122], S. Nemecek[129], P. Nemethy[112], M. Nessi[32,ak], M.S. Neubauer[169], M. Neumann[178], P.R. Newman[19], T.Y. Ng[62c], Y.S. Ng[17], T. Nguyen Manh[97], R.B. Nickerson[122], R. Nicolaidou[138], J. Nielsen[139], N. Nikiforou[11], V. Nikolaenko[132,aj], I. Nikolic-Audit[83], K. Nikolopoulos[19], J.K. Nilsen[121], P. Nilsson[27], Y. Ninomiya[69], A. Nisati[134a], N. Nishu[36c], R. Nisius[103], I. Nitsche[46], T. Nitta[174], T. Nobe[157], Y. Noguchi[71], M. Nomachi[120], I. Nomidis[31], M.A. Nomura[27], T. Nooney[79], M. Nordberg[32], N. Norjoharuddeen[122], O. Novgorodova[47], M. Nozaki[69], L. Nozka[117], K. Ntekas[166], E. Nurse[81], F. Nuti[91], K. O'connor[25], D.C. O'Neil[144], A.A. O'Rourke[45], V. O'Shea[56], F.G. Oakham[31,d], H. Oberlack[103], T. Obermann[23], J. Ocariz[83], A. Ochi[70], I. Ochoa[38], J.P. Ochoa-Ricoux[34a], S. Oda[73], S. Odaka[69], A. Oh[87], S.H. Oh[48], C.C. Ohm[149], H. Ohman[168], H. Oide[53a,53b], H. Okawa[164], Y. Okumura[157], T. Okuyama[69], A. Olariu[28b], L.F. Oleiro Seabra[128a], S.A. Olivares Pino[34a], D. Oliveira Damazio[27], A. Olszewski[42], J. Olszowska[42], A. Onofre[128a,128e], K. Onogi[105], P.U.E. Onyisi[11,aa], H. Oppen[121], M.J. Oreglia[33], Y. Oren[155], D. Orestano[136a,136b], N. Orlando[62b], R.S. Orr[161], B. Osculati[53a,53b,*], R. Ospanov[36a], G. Otero y Garzon[29], H. Otono[73], M. Ouchrif[137d], F. Ould-Saada[121], A. Ouraou[138], K.P. Oussoren[109], Q. Ouyang[35a], M. Owen[56], R.E. Owen[19], V.E. Ozcan[20a], N. Ozturk[8], K. Pachal[144], A. Pacheco Pages[13], L. Pacheco Rodriguez[138], C. Padilla Aranda[13],

JHEP05(2018)195

S. Pagan Griso[16], M. Paganini[179], F. Paige[27], G. Palacino[64], S. Palazzo[40a,40b], S. Palestini[32], M. Palka[41b], D. Pallin[37], E.St. Panagiotopoulou[10], I. Panagoulias[10], C.E. Pandini[52], J.G. Panduro Vazquez[80], P. Pani[32], S. Panitkin[27], D. Pantea[28b], L. Paolozzi[52], Th.D. Papadopoulou[10], K. Papageorgiou[9,s], A. Paramonov[6], D. Paredes Hernandez[179], A.J. Parker[75], M.A. Parker[30], K.A. Parker[45], F. Parodi[53a,53b], J.A. Parsons[38], U. Parzefall[51], V.R. Pascuzzi[161], J.M. Pasner[139], E. Pasqualucci[134a], S. Passaggio[53a], Fr. Pastore[80], S. Pataraia[86], J.R. Pater[87], T. Pauly[32], B. Pearson[103], S. Pedraza Lopez[170], R. Pedro[128a,128b], S.V. Peleganchuk[111,c], O. Penc[129], C. Peng[35a,35d], H. Peng[36a], J. Penwell[64], B.S. Peralva[26b], M.M. Perego[138], D.V. Perepelitsa[27], F. Peri[17], L. Perini[94a,94b], H. Pernegger[32], S. Perrella[106a,106b], R. Peschke[45], V.D. Peshekhonov[68,*], K. Peters[45], R.F.Y. Peters[87], B.A. Petersen[32], T.C. Petersen[39], E. Petit[58], A. Petridis[1], C. Petridou[156], P. Petroff[119], E. Petrolo[134a], M. Petrov[122], F. Petrucci[136a,136b], N.E. Pettersson[89], A. Peyaud[138], R. Pezoa[34b], F.H. Phillips[93], P.W. Phillips[133], G. Piacquadio[150], E. Pianori[173], A. Picazio[89], M.A. Pickering[122], R. Piegaia[29], J.E. Pilcher[33], A.D. Pilkington[87], M. Pinamonti[135a,135b], J.L. Pinfold[3], H. Pirumov[45], M. Pitt[175], L. Plazak[146a], M.-A. Pleier[27], V. Pleskot[86], E. Plotnikova[68], D. Pluth[67], P. Podberezko[111], R. Poettgen[84], R. Poggi[123a,123b], L. Poggioli[119], I. Pogrebnyak[93], D. Pohl[23], I. Pokharel[57], G. Polesello[123a], A. Poley[45], A. Policicchio[40a,40b], R. Polifka[32], A. Polini[22a], C.S. Pollard[56], V. Polychronakos[27], K. Pommès[32], D. Ponomarenko[100], L. Pontecorvo[134a], G.A. Popeneciu[28d], D.M. Portillo Quintero[83], S. Pospisil[130], K. Potamianos[45], I.N. Potrap[68], C.J. Potter[30], H. Potti[11], T. Poulsen[84], J. Poveda[32], M.E. Pozo Astigarraga[32], P. Pralavorio[88], A. Pranko[16], S. Prell[67], D. Price[87], M. Primavera[76a], S. Prince[90], N. Proklova[100], K. Prokofiev[62c], F. Prokoshin[34b], S. Protopopescu[27], J. Proudfoot[6], M. Przybycien[41a], A. Puri[169], P. Puzo[119], J. Qian[92], G. Qin[56], Y. Qin[87], A. Quadt[57], M. Queitsch-Maitland[45], D. Quilty[56], S. Raddum[121], V. Radeka[27], V. Radescu[122], S.K. Radhakrishnan[150], P. Radloff[118], P. Rados[91], F. Ragusa[94a,94b], G. Rahal[181], J.A. Raine[87], S. Rajagopalan[27], C. Rangel-Smith[168], T. Rashid[119], S. Raspopov[5], M.G. Ratti[94a,94b], D.M. Rauch[45], F. Rauscher[102], S. Rave[86], I. Ravinovich[175], J.H. Rawling[87], M. Raymond[32], A.L. Read[121], N.P. Readioff[58], M. Reale[76a,76b], D.M. Rebuzzi[123a,123b], A. Redelbach[177], G. Redlinger[27], R. Reece[139], R.G. Reed[147c], K. Reeves[44], L. Rehnisch[17], J. Reichert[124], A. Reiss[86], C. Rembser[32], H. Ren[35a,35d], M. Rescigno[134a], S. Resconi[94a], E.D. Resseguie[124], S. Rettie[171], E. Reynolds[19], O.L. Rezanova[111,c], P. Reznicek[131], R. Rezvani[97], R. Richter[103], S. Richter[81], E. Richter-Was[41b], O. Ricken[23], M. Ridel[83], P. Rieck[103], C.J. Riegel[178], J. Rieger[57], O. Rifki[115], M. Rijssenbeek[150], A. Rimoldi[123a,123b], M. Rimoldi[18], L. Rinaldi[22a], G. Ripellino[149], B. Ristić[32], E. Ritsch[32], I. Riu[13], F. Rizatdinova[116], E. Rizvi[79], C. Rizzi[13], R.T. Roberts[87], S.H. Robertson[90,o], A. Robichaud-Veronneau[90], D. Robinson[30], J.E.M. Robinson[45], A. Robson[56], E. Rocco[86], C. Roda[126a,126b], Y. Rodina[88,al], S. Rodriguez Bosca[170], A. Rodriguez Perez[13], D. Rodriguez Rodriguez[170], S. Roe[32], C.S. Rogan[59], O. Røhne[121], J. Roloff[59], A. Romaniouk[100], M. Romano[22a,22b], S.M. Romano Saez[37], E. Romero Adam[170], N. Rompotis[77], M. Ronzani[51], L. Roos[83], S. Rosati[134a], K. Rosbach[51], P. Rose[139], N.-A. Rosien[57], E. Rossi[106a,106b], L.P. Rossi[53a], J.H.N. Rosten[30], R. Rosten[140], M. Rotaru[28b], J. Rothberg[140], D. Rousseau[119], A. Rozanov[88], Y. Rozen[154], X. Ruan[147c], F. Rubbo[145], F. Rühr[51], A. Ruiz-Martinez[31], Z. Rurikova[51], N.A. Rusakovich[68], H.L. Russell[90], J.P. Rutherfoord[7], N. Ruthmann[32], E.M. Rüttinger[45], Y.F. Ryabov[125], M. Rybar[169], G. Rybkin[119], S. Ryu[6], A. Ryzhov[132], G.F. Rzehorz[57], A.F. Saavedra[152], G. Sabato[109], S. Sacerdoti[29], H.F-W. Sadrozinski[139], R. Sadykov[68], F. Safai Tehrani[134a], P. Saha[110], M. Sahinsoy[60a], M. Saimpert[45], M. Saito[157], T. Saito[157], H. Sakamoto[157], Y. Sakurai[174], G. Salamanna[136a,136b], J.E. Salazar Loyola[34b], D. Salek[109], P.H. Sales De Bruin[168], D. Salihagic[103], A. Salnikov[145], J. Salt[170], D. Salvatore[40a,40b], F. Salvatore[151], A. Salvucci[62a,62b,62c], A. Salzburger[32], D. Sammel[51], D. Sampsonidis[156], D. Sampsonidou[156],

JHEP05(2018)195

J. Sánchez[170], V. Sanchez Martinez[170], A. Sanchez Pineda[167a,167c], H. Sandaker[121], R.L. Sandbach[79], C.O. Sander[45], M. Sandhoff[178], C. Sandoval[21], D.P.C. Sankey[133], M. Sannino[53a,53b], Y. Sano[105], A. Sansoni[50], C. Santoni[37], H. Santos[128a], I. Santoyo Castillo[151], A. Sapronov[68], J.G. Saraiva[128a,128d], B. Sarrazin[23], O. Sasaki[69], K. Sato[164], E. Sauvan[5], G. Savage[80], P. Savard[161,d], N. Savic[103], C. Sawyer[133], L. Sawyer[82,u], J. Saxon[33], C. Sbarra[22a], A. Sbrizzi[22a,22b], T. Scanlon[81], D.A. Scannicchio[166], J. Schaarschmidt[140], P. Schacht[103], B.M. Schachtner[102], D. Schaefer[33], L. Schaefer[124], R. Schaefer[45], J. Schaeffer[86], S. Schaepe[32], S. Schaetzel[60b], U. Schäfer[86], A.C. Schaffer[119], D. Schaile[102], R.D. Schamberger[150], V.A. Schegelsky[125], D. Scheirich[131], M. Schernau[166], C. Schiavi[53a,53b], S. Schier[139], L.K. Schildgen[23], C. Schillo[51], M. Schioppa[40a,40b], S. Schlenker[32], K.R. Schmidt-Sommerfeld[103], K. Schmieden[32], C. Schmitt[86], S. Schmitt[45], S. Schmitz[86], U. Schnoor[51], L. Schoeffel[138], A. Schoening[60b], B.D. Schoenrock[93], E. Schopf[23], M. Schott[86], J.F.P. Schouwenberg[108], J. Schovancova[32], S. Schramm[52], N. Schuh[86], A. Schulte[86], M.J. Schultens[23], H.-C. Schultz-Coulon[60a], H. Schulz[17], M. Schumacher[51], B.A. Schumm[139], Ph. Schune[138], A. Schwartzman[145], T.A. Schwarz[92], H. Schweiger[87], Ph. Schwemling[138], R. Schwienhorst[93], J. Schwindling[138], A. Sciandra[23], G. Sciolla[25], M. Scornajenghi[40a,40b], F. Scuri[126a], F. Scutti[91], J. Searcy[92], P. Seema[23], S.C. Seidel[107], A. Seiden[139], J.M. Seixas[26a], G. Sekhniaidze[106a], K. Sekhon[92], S.J. Sekula[43], N. Semprini-Cesari[22a,22b], S. Senkin[37], C. Serfon[121], L. Serin[119], L. Serkin[167a,167b], M. Sessa[136a,136b], R. Seuster[172], H. Severini[115], T. Šfiligoj[78], F. Sforza[165], A. Sfyrla[52], E. Shabalina[57], N.W. Shaikh[148a,148b], L.Y. Shan[35a], R. Shang[169], J.T. Shank[24], M. Shapiro[16], P.B. Shatalov[99], K. Shaw[167a,167b], S.M. Shaw[87], A. Shcherbakova[148a,148b], C.Y. Shehu[151], Y. Shen[115], N. Sherafati[31], A.D. Sherman[24], P. Sherwood[81], L. Shi[153,am], S. Shimizu[70], C.O. Shimmin[179], M. Shimojima[104], I.P.J. Shipsey[122], S. Shirabe[73], M. Shiyakova[68,an], J. Shlomi[175], A. Shmeleva[98], D. Shoaleh Saadi[97], M.J. Shochet[33], S. Shojaii[94a,94b], D.R. Shope[115], S. Shrestha[113], E. Shulga[100], M.A. Shupe[7], P. Sicho[129], A.M. Sickles[169], P.E. Sidebo[149], E. Sideras Haddad[147c], O. Sidiropoulou[177], A. Sidoti[22a,22b], F. Siegert[47], Dj. Sijacki[14], J. Silva[128a,128d], S.B. Silverstein[148a], V. Simak[130], L. Simic[68], S. Simion[119], E. Simioni[86], B. Simmons[81], M. Simon[86], P. Sinervo[161], N.B. Sinev[118], M. Sioli[22a,22b], G. Siragusa[177], I. Siral[92], S.Yu. Sivoklokov[101], J. Sjölin[148a,148b], M.B. Skinner[75], P. Skubic[115], M. Slater[19], T. Slavicek[130], M. Slawinska[42], K. Sliwa[165], R. Slovak[131], V. Smakhtin[175], B.H. Smart[5], J. Smiesko[146a], N. Smirnov[100], S.Yu. Smirnov[100], Y. Smirnov[100], L.N. Smirnova[101,ao], O. Smirnova[84], J.W. Smith[57], M.N.K. Smith[38], R.W. Smith[38], M. Smizanska[75], K. Smolek[130], A.A. Snesarev[98], I.M. Snyder[118], S. Snyder[27], R. Sobie[172,o], F. Socher[47], A. Soffer[155], A. Søgaard[49], D.A. Soh[153], G. Sokhrannyi[78], C.A. Solans Sanchez[32], M. Solar[130], E.Yu. Soldatov[100], U. Soldevila[170], A.A. Solodkov[132], A. Soloshenko[68], O.V. Solovyanov[132], V. Solovyev[125], P. Sommer[141], H. Son[165], A. Sopczak[130], D. Sosa[60b], C.L. Sotiropoulou[126a,126b], S. Sottocornola[123a,123b], R. Soualah[167a,167c], A.M. Soukharev[111,c], D. South[45], B.C. Sowden[80], S. Spagnolo[76a,76b], M. Spalla[126a,126b], M. Spangenberg[173], F. Spanò[80], D. Sperlich[17], F. Spettel[103], T.M. Spieker[60a], R. Spighi[22a], G. Spigo[32], L.A. Spiller[91], M. Spousta[131], R.D. St. Denis[56,*], A. Stabile[94a,94b], R. Stamen[60a], S. Stamm[17], E. Stanecka[42], R.W. Stanek[6], C. Stanescu[136a], M.M. Stanitzki[45], B.S. Stapf[109], S. Stapnes[121], E.A. Starchenko[132], G.H. Stark[33], J. Stark[58], S.H Stark[39], P. Staroba[129], P. Starovoitov[60a], S. Stärz[32], R. Staszewski[42], M. Stegler[45], P. Steinberg[27], B. Stelzer[144], H.J. Stelzer[32], O. Stelzer-Chilton[163a], H. Stenzel[55], T.J. Stevenson[79], G.A. Stewart[56], M.C. Stockton[118], M. Stoebe[90], G. Stoicea[28b], P. Stolte[57], S. Stonjek[103], A.R. Stradling[8], A. Straessner[47], M.E. Stramaglia[18], J. Strandberg[149], S. Strandberg[148a,148b], M. Strauss[115], P. Strizenec[146b], R. Ströhmer[177], D.M. Strom[118], R. Stroynowski[43], A. Strubig[49], S.A. Stucci[27], B. Stugu[15], N.A. Styles[45], D. Su[145], J. Su[127], S. Suchek[60a], Y. Sugaya[120], M. Suk[130], V.V. Sulin[98],

JHEP05(2018)195

DMS Sultan[162a,162b], S. Sultansoy[4c], T. Sumida[71], S. Sun[59], X. Sun[3], K. Suruliz[151], C.J.E. Suster[152], M.R. Sutton[151], S. Suzuki[69], M. Svatos[129], M. Swiatlowski[33], S.P. Swift[2], I. Sykora[146a], T. Sykora[131], D. Ta[51], K. Tackmann[45], J. Taenzer[155], A. Taffard[166], R. Tafirout[163a], E. Tahirovic[79], N. Taiblum[155], H. Takai[27], R. Takashima[72], E.H. Takasugi[103], K. Takeda[70], T. Takeshita[142], Y. Takubo[69], M. Talby[88], A.A. Talyshev[111,c], J. Tanaka[157], M. Tanaka[159], R. Tanaka[119], S. Tanaka[69], R. Tanioka[70], B.B. Tannenwald[113], S. Tapia Araya[34b], S. Tapprogge[86], S. Tarem[154], G.F. Tartarelli[94a], P. Tas[131], M. Tasevsky[129], T. Tashiro[71], E. Tassi[40a,40b], A. Tavares Delgado[128a,128b], Y. Tayalati[137e], A.C. Taylor[107], A.J. Taylor[49], G.N. Taylor[91], P.T.E. Taylor[91], W. Taylor[163b], P. Teixeira-Dias[80], D. Temple[144], H. Ten Kate[32], P.K. Teng[153], J.J. Teoh[120], F. Tepel[178], S. Terada[69], K. Terashi[157], J. Terron[85], S. Terzo[13], M. Testa[50], R.J. Teuscher[161,o], S.J. Thais[179], T. Theveneaux-Pelzer[88], F. Thiele[39], J.P. Thomas[19], J. Thomas-Wilsker[80], P.D. Thompson[19], A.S. Thompson[56], L.A. Thomsen[179], E. Thomson[124], Y. Tian[38], M.J. Tibbetts[16], R.E. Ticse Torres[57], V.O. Tikhomirov[98,ap], Yu.A. Tikhonov[111,c], S. Timoshenko[100], P. Tipton[179], S. Tisserant[88], K. Todome[159], S. Todorova-Nova[5], S. Todt[47], J. Tojo[73], S. Tokár[146a], K. Tokushuku[69], E. Tolley[113], L. Tomlinson[87], M. Tomoto[105], L. Tompkins[145,aq], K. Toms[107], B. Tong[59], P. Tornambe[51], E. Torrence[118], H. Torres[47], E. Torró Pastor[140], J. Toth[88,ar], F. Touchard[88], D.R. Tovey[141], C.J. Treado[112], T. Trefzger[177], F. Tresoldi[151], A. Tricoli[27], I.M. Trigger[163a], S. Trincaz-Duvoid[83], M.F. Tripiana[13], W. Trischuk[161], B. Trocmé[58], A. Trofymov[45], C. Troncon[94a], M. Trottier-McDonald[16], M. Trovatelli[172], L. Truong[147b], M. Trzebinski[42], A. Trzupek[42], K.W. Tsang[62a], J.C-L. Tseng[122], P.V. Tsiareshka[95], G. Tsipolitis[10], N. Tsirintanis[9], S. Tsiskaridze[13], V. Tsiskaridze[51], E.G. Tskhadadze[54a], I.I. Tsukerman[99], V. Tsulaia[16], S. Tsuno[69], D. Tsybychev[150], Y. Tu[62b], A. Tudorache[28b], V. Tudorache[28b], T.T. Tulbure[28a], A.N. Tuna[59], S. Turchikhin[68], D. Turgeman[175], I. Turk Cakir[4b,as], R. Turra[94a], P.M. Tuts[38], G. Ucchielli[22a,22b], I. Ueda[69], M. Ughetto[148a,148b], F. Ukegawa[164], G. Unal[32], A. Undrus[27], G. Unel[166], F.C. Ungaro[91], Y. Unno[69], K. Uno[157], C. Unverdorben[102], J. Urban[146b], P. Urquijo[91], P. Urrejola[86], G. Usai[8], J. Usui[69], L. Vacavant[88], V. Vacek[130], B. Vachon[90], K.O.H. Vadla[121], A. Vaidya[81], C. Valderanis[102], E. Valdes Santurio[148a,148b], M. Valente[52], S. Valentinetti[22a,22b], A. Valero[170], L. Valéry[13], S. Valkar[131], A. Vallier[5], J.A. Valls Ferrer[170], W. Van Den Wollenberg[109], H. van der Graaf[109], P. van Gemmeren[6], J. Van Nieuwkoop[144], I. van Vulpen[109], M.C. van Woerden[109], M. Vanadia[135a,135b], W. Vandelli[32], A. Vaniachine[160], P. Vankov[109], G. Vardanyan[180], R. Vari[134a], E.W. Varnes[7], C. Varni[53a,53b], T. Varol[43], D. Varouchas[119], A. Vartapetian[8], K.E. Varvell[152], J.G. Vasquez[179], G.A. Vasquez[34b], F. Vazeille[37], D. Vazquez Furelos[13], T. Vazquez Schroeder[90], J. Veatch[57], V. Veeraraghavan[7], L.M. Veloce[161], F. Veloso[128a,128c], S. Veneziano[134a], A. Ventura[76a,76b], M. Venturi[172], N. Venturi[32], A. Venturini[25], V. Vercesi[123a], M. Verducci[136a,136b], W. Verkerke[109], A.T. Vermeulen[109], J.C. Vermeulen[109], M.C. Vetterli[144,d], N. Viaux Maira[34b], O. Viazlo[84], I. Vichou[169,*], T. Vickey[141], O.E. Vickey Boeriu[141], G.H.A. Viehhauser[122], S. Viel[16], L. Vigani[122], M. Villa[22a,22b], M. Villaplana Perez[94a,94b], E. Vilucchi[50], M.G. Vincter[31], V.B. Vinogradov[68], A. Vishwakarma[45], C. Vittori[22a,22b], I. Vivarelli[151], S. Vlachos[10], M. Vogel[178], P. Vokac[130], G. Volpi[13], H. von der Schmitt[103], E. von Toerne[23], V. Vorobel[131], K. Vorobev[100], M. Vos[170], R. Voss[32], J.H. Vossebeld[77], N. Vranjes[14], M. Vranjes Milosavljevic[14], V. Vrba[130], M. Vreeswijk[109], R. Vuillermet[32], I. Vukotic[33], P. Wagner[23], W. Wagner[178], J. Wagner-Kuhr[102], H. Wahlberg[74], S. Wahrmund[47], J. Walder[75], R. Walker[102], W. Walkowiak[143], V. Wallangen[148a,148b], C. Wang[35b], C. Wang[36b,at], F. Wang[176], H. Wang[16], H. Wang[3], J. Wang[45], J. Wang[152], Q. Wang[115], R.-J. Wang[83], R. Wang[6], S.M. Wang[153], T. Wang[38], W. Wang[153,au], W. Wang[36a,av], Z. Wang[36c], C. Wanotayaroj[45], A. Warburton[90], C.P. Ward[30], D.R. Wardrope[81], A. Washbrook[49], P.M. Watkins[19], A.T. Watson[19], M.F. Watson[19], G. Watts[140], S. Watts[87],

JHEP05(2018)195

B.M. Waugh[81], A.F. Webb[11], S. Webb[86], M.S. Weber[18], S.M. Weber[60a], S.W. Weber[177], S.A. Weber[31], J.S. Webster[6], A.R. Weidberg[122], B. Weinert[64], J. Weingarten[57], M. Weirich[86], C. Weiser[51], H. Weits[109], P.S. Wells[32], T. Wenaus[27], T. Wengler[32], S. Wenig[32], N. Wermes[23], M.D. Werner[67], P. Werner[32], M. Wessels[60a], T.D. Weston[18], K. Whalen[118], N.L. Whallon[140], A.M. Wharton[75], A.S. White[92], A. White[8], M.J. White[1], R. White[34b], D. Whiteson[166], B.W. Whitmore[75], F.J. Wickens[133], W. Wiedenmann[176], M. Wielers[133], C. Wiglesworth[39], L.A.M. Wiik-Fuchs[51], A. Wildauer[103], F. Wilk[87], H.G. Wilkens[32], H.H. Williams[124], S. Williams[109], C. Willis[93], S. Willocq[89], J.A. Wilson[19], I. Wingerter-Seez[5], E. Winkels[151], F. Winklmeier[118], O.J. Winston[151], B.T. Winter[23], M. Wittgen[145], M. Wobisch[82,u], T.M.H. Wolf[109], R. Wolff[88], M.W. Wolter[42], H. Wolters[128a,128c], V.W.S. Wong[171], N.L. Woods[139], S.D. Worm[19], B.K. Wosiek[42], J. Wotschack[32], K.W. Wozniak[42], M. Wu[33], S.L. Wu[176], X. Wu[52], Y. Wu[92], T.R. Wyatt[87], B.M. Wynne[49], S. Xella[39], Z. Xi[92], L. Xia[35c], D. Xu[35a], L. Xu[27], T. Xu[138], W. Xu[92], B. Yabsley[152], S. Yacoob[147a], D. Yamaguchi[159], Y. Yamaguchi[159], A. Yamamoto[69], S. Yamamoto[157], T. Yamanaka[157], F. Yamane[70], M. Yamatani[157], T. Yamazaki[157], Y. Yamazaki[70], Z. Yan[24], H. Yang[36c], H. Yang[16], Y. Yang[153], Z. Yang[15], W-M. Yao[16], Y.C. Yap[45], Y. Yasu[69], E. Yatsenko[5], K.H. Yau Wong[23], J. Ye[43], S. Ye[27], I. Yeletskikh[68], E. Yigitbasi[24], E. Yildirim[86], K. Yorita[174], K. Yoshihara[124], C. Young[145], C.J.S. Young[32], J. Yu[8], J. Yu[67], S.P.Y. Yuen[23], I. Yusuff[30,aw], B. Zabinski[42], G. Zacharis[10], R. Zaidan[13], A.M. Zaitsev[132,aj], N. Zakharchuk[45], J. Zalieckas[15], A. Zaman[150], S. Zambito[59], D. Zanzi[91], C. Zeitnitz[178], G. Zemaityte[122], A. Zemla[41a], J.C. Zeng[169], Q. Zeng[145], O. Zenin[132], T. Ženiš[146a], D. Zerwas[119], D. Zhang[36b], D. Zhang[92], F. Zhang[176], G. Zhang[36a,av], H. Zhang[119], J. Zhang[6], L. Zhang[51], L. Zhang[36a], M. Zhang[169], P. Zhang[35b], R. Zhang[23], R. Zhang[36a,at], X. Zhang[36b], Y. Zhang[35a,35d], Z. Zhang[119], X. Zhao[43], Y. Zhao[36b,ax], Z. Zhao[36a], A. Zhemchugov[68], B. Zhou[92], C. Zhou[176], L. Zhou[43], M. Zhou[35a,35d], M. Zhou[150], N. Zhou[36c], Y. Zhou[7], C.G. Zhu[36b], H. Zhu[35a], J. Zhu[92], Y. Zhu[36a], X. Zhuang[35a], K. Zhukov[98], A. Zibell[177], D. Zieminska[64], N.I. Zimine[68], C. Zimmermann[86], S. Zimmermann[51], Z. Zinonos[103], M. Zinser[86], M. Ziolkowski[143], L. Živković[14], G. Zobernig[176], A. Zoccoli[22a,22b], R. Zou[33], M. zur Nedden[17], L. Zwalinski[32]

[1] *Department of Physics, University of Adelaide, Adelaide, Australia*
[2] *Physics Department, SUNY Albany, Albany NY, United States of America*
[3] *Department of Physics, University of Alberta, Edmonton AB, Canada*
[4] [(a)] *Department of Physics, Ankara University, Ankara;* [(b)] *Istanbul Aydin University, Istanbul;* [(c)] *Division of Physics, TOBB University of Economics and Technology, Ankara, Turkey*
[5] *LAPP, CNRS/IN2P3 and Université Savoie Mont Blanc, Annecy-le-Vieux, France*
[6] *High Energy Physics Division, Argonne National Laboratory, Argonne IL, United States of America*
[7] *Department of Physics, University of Arizona, Tucson AZ, United States of America*
[8] *Department of Physics, The University of Texas at Arlington, Arlington TX, United States of America*
[9] *Physics Department, National and Kapodistrian University of Athens, Athens, Greece*
[10] *Physics Department, National Technical University of Athens, Zografou, Greece*
[11] *Department of Physics, The University of Texas at Austin, Austin TX, United States of America*
[12] *Institute of Physics, Azerbaijan Academy of Sciences, Baku, Azerbaijan*
[13] *Institut de Física d'Altes Energies (IFAE), The Barcelona Institute of Science and Technology, Barcelona, Spain*
[14] *Institute of Physics, University of Belgrade, Belgrade, Serbia*
[15] *Department for Physics and Technology, University of Bergen, Bergen, Norway*
[16] *Physics Division, Lawrence Berkeley National Laboratory and University of California, Berkeley CA, United States of America*

JHEP05(2018)195

[17] Department of Physics, Humboldt University, Berlin, Germany
[18] Albert Einstein Center for Fundamental Physics and Laboratory for High Energy Physics, University of Bern, Bern, Switzerland
[19] School of Physics and Astronomy, University of Birmingham, Birmingham, United Kingdom
[20] [(a)] Department of Physics, Bogazici University, Istanbul; [(b)] Department of Physics Engineering, Gaziantep University, Gaziantep; [(d)] Istanbul Bilgi University, Faculty of Engineering and Natural Sciences, Istanbul; [(e)] Bahcesehir University, Faculty of Engineering and Natural Sciences, Istanbul, Turkey
[21] Centro de Investigaciones, Universidad Antonio Narino, Bogota, Colombia
[22] [(a)] INFN Sezione di Bologna; [(b)] Dipartimento di Fisica e Astronomia, Università di Bologna, Bologna, Italy
[23] Physikalisches Institut, University of Bonn, Bonn, Germany
[24] Department of Physics, Boston University, Boston MA, United States of America
[25] Department of Physics, Brandeis University, Waltham MA, United States of America
[26] [(a)] Universidade Federal do Rio De Janeiro COPPE/EE/IF, Rio de Janeiro; [(b)] Electrical Circuits Department, Federal University of Juiz de Fora (UFJF), Juiz de Fora; [(c)] Federal University of Sao Joao del Rei (UFSJ), Sao Joao del Rei; [(d)] Instituto de Fisica, Universidade de Sao Paulo, Sao Paulo, Brazil
[27] Physics Department, Brookhaven National Laboratory, Upton NY, United States of America
[28] [(a)] Transilvania University of Brasov, Brasov; [(b)] Horia Hulubei National Institute of Physics and Nuclear Engineering, Bucharest; [(c)] Department of Physics, Alexandru Ioan Cuza University of Iasi, Iasi; [(d)] National Institute for Research and Development of Isotopic and Molecular Technologies, Physics Department, Cluj Napoca; [(e)] University Politehnica Bucharest, Bucharest; [(f)] West University in Timisoara, Timisoara, Romania
[29] Departamento de Física, Universidad de Buenos Aires, Buenos Aires, Argentina
[30] Cavendish Laboratory, University of Cambridge, Cambridge, United Kingdom
[31] Department of Physics, Carleton University, Ottawa ON, Canada
[32] CERN, Geneva, Switzerland
[33] Enrico Fermi Institute, University of Chicago, Chicago IL, United States of America
[34] [(a)] Departamento de Física, Pontificia Universidad Católica de Chile, Santiago; [(b)] Departamento de Física, Universidad Técnica Federico Santa María, Valparaíso, Chile
[35] [(a)] Institute of High Energy Physics, Chinese Academy of Sciences, Beijing; [(b)] Department of Physics, Nanjing University, Jiangsu; [(c)] Physics Department, Tsinghua University, Beijing 100084; [(d)] University of Chinese Academy of Science (UCAS), Beijing, China
[36] [(a)] Department of Modern Physics and State Key Laboratory of Particle Detection and Electronics, University of Science and Technology of China, Anhui; [(b)] School of Physics, Shandong University, Shandong; [(c)] School of Physics and Astronomy, Key Laboratory for Particle Physics, Astrophysics and Cosmology, Ministry of Education; Shanghai Key Laboratory for Particle Physics and Cosmology, Tsung-Dao Lee Institute, Shanghai Jiao Tong University, China
[37] Université Clermont Auvergne, CNRS/IN2P3, LPC, Clermont-Ferrand, France
[38] Nevis Laboratory, Columbia University, Irvington NY, United States of America
[39] Niels Bohr Institute, University of Copenhagen, Kobenhavn, Denmark
[40] [(a)] INFN Gruppo Collegato di Cosenza, Laboratori Nazionali di Frascati; [(b)] Dipartimento di Fisica, Università della Calabria, Rende, Italy
[41] [(a)] AGH University of Science and Technology, Faculty of Physics and Applied Computer Science, Krakow; [(b)] Marian Smoluchowski Institute of Physics, Jagiellonian University, Krakow, Poland
[42] Institute of Nuclear Physics Polish Academy of Sciences, Krakow, Poland
[43] Physics Department, Southern Methodist University, Dallas TX, United States of America
[44] Physics Department, University of Texas at Dallas, Richardson TX, United States of America
[45] DESY, Hamburg and Zeuthen, Germany
[46] Lehrstuhl für Experimentelle Physik IV, Technische Universität Dortmund, Dortmund, Germany
[47] Institut für Kern- und Teilchenphysik, Technische Universität Dresden, Dresden, Germany

JHEP05(2018)195

[48] Department of Physics, Duke University, Durham NC, United States of America
[49] SUPA — School of Physics and Astronomy, University of Edinburgh, Edinburgh, United Kingdom
[50] INFN e Laboratori Nazionali di Frascati, Frascati, Italy
[51] Fakultät für Mathematik und Physik, Albert-Ludwigs-Universität, Freiburg, Germany
[52] Departement de Physique Nucleaire et Corpusculaire, Université de Genève, Geneva, Switzerland
[53] [(a)] INFN Sezione di Genova; [(b)] Dipartimento di Fisica, Università di Genova, Genova, Italy
[54] [(a)] E. Andronikashvili Institute of Physics, Iv. Javakhishvili Tbilisi State University, Tbilisi; [(b)] High Energy Physics Institute, Tbilisi State University, Tbilisi, Georgia
[55] II Physikalisches Institut, Justus-Liebig-Universität Giessen, Giessen, Germany
[56] SUPA — School of Physics and Astronomy, University of Glasgow, Glasgow, United Kingdom
[57] II Physikalisches Institut, Georg-August-Universität, Göttingen, Germany
[58] Laboratoire de Physique Subatomique et de Cosmologie, Université Grenoble-Alpes, CNRS/IN2P3, Grenoble, France
[59] Laboratory for Particle Physics and Cosmology, Harvard University, Cambridge MA, United States of America
[60] [(a)] Kirchhoff-Institut für Physik, Ruprecht-Karls-Universität Heidelberg, Heidelberg; [(b)] Physikalisches Institut, Ruprecht-Karls-Universität Heidelberg, Heidelberg, Germany
[61] Faculty of Applied Information Science, Hiroshima Institute of Technology, Hiroshima, Japan
[62] [(a)] Department of Physics, The Chinese University of Hong Kong, Shatin, N.T., Hong Kong; [(b)] Department of Physics, The University of Hong Kong, Hong Kong; [(c)] Department of Physics and Institute for Advanced Study, The Hong Kong University of Science and Technology, Clear Water Bay, Kowloon, Hong Kong, China
[63] Department of Physics, National Tsing Hua University, Taiwan, Taiwan
[64] Department of Physics, Indiana University, Bloomington IN, United States of America
[65] Institut für Astro- und Teilchenphysik, Leopold-Franzens-Universität, Innsbruck, Austria
[66] University of Iowa, Iowa City IA, United States of America
[67] Department of Physics and Astronomy, Iowa State University, Ames IA, United States of America
[68] Joint Institute for Nuclear Research, JINR Dubna, Dubna, Russia
[69] KEK, High Energy Accelerator Research Organization, Tsukuba, Japan
[70] Graduate School of Science, Kobe University, Kobe, Japan
[71] Faculty of Science, Kyoto University, Kyoto, Japan
[72] Kyoto University of Education, Kyoto, Japan
[73] Research Center for Advanced Particle Physics and Department of Physics, Kyushu University, Fukuoka, Japan
[74] Instituto de Física La Plata, Universidad Nacional de La Plata and CONICET, La Plata, Argentina
[75] Physics Department, Lancaster University, Lancaster, United Kingdom
[76] [(a)] INFN Sezione di Lecce; [(b)] Dipartimento di Matematica e Fisica, Università del Salento, Lecce, Italy
[77] Oliver Lodge Laboratory, University of Liverpool, Liverpool, United Kingdom
[78] Department of Experimental Particle Physics, Jožef Stefan Institute and Department of Physics, University of Ljubljana, Ljubljana, Slovenia
[79] School of Physics and Astronomy, Queen Mary University of London, London, United Kingdom
[80] Department of Physics, Royal Holloway University of London, Surrey, United Kingdom
[81] Department of Physics and Astronomy, University College London, London, United Kingdom
[82] Louisiana Tech University, Ruston LA, United States of America
[83] Laboratoire de Physique Nucléaire et de Hautes Energies, UPMC and Université Paris-Diderot and CNRS/IN2P3, Paris, France
[84] Fysiska institutionen, Lunds universitet, Lund, Sweden
[85] Departamento de Fisica Teorica C-15, Universidad Autonoma de Madrid, Madrid, Spain
[86] Institut für Physik, Universität Mainz, Mainz, Germany
[87] School of Physics and Astronomy, University of Manchester, Manchester, United Kingdom
[88] CPPM, Aix-Marseille Université and CNRS/IN2P3, Marseille, France

JHEP05(2018)195

[89] Department of Physics, University of Massachusetts, Amherst MA, United States of America
[90] Department of Physics, McGill University, Montreal QC, Canada
[91] School of Physics, University of Melbourne, Victoria, Australia
[92] Department of Physics, The University of Michigan, Ann Arbor MI, United States of America
[93] Department of Physics and Astronomy, Michigan State University, East Lansing MI, United States of America
[94] [(a)] INFN Sezione di Milano; [(b)] Dipartimento di Fisica, Università di Milano, Milano, Italy
[95] B.I. Stepanov Institute of Physics, National Academy of Sciences of Belarus, Minsk, Republic of Belarus
[96] Research Institute for Nuclear Problems of Byelorussian State University, Minsk, Republic of Belarus
[97] Group of Particle Physics, University of Montreal, Montreal QC, Canada
[98] P.N. Lebedev Physical Institute of the Russian Academy of Sciences, Moscow, Russia
[99] Institute for Theoretical and Experimental Physics (ITEP), Moscow, Russia
[100] National Research Nuclear University MEPhI, Moscow, Russia
[101] D.V. Skobeltsyn Institute of Nuclear Physics, M.V. Lomonosov Moscow State University, Moscow, Russia
[102] Fakultät für Physik, Ludwig-Maximilians-Universität München, München, Germany
[103] Max-Planck-Institut für Physik (Werner-Heisenberg-Institut), München, Germany
[104] Nagasaki Institute of Applied Science, Nagasaki, Japan
[105] Graduate School of Science and Kobayashi-Maskawa Institute, Nagoya University, Nagoya, Japan
[106] [(a)] INFN Sezione di Napoli; [(b)] Dipartimento di Fisica, Università di Napoli, Napoli, Italy
[107] Department of Physics and Astronomy, University of New Mexico, Albuquerque NM, United States of America
[108] Institute for Mathematics, Astrophysics and Particle Physics, Radboud University Nijmegen/Nikhef, Nijmegen, Netherlands
[109] Nikhef National Institute for Subatomic Physics and University of Amsterdam, Amsterdam, Netherlands
[110] Department of Physics, Northern Illinois University, DeKalb IL, United States of America
[111] Budker Institute of Nuclear Physics, SB RAS, Novosibirsk, Russia
[112] Department of Physics, New York University, New York NY, United States of America
[113] Ohio State University, Columbus OH, United States of America
[114] Faculty of Science, Okayama University, Okayama, Japan
[115] Homer L. Dodge Department of Physics and Astronomy, University of Oklahoma, Norman OK, United States of America
[116] Department of Physics, Oklahoma State University, Stillwater OK, United States of America
[117] Palacký University, RCPTM, Olomouc, Czech Republic
[118] Center for High Energy Physics, University of Oregon, Eugene OR, United States of America
[119] LAL, Univ. Paris-Sud, CNRS/IN2P3, Université Paris-Saclay, Orsay, France
[120] Graduate School of Science, Osaka University, Osaka, Japan
[121] Department of Physics, University of Oslo, Oslo, Norway
[122] Department of Physics, Oxford University, Oxford, United Kingdom
[123] [(a)] INFN Sezione di Pavia; [(b)] Dipartimento di Fisica, Università di Pavia, Pavia, Italy
[124] Department of Physics, University of Pennsylvania, Philadelphia PA, United States of America
[125] National Research Centre "Kurchatov Institute" B.P.Konstantinov Petersburg Nuclear Physics Institute, St. Petersburg, Russia
[126] [(a)] INFN Sezione di Pisa; [(b)] Dipartimento di Fisica E. Fermi, Università di Pisa, Pisa, Italy
[127] Department of Physics and Astronomy, University of Pittsburgh, Pittsburgh PA, United States of America
[128] [(a)] Laboratório de Instrumentação e Física Experimental de Partículas — LIP, Lisboa; [(b)] Faculdade de Ciências, Universidade de Lisboa, Lisboa; [(c)] Department of Physics, University of Coimbra, Coimbra; [(d)] Centro de Física Nuclear da Universidade de Lisboa, Lisboa; [(e)]

JHEP05(2018)195

Departamento de Fisica, Universidade do Minho, Braga; [(f)] *Departamento de Fisica Teorica y del Cosmos, Universidad de Granada, Granada;* [(g)] *Dep Fisica and CEFITEC of Faculdade de Ciencias e Tecnologia, Universidade Nova de Lisboa, Caparica, Portugal*

[129] *Institute of Physics, Academy of Sciences of the Czech Republic, Praha, Czech Republic*

[130] *Czech Technical University in Prague, Praha, Czech Republic*

[131] *Charles University, Faculty of Mathematics and Physics, Prague, Czech Republic*

[132] *State Research Center Institute for High Energy Physics (Protvino), NRC KI, Russia*

[133] *Particle Physics Department, Rutherford Appleton Laboratory, Didcot, United Kingdom*

[134] [(a)] *INFN Sezione di Roma;* [(b)] *Dipartimento di Fisica, Sapienza Università di Roma, Roma, Italy*

[135] [(a)] *INFN Sezione di Roma Tor Vergata;* [(b)] *Dipartimento di Fisica, Università di Roma Tor Vergata, Roma, Italy*

[136] [(a)] *INFN Sezione di Roma Tre;* [(b)] *Dipartimento di Matematica e Fisica, Università Roma Tre, Roma, Italy*

[137] [(a)] *Faculté des Sciences Ain Chock, Réseau Universitaire de Physique des Hautes Energies — Université Hassan II, Casablanca;* [(b)] *Centre National de l'Energie des Sciences Techniques Nucleaires, Rabat;* [(c)] *Faculté des Sciences Semlalia, Université Cadi Ayyad, LPHEA-Marrakech;* [(d)] *Faculté des Sciences, Université Mohamed Premier and LPTPM, Oujda;* [(e)] *Faculté des sciences, Université Mohammed V, Rabat, Morocco*

[138] *DSM/IRFU (Institut de Recherches sur les Lois Fondamentales de l'Univers), CEA Saclay (Commissariat à l'Energie Atomique et aux Energies Alternatives), Gif-sur-Yvette, France*

[139] *Santa Cruz Institute for Particle Physics, University of California Santa Cruz, Santa Cruz CA, United States of America*

[140] *Department of Physics, University of Washington, Seattle WA, United States of America*

[141] *Department of Physics and Astronomy, University of Sheffield, Sheffield, United Kingdom*

[142] *Department of Physics, Shinshu University, Nagano, Japan*

[143] *Department Physik, Universität Siegen, Siegen, Germany*

[144] *Department of Physics, Simon Fraser University, Burnaby BC, Canada*

[145] *SLAC National Accelerator Laboratory, Stanford CA, United States of America*

[146] [(a)] *Faculty of Mathematics, Physics & Informatics, Comenius University, Bratislava;* [(b)] *Department of Subnuclear Physics, Institute of Experimental Physics of the Slovak Academy of Sciences, Kosice, Slovak Republic*

[147] [(a)] *Department of Physics, University of Cape Town, Cape Town;* [(b)] *Department of Physics, University of Johannesburg, Johannesburg;* [(c)] *School of Physics, University of the Witwatersrand, Johannesburg, South Africa*

[148] [(a)] *Department of Physics, Stockholm University;* [(b)] *The Oskar Klein Centre, Stockholm, Sweden*

[149] *Physics Department, Royal Institute of Technology, Stockholm, Sweden*

[150] *Departments of Physics & Astronomy and Chemistry, Stony Brook University, Stony Brook NY, United States of America*

[151] *Department of Physics and Astronomy, University of Sussex, Brighton, United Kingdom*

[152] *School of Physics, University of Sydney, Sydney, Australia*

[153] *Institute of Physics, Academia Sinica, Taipei, Taiwan*

[154] *Department of Physics, Technion: Israel Institute of Technology, Haifa, Israel*

[155] *Raymond and Beverly Sackler School of Physics and Astronomy, Tel Aviv University, Tel Aviv, Israel*

[156] *Department of Physics, Aristotle University of Thessaloniki, Thessaloniki, Greece*

[157] *International Center for Elementary Particle Physics and Department of Physics, The University of Tokyo, Tokyo, Japan*

[158] *Graduate School of Science and Technology, Tokyo Metropolitan University, Tokyo, Japan*

[159] *Department of Physics, Tokyo Institute of Technology, Tokyo, Japan*

[160] *Tomsk State University, Tomsk, Russia*

[161] *Department of Physics, University of Toronto, Toronto ON, Canada*

[162] [(a)] *INFN-TIFPA;* [(b)] *University of Trento, Trento, Italy*

JHEP05(2018)195

[163] [(a)] TRIUMF, Vancouver BC; [(b)] Department of Physics and Astronomy, York University, Toronto ON, Canada
[164] Faculty of Pure and Applied Sciences, and Center for Integrated Research in Fundamental Science and Engineering, University of Tsukuba, Tsukuba, Japan
[165] Department of Physics and Astronomy, Tufts University, Medford MA, United States of America
[166] Department of Physics and Astronomy, University of California Irvine, Irvine CA, United States of America
[167] [(a)] INFN Gruppo Collegato di Udine, Sezione di Trieste, Udine; [(b)] ICTP, Trieste; [(c)] Dipartimento di Chimica, Fisica e Ambiente, Università di Udine, Udine, Italy
[168] Department of Physics and Astronomy, University of Uppsala, Uppsala, Sweden
[169] Department of Physics, University of Illinois, Urbana IL, United States of America
[170] Instituto de Fisica Corpuscular (IFIC), Centro Mixto Universidad de Valencia — CSIC, Spain
[171] Department of Physics, University of British Columbia, Vancouver BC, Canada
[172] Department of Physics and Astronomy, University of Victoria, Victoria BC, Canada
[173] Department of Physics, University of Warwick, Coventry, United Kingdom
[174] Waseda University, Tokyo, Japan
[175] Department of Particle Physics, The Weizmann Institute of Science, Rehovot, Israel
[176] Department of Physics, University of Wisconsin, Madison WI, United States of America
[177] Fakultät für Physik und Astronomie, Julius-Maximilians-Universität, Würzburg, Germany
[178] Fakultät für Mathematik und Naturwissenschaften, Fachgruppe Physik, Bergische Universität Wuppertal, Wuppertal, Germany
[179] Department of Physics, Yale University, New Haven CT, United States of America
[180] Yerevan Physics Institute, Yerevan, Armenia
[181] Centre de Calcul de l'Institut National de Physique Nucléaire et de Physique des Particules (IN2P3), Villeurbanne, France
[182] Academia Sinica Grid Computing, Institute of Physics, Academia Sinica, Taipei, Taiwan

[a] Also at Department of Physics, King's College London, London, United Kingdom
[b] Also at Institute of Physics, Azerbaijan Academy of Sciences, Baku, Azerbaijan
[c] Also at Novosibirsk State University, Novosibirsk, Russia
[d] Also at TRIUMF, Vancouver BC, Canada
[e] Also at Department of Physics & Astronomy, University of Louisville, Louisville, KY, United States of America
[f] Also at Physics Department, An-Najah National University, Nablus, Palestine
[g] Also at Department of Physics, California State University, Fresno CA, United States of America
[h] Also at Department of Physics, University of Fribourg, Fribourg, Switzerland
[i] Also at II Physikalisches Institut, Georg-August-Universität, Göttingen, Germany
[j] Also at Departament de Fisica de la Universitat Autonoma de Barcelona, Barcelona, Spain
[k] Also at Departamento de Fisica e Astronomia, Faculdade de Ciencias, Universidade do Porto, Portugal
[l] Also at Tomsk State University, Tomsk, and Moscow Institute of Physics and Technology State University, Dolgoprudny, Russia
[m] Also at The Collaborative Innovation Center of Quantum Matter (CICQM), Beijing, China
[n] Also at Universita di Napoli Parthenope, Napoli, Italy
[o] Also at Institute of Particle Physics (IPP), Canada
[p] Also at Horia Hulubei National Institute of Physics and Nuclear Engineering, Bucharest, Romania
[q] Also at Department of Physics, St. Petersburg State Polytechnical University, St. Petersburg, Russia
[r] Also at Borough of Manhattan Community College, City University of New York, New York City, United States of America
[s] Also at Department of Financial and Management Engineering, University of the Aegean, Chios, Greece

JHEP05(2018)195

[t] Also at Centre for High Performance Computing, CSIR Campus, Rosebank, Cape Town, South Africa
[u] Also at Louisiana Tech University, Ruston LA, United States of America
[v] Also at Institucio Catalana de Recerca i Estudis Avancats, ICREA, Barcelona, Spain
[w] Also at Department of Physics, The University of Michigan, Ann Arbor MI, United States of America
[x] Also at Graduate School of Science, Osaka University, Osaka, Japan
[y] Also at Fakultät für Mathematik und Physik, Albert-Ludwigs-Universität, Freiburg, Germany
[z] Also at Institute for Mathematics, Astrophysics and Particle Physics, Radboud University Nijmegen/Nikhef, Nijmegen, Netherlands
[aa] Also at Department of Physics, The University of Texas at Austin, Austin TX, United States of America
[ab] Also at Institute of Theoretical Physics, Ilia State University, Tbilisi, Georgia
[ac] Also at CERN, Geneva, Switzerland
[ad] Also at Georgian Technical University (GTU),Tbilisi, Georgia
[ae] Also at Ochadai Academic Production, Ochanomizu University, Tokyo, Japan
[af] Also at Manhattan College, New York NY, United States of America
[ag] Also at The City College of New York, New York NY, United States of America
[ah] Also at Departamento de Fisica Teorica y del Cosmos, Universidad de Granada, Granada, Portugal
[ai] Also at Department of Physics, California State University, Sacramento CA, United States of America
[aj] Also at Moscow Institute of Physics and Technology State University, Dolgoprudny, Russia
[ak] Also at Departement de Physique Nucleaire et Corpusculaire, Université de Genève, Geneva, Switzerland
[al] Also at Institut de Física d'Altes Energies (IFAE), The Barcelona Institute of Science and Technology, Barcelona, Spain
[am] Also at School of Physics, Sun Yat-sen University, Guangzhou, China
[an] Also at Institute for Nuclear Research and Nuclear Energy (INRNE) of the Bulgarian Academy of Sciences, Sofia, Bulgaria
[ao] Also at Faculty of Physics, M.V.Lomonosov Moscow State University, Moscow, Russia
[ap] Also at National Research Nuclear University MEPhI, Moscow, Russia
[aq] Also at Department of Physics, Stanford University, Stanford CA, United States of America
[ar] Also at Institute for Particle and Nuclear Physics, Wigner Research Centre for Physics, Budapest, Hungary
[as] Also at Giresun University, Faculty of Engineering, Turkey
[at] Also at CPPM, Aix-Marseille Université and CNRS/IN2P3, Marseille, France
[au] Also at Department of Physics, Nanjing University, Jiangsu, China
[av] Also at Institute of Physics, Academia Sinica, Taipei, Taiwan
[aw] Also at University of Malaya, Department of Physics, Kuala Lumpur, Malaysia
[ax] Also at LAL, Univ. Paris-Sud, CNRS/IN2P3, Université Paris-Saclay, Orsay, France
[*] Deceased

JHEP05(2018)195